Indian Summer Monsoon

critical transition, predictability and extremes

D I S S E R T A T I O N

zur Erlangung des akademischen Grades

d o c t o r   r e r u m   n a t u r a l i u m
(Dr. rer. nat.)
im Fach Physik

eingereicht an der
Mathematisch-Naturwissenschaftlichen Fakultät
der Humboldt-Universität zu Berlin

von
Dipl.-Phys. Veronika Stolbova

Präsident der Humboldt-Universität zu Berlin:
Prof. Dr. Jan-Hendrik Olbertz

Dekan der Mathematisch-Naturwissenschaftlichen Fakultät:
Prof. Dr. Elmar Kulke

Gutachter:

1. Prof. Dr. Dr. h.c. J. Kurths

2. Prof. Dr. Ir. H.A. Dijkstra

3. Prof. R. Krishnan

Tag der mündlichen Prüfung: 29. Januar 2016

To my family

Abstract

The aim of this thesis is to uncover some of the mysteries surrounding the Indian Monsoon - a large-scale climatic phenomenon affecting more than 1.7 billion people - by using modern methods of complex systems science. The variability, strength, onset and withdrawal of monsoonal rainfall have an enormous effect on Indian agriculture, economy, life and prosperity of the inhabitants of the Indian subcontinent. Consequently, understanding the mechanisms of the Indian monsoon and its successful forecasting is not only a question of great interest, but also a significant scientific challenge.

The first part of this thesis is devoted to extreme rainfall events over the Indian subcontinent before, during and after the Indian monsoon season. I have employed and generalized the tools of complex networks and a nonlinear correlation measure - event synchronization - to study spatial structures and synchronicity of rainfall extremes. The analysis reveals a coincidence between the occurrence of extreme rainfall events in a pair of geographical regions: the Eastern Ghats and North Pakistan. In this thesis, I have shown that a synchronicity between extreme rainfall events in the Eastern Ghats and North Pakistan regions is caused by the interplay between the Indian Monsoon and a non-monsoonal precipitation pattern driven by the Westerlies - Western Disturbances. This result highlights the importance of the North Pakistan region for inferring the interaction between the Indian Monsoon system and Western Disturbances, and, therefore, improves the understanding of the Indian Monsoon coupling with the extratropics.

The second part of this dissertation is concerned with the problem of the spatial and temporal organization of the abrupt transition to the Indian monsoon. The analysis of observational data uncovers that a threshold behavior at the transition to monsoon over the central part of India corresponds to the well-defined critical transition of the cusp catastrophe type. Based on these observations, I have proposed a novel mechanism of a spatio-temporal transition to monsoon. It has several advantages in comparison to existing explanations of the Indian Monsoon nature: it describes the abrupt transition to monsoon in a chosen region of the Indian subcontinent, as well as the spatial propagation and variability of the Indian Monsoon onset along the axis of advance of monsoon.

The third part of this thesis focuses on the problem of predictability of the Indian Monsoon. I have developed a novel method for prediction of monsoon timing based on a critical transition precursor. The main idea of the method is to identify geographic regions - tipping elements of the monsoon - and to use them as observation locations for predicting onset and withdrawal dates. Unlike most predictability methods, this approach does not rely on precipitation analysis, but on air temperature and relative humidity, which are well-represented both in models and observations. The proposed method predicts the onset and withdrawal dates more than two weeks and a month earlier than existing methods, respectively. In addition, the scheme allows the inclusion of the information about the El-Niño–Southern Oscillation in the forecasting of onset and withdrawal dates, thereby, significantly improving the prediction of monsoon timing during anomalous years associated with the El-Niño–Southern Oscillation. Finally, the proposed scheme can be directly implemented into the existing long-range forecasting system of the monsoon's timing.

Zusammenfassung

Das Ziel dieser Arbeit ist es, mittels moderner Methoden der Wissenschaft komplexer Systeme einige Geheimnisse des Indischen Monsuns aufzudecken - ein groß-skaliges Klimaphänomen, das mehr als 1,7 Milliarden Menschen stark beeinflußt. Die Variabilität des Monsunregenfälle, seine Stärke, Beginn und Ende haben einen enormen Einfluss auf die Indische Landwirtschaft, Wirtschaft, Leben und Wohlstand der Bewohner des indischen Subkontinents. Folglich ist das Verständnis der Mechanismen des Indischen Monsuns und seine erfolgreiche Prognose nicht nur eine Frage von größtem Interesse, sondern auch eine bedeutende wissenschaftliche Herausforderung.

Der erste Teil dieser Arbeit ist den extremen Niederschlagsereignissen über dem Indischen Subkontinent vor, während und nach der Indischen Monsunzeit gewidmet. Ich habe Methoden komplexer Netzwerke und nichtlinearer Korrelationsmaße sowie Ereignissynchronisation angewendet, um räumliche Strukturen der extremer Niederschläge und ihre Synchronizität zu studieren. Die Analyse ergab eine Übereinstimmung zwischen dem Auftreten von extremen Niederschlagsereignissen in einem Paar von geographischen Regionen: der Eastern Ghats und Nord Pakistan. In dieser Arbeit wurde gezeigt, dass eine Synchronizität zwischen extremen Niederschlagsereignissen in den Eastern Ghats und Nord Pakistan Regionen durch das Zusammenspiel zwischen dem indischen Monsun und einem nicht-Monsunniederschlagsmuster, das durch die Westwinde angetrieben wird, verursacht wird. Dieses Ergebnis unterstreicht die Bedeutung der Region Nord-Pakistan zur Ableitung der Wechselwirkung zwischen dem indischen Monsun-System und den West-Störungen, und verbessert daher das Verständnis der Kopplung des indischen Monsuns mit den Extratropen.

Der zweite Teil der Arbeit befasst sich mit dem Problem der räumlichen und zeitlichen Organisation des abrupten Übergangs auf den indischen Monsun. Die Analyse von Beobachtungsdaten zeigt, dass ein Schwellenverhalten beim Übergang zum Monsun im mittleren Teil von Indien dem wohlbekannten kritischen Übergang einer Gipfel- Katastrophe entspricht. Basierend auf diesen Beobachtungen wird ein neuartiger Mechanismus des räumlich-zeitlichen Übergangs zur Regenperiode vorgeschlagen. Er hat mehrere Vorteile gegenüber bestehenden Erklärungen der Natur des indischen Monsuns: Es beschreibt den abrupten Übergang in einer gewählten Region des indischen Subkontinents sowie die räumliche Ausbreitung und Variabilität des indischen Monsuns beim Einsetzen entlang der Achse des Monsuns.

Der dritte Teil dieser Arbeit konzentriert sich auf das Problem der Vorhersagbarkeit des indischen Monsuns. Ich habe neuartige Verfahren zur Vorhersage der Regenzeit auf der Grundlage von Vorläufern kritischer Übergänge vorgeschlagen. Die Grundidee des Verfahrens ist, geografische Regionen als Kipp-Elemente des Monsuns zu identifizieren und sie als Beobachtungsstellen für die Vorhersage des Einsetzens und Endens aus Daten zu verwenden. Anders als die meisten Vorhersagemethoden, basiert dieser Ansatz nicht auf Niederschlagsdaten, sondern auf der Lufttemperatur und der relativen Luftfeuchtigkeit, die gut sowohl in Modellen als auch Beobachtungen vertreten sind. Das vorgeschlagene Verfahren ermöglicht die Vorhersage des Einsetzens und Endens über einen mehr als zwei Wochen bzw.einen Monat früheren Zeitraum im Vergleich zu bisher bekannten

Methoden. Darüber hinaus ermöglicht das System unter Einbezug von Informationen über die El-Niño - Southern Oscillation eine Prognose des Auftretens und Endens, dass in anomalen El-Niño Jahren die Vorhersage deutlich verbessert werden kann. Schließlich kann die vorgeschlagene Instrumentarium direkt in das bestehende lang-reichweitige Vorhersagesystem für den Monsuns implementiert werden.

List of publications

This dissertation is partly based on the following publications. The identifiers, *e.g.*, P1, given below are cited in the text to highlight passages that are connected to these papers.

Papers

P1 **Stolbova V.**, Martin P., Bookhagen B., Marwan N. and Kurths J., *Topology and seasonal evolution of the network of extreme precipitation over the Indian subcontinent and Sri Lanka*, Nonlinear Processes in Geophysics, 21, 4, 901-917, 2014; doi:10.5194/npg-21-901-2014.

P2 Molkenthin N., Rehfeld K., **Stolbova V.**, Tupikina L., Kurths J., *On the influence of spatial sampling on climate networks*, Nonlinear Processes in Geophysics, 21, 3, 651-657, 2014; doi:10.5194/npg-21-651-2014.

P3 Tupikina L., Rehfeld K., Molkenthin N., **Stolbova V.**, Marwan N., Kurths J., *Characterizing the evolution of climate networks*, Nonlinear Processes in Geophysics , 21, 4, 705-711, 2014; doi:10.5194/npg-21-705-2014.

P4 **Stolbova V.**, Surovyatkina E., Bookhagen B., Kurths J., *Mechanism of spatio-temporal abrupt transition to monsoon*, submitted, 2016.

P5 **Stolbova V.**, Surovyatkina E., Bookhagen B., Kurths J., *Tipping elements of the Indian monsoon: prediction of onset and withdrawal*, Geophysical Research Letters, 43, 2016; doi:10.1002/2016GL068392.

P6 Donges J. F., Heitzig J., Beronov, B., Dijkstra, H. A., Donner, R. V., Feng, Qing Yi, Marwan, Runge,J., **Stolbova V.**, Tupikina, L., Wiedermann, M. and Kurths, J., *Unied functional network and nonlinear time series analysis for complex systems science: The pyunicorn package*, Chaos 25, 113101, 2015; doi: 10.1063/1.4934554

P7 Donner R., **Stolbova V.**, Balasis G., Donges J., Georgiou M., Potirakis S., Kurths J., *Dynamical complexity in the magnetosphere - A recurrence perspective*, under review in Journal of Geophysical Research, 2016.

Acknowledgements

First, I would like to express my deepest appreciation to my supervisor Prof. Jürgen Kurths for his wisdom, inspiration and gentle guidance in overseeing the direction and content of this thesis. Please receive my sincere gratitude for your encouragement and patient support during these years. I appreciate it very much and will never forget it.

I am enormously indebted to Elena Surovyatkina for opening my mind to the bifurcations and showing me what true interdisciplinarity means. Thank you so much for sharing your experience with me, encouragement to proceed with ideas and enthusiasm which kept me going until the discovery of the solutions.

My greatest gratitude goes to Bodo Bookhagen for encouraging me to learn about Monsoon and our scientific discussions which shaped my research interests and resulted in our interesting and productive collaboration.

I thank Norbert Marwan for kind and friendly attention, and for your disposition to share your experience with me. Paige Martin - thank you so much for your always positive scientific input and for being such a great friend! Big thanks to my amazing office mates: Liuba, Jakob and Marc! It was a great pleasure working and spending time with you guys! No matter office buildings or countries, I hope we stay in touch! Special thanks goes to Jakob for his valuable comments.

I am grateful to Reik Donner for the wisdom: "There are no problems in science, there are challenges", and expending my knowledge in the field of nonlinear time series analysis. I thank Kira Rehfeld for showing me what efficiency and time management means during our productive "girl team" writing of papers, Nora Molkenthin - for showing by your example that science is never boring. Big thanks to all members of the group: Deniz, Bedartha, Niklas, Aljoscha, Jonathan, Maik, Thomas, Jobst, Tim, Chiranjit, Julian, Jonathan, Carsten, Peng, Sabine, Paul, Frank, Gabi, Heike, Anja, Nadine - I am happy I work with you!

I pass my big gratitude to Prof. Henk Dijkstra for encouraging scientific discussions and hospitality during my research visit to his group. I am very happy I had a chance to be a part of a wonderful LINC project and "get linked" to the great scientists and friends! Thanks to: Prof. Cristina Masoller, Prof. Marcelo Bareirro, Prof. Shlomo Havlin, Prof. Emilio Hernandez Garcia, Avi Gozolchiani, Ignacio, Giulio, Veronica, Fernando, Alexis, Hisham, Marc, Miguel, Yang, Dong. It has been a pleasure working and spending time with you, guys! Greatest thanks to you Qingyi for inspiring me with your elegant attitude to life and science, for your support and being such a great friend!

The biggest gratitude I pass to my family for making me who I am and always supporting me no matter what.

Contents

Contents

List of Figures

List of Tables

List of frequently used mathematical symbols

Climatological and geographical abbreviations

ISM	Indian Summer Monsoon
ITCZ	Intertropical Convergence Zone
EG	Eastern Ghats
NP	North Pakistan
TP	Tibetan Plateau
WG	Western Ghats
BoB	Bay of Bengal
AS	Arabian Sea
OD	onset date of monsoon
WD	withdrawal date of monsoon

Mathematical abbreviations

A	adjacency matrix of a network
D	network measure Degree
B	network measure Betweenness
MGLL	network measure Mean Geographical Link Length

Chapter 1.

Introduction

> "May the rain come down in the proper time,
> may the earth yield plenty of corn ..."
>
> – *Daily prayer*

1.1. Motivation

The Indian Monsoon has been identified as a one of the tipping elements of the Earth's system - large-scale components of the Earth's system where qualitative changes in the state of the component can lead to drastic and abrupt changes in the state of the Earth's climate (Lenton et al., 2008; Levermann et al., 2009). The effects of the Indian Monsoon are enormous as on regional scale, through the agriculture and economy of the Indian subcontinent, as well on a global scale, through the monsoon's coupling with other large-scale climatic phenomena, including the El-Niño-Southern Oscillation, Indian Ocean Dipole and Equatorial Indian Ocean Oscillation (Sankar et al., 2011; Achuthavarier et al., 2012; Sabeerali et al., 2011; Wu and Kirtman, 2003; Wu et al., 2012; Gadgil, 2004). Nowadays, the Indian Monsoon directly affects life and prosperity of more than 1.7 billion people - near 1/4-th of the world's population.

The importance of the Indian Monsoon has been recognized several centuries ago, and documented studies of the monsoon variability and forecasts of monsoonal rainfall have been issued by the Indian Meteorological Department (IMD) since the late 19-th century. The most remarkable feature of the monsoon – the regularity of its occurrence from June to September – strictly tightened the agricultural activities on the Indian subcontinent with monsoon. Another important feature of the monsoon - the variability in the amount of rainfall and timing, including arrival and withdrawal of the monsoon, as well as intra-seasonal variability of "wet" and "dry" spells – up to now governs the life and prosperity of the inhabitants of the Indian subcontinent (Krishnamurthy and Shukla, 2007).

The monsoon is highly awaited by the population as it provides water for the crops, and is a main source of drinking water for most parts of the Indian subcontinent. Small variations of the timing and quantity of the rainfall strongly affect the agricultural planning and crop yields. For example, weak monsoon years (i.e., with the amount of rainfall significantly less than normal) generally correspond to low crop yields, thus, leading to farmer suicides, which account for 11.2% of all suicides in India (Das, 2011).
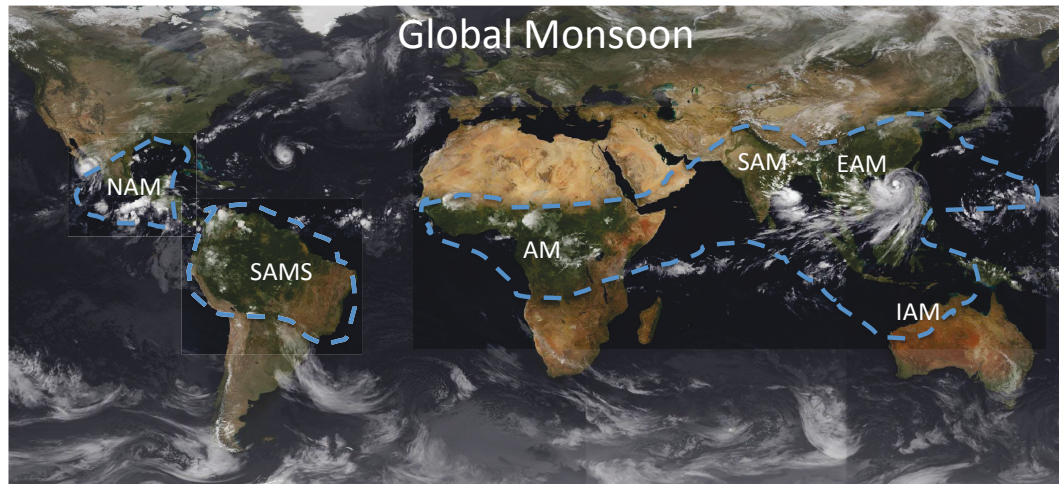
Figure 1.1.: Global Monsoon: SAM – South Asian Monsoon (includes Indian Summer Monsoon - ISM - during June-September and Winter Monsoon: October-December), EAM – East Asian Monsoon, IAM – Indo-Australian Monsoon, AM – African Monsoon, NAM – North American Monsoon, SAMS – South American Monsoon System. The Intertropical Convergence Zone (ITCZ) is one of the main drivers of monsoon, and is shown as a belt of clouds circling the globe and passing through the monsoon regions.

Strong monsoon years usually produce abundant crops, however, they may also lead to landslides, losses of crops and households (Webster et al., 1998). Additional danger of the monsoon is the occurence extreme rainfall events which is the main cause of the floods over the Indian subcontinent. The timing of the monsoon - the onset and withdrawal - is of particular interest for agricultural planning. A late or early onset and withdrawal of the monsoon may have devastating effects on agriculture even during the years when the mean annual rainfall during the monsoon season is normal. A delay of a few days in the arrival of the monsoon can badly affect the economy, as, for example, was shown by the numerous droughts in India in the 1990s, 2002 and 2009, while early monsoon arrival can lead to flooding of crops (Wang et al., 2009; Goswami et al., 2010).

Numerous studies of the Indian Monsoon during the last century significantly improved the understanding of the monsoon regularities and its variability from millennial to inter-annual and intra-seasonal time scales. However, there are still open crucial questions in the understanding of the present-day monsoon variability, which prevent its successful forecasting (Webster et al., 1998). In this thesis, I have attempted to address the questions related to extreme rainfall events of the Indian Monsoon, the mechanism of the abrupt transition to monsoon and the predictability of the monsoonal timing.
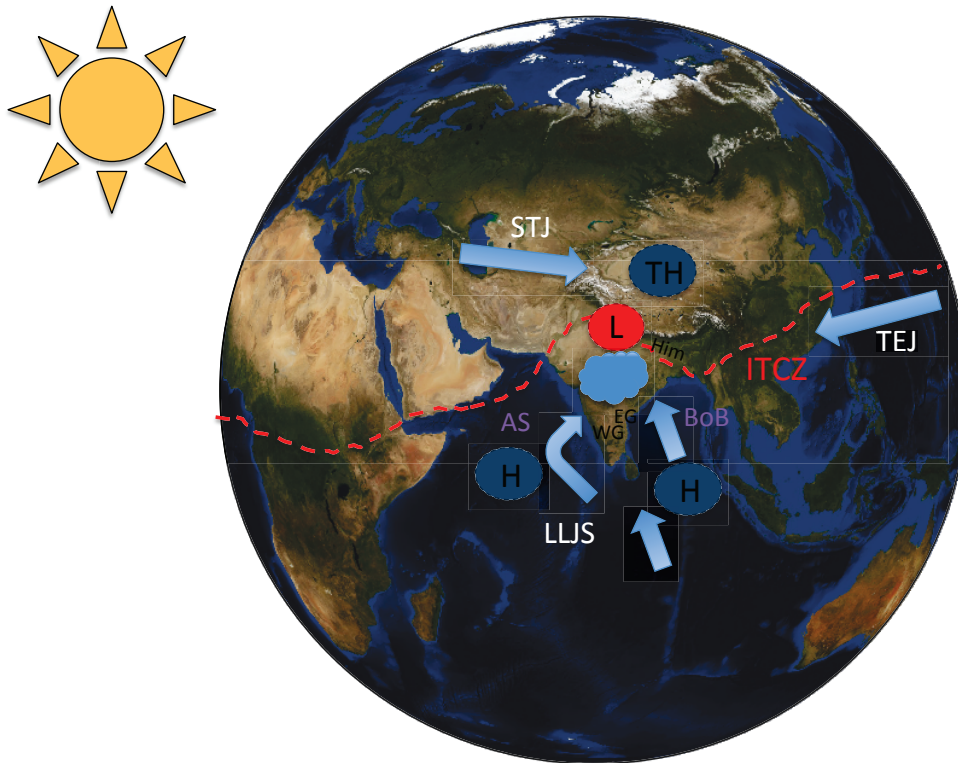
Figure 1.2.: Schematic illustration of the Indian Summer Monsoon circulation. The circulation is driven by seasonal insolation changes, differential heating between the land and surrounding Arabian Sea (AS) and Bay of Bengal (BoB), migration of the Intertropical Convergence Zone (ITCZ) together with tropical easterly jet (TEJ), and westerly sub-tropical jet stream (STJ). Tibetan upper troposphere High (TH) establishes over the Tibet and Low Level Jet stream (LLJ) splits into two monsoon branches. Topographical features: Himalayas (Him), Tibetan Plateau, Western Ghats (WG) and Eastern Ghats (EG). Areas of high and low pressure are marked with H and L, respectively.

1.2. Indian Monsoon: mechanism, extreme rainfall, transition to monsoon and predictability

Early studies defined *monsoon* as a regional phenomenon of sea breeze, caused by the seasonal reversal of the wind direction due to the differential heating of the land and the surrounded ocean. This word came from the Arabic word *mausim*, meaning season, which was used by sailors in the XVI century to describe the reversal of winds in the Arabian sea. More mordern studies, starting from (Saha and Saha, 1980), consider the monsoon as a part of the global atmospheric circulation system, and therefore, as a global phenomenon. In the frame of this theory, it is the Intertropical Convergenze Zone (ITCZ) – a belt circling the Earth, where trade winds from the Northern and Southern Hemispheres meet – what is responsible for the monsoon. This theory broadens the definition of the monsoon from the rainy season in the Indian subcontinent, to the so-called "Monsoon Zone", which consists of several "classical monsoons": South Asian or Indian Monsoon (SAM), East-Asian Monsoon (EAM), Indo-Australian Monsoon (IAM), African Monsoon (AM). Some researchers also define South - American Monsoon System (SAMS) and North American Monsoon (NAM) (see Figure 1.1). This work is fully dedicated to the study of the main and strongest monsoon on Earth - the Indian Monsoon.

1.2.1. Basic mechanism and variability

The Indian monsoon is a large-scale atmospheric pattern and one of the active components in the global climate system in the tropics. The ISM is driven by several factors which include the land-ocean surface temperature gradient between the Indian subcontinent and surrounding bodies of water (Arabian Sea and Bay of Bengal), the migration of the Intertropical Convergence Zone (ITCZ) northward during the Northern Hemisphere summer, northward shifting of westerly sub-tropical jet stream (STJ), the establishment of tropical easterly jet (TEJ), the Tibetan upper troposphere High (TH) and Low Level Jet stream (LLJ), which splits into two monsoon branches (see Fig. 2.1). These factors, combined together with topography of the Indian subcontinent, dominated by the Himalayas and Tibetan Plateau in the north, the Western Ghats from the Arabian Sea and Eastern Ghats from the Bay of Bengal, create a low pressure monsoon trough, and an area of deep convection establishes over the Indian subcontinent (Joseph et al., 1994; Ananthakrishnan and Soman, 1990).

Understanding the ISM as a giant sea-land breeze explains theannual regularity of the ISM occurrence, caused by the sea-land temperature gradient (Webster et al., 1998). However, it does not account for high temporal and spatial variability of the monsoonal rainfall (Gadgil, 2003). The monsoon variability is believed to be caused by the internal dynamics of monsoon, teleconnections with other climatic phenomena, such as El-Niño Southern Oscillation, Indian Ocean Dipole etc., and, lately, by the anthropogenic forcing (CO_2, aerosols) (Gadgil, 2004).

Climate Networks
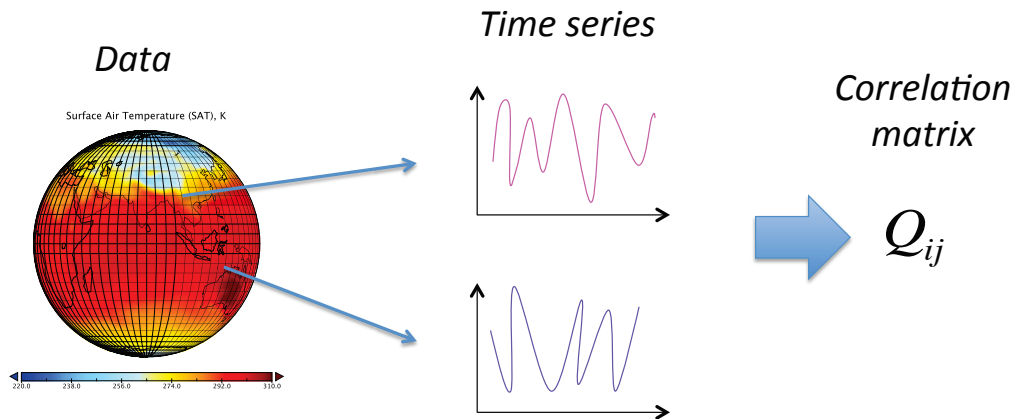
Figure 1.3.: Schematic illustration of the Climate Network approach. The data used are gridded: each grid cell is represented by a time series of a climatic variable (e.g. temperature, pressure or precipitation). In a climate network, nodes are geographical locations. Links are determined statistically as a similarity in dynamics between two geographical locations using a chosen correlation measure (e.g. Pearson correlation coefficient, mutual information, or event synchronization). The procedure of intercomparison is carried out for all pairs of locations. In order to obtain only significant correlation and the "strongest" links, the correlation matrix Q_{ij} is thresholded, and transformed into the adjacency matrix A_{ij}, which fully determines an undirected, unweighted climate network.

1.2.2. Extreme rainfall

One of the most important features accompanying the Indian Monsoon season is heavy rainfall. In cases, when the amount of rainfall in a region of the Indian subcontinent exceeds a certain threshold for the region of interest, the rainfall is considered extreme. Extreme rainfall events occur over the whole Indian subcontinent, mostly during the monsoon season, causing extensive damage to property, households, infrastructure and crops through landslides and flash floods. As a result, they have major impacts on society, the environment and the economy of the countries of the subcontinent. Therefore, understanding the regularities in the extreme rainfall and its predictability is a vital question for the subcontinent.

Extreme rainfall events over the Indian subcontinent have been extensively studied over the past decades (Goswami et al., 2006; Pattanaik and Rajeevan, 2009; Malik et al., 2010; Stolbova et al., 2014). Many studies focus on uncovering the statistical properties of extreme rainfall events (Goswami et al., 2006). Others, are concerned with changes in the general trend of the extreme rainfall events and its response to anthropogenic forcing - which points out that the number of extreme rainfall events tends to increase in the warming climate (Goswami et al., 2006). However, for the purpose of disaster preparedness and predictability of the extreme rainfall

Figure 1.4.: Visualization of a climate network derived from rainfall data over the Indian subcontinent.

events, it is crucial to focus on the study of the spatial structures of extreme rainfall events and their spatial and temporal properties. Recently, a novel methodology for investigation of the spatial structures of extreme rainfall events was proposed based on the climate network approach, which reveals the spatial structures and regularities in the synchronicity of the extreme rainfall events (Malik et al., 2010).

An extreme rainfall rarely comes alone. When extreme rainfall occurs in a certain place, it is important to detect other regions, which are vulnerable for extreme rainfall, in order to increase the awareness of the approaching extreme rainfall. Of course, depending on where the extreme rainfall occurs first, the configuration of the vulnerable regions changes. In order to detect the spatial structures of vulnerable regions as a function of location of extreme rainfall event, in this thesis I apply the climate network approach. A schematic illustration of the climate network approach is shown on Figure 1.3, while the visualization of the climate network in Figure 1.4. In Chapter 2 of this thesis, I present a detailed analysis of the spatial structures of the synchronized extreme rainfall events, taking into account their seasonal evolution, and identify the key regions on the Indian subcontinent governing the sychronization

of the extreme rainfall events during the monsoon season.

The big step towards the understanding of the regularities of the extreme events was, to a large extent, made due to the variety of high temporal and spatial resolution data sets that became available during the last years including model outputs from General Circulation Models (GSM), re-analysis observational and satellite-derived data (NCEP/NCAR, 2015; ERA40, 2015; TRMM, 2015). Such broad variety of the data sets rises the question of the data set inter-comparison, specifically, the comparison of the re-analysis and model-output data with observations, as precipitation is one the hardest climatic variables to model. While the comparison of the trends and the mean values is straightforward, it is more challenging task for the spatial structures. In Chapter 2 of this thesis, I discuss a spatial inter-comparison of two data sets using a climate network approach and network measures. It will be shown that this method is particularly useful for the patterns inter-comparison.

1.2.3. Transition to monsoon

The Indian Monsoon undergoes transitions on many time scales from millennial to yearly, which has been studied extensively by many researchers (Levermann et al., 2009; Lenton et al., 2008). However, the most crucial for the inhabitants of the Indian subcontinent transition associated with monsoon is the monsoon onset which governs agricultural activities. While the main drivers of monsoon and its basic mechanism are well described and understood, there are certain gaps in the understanding of the mechanism of abrupt transition to monsoon, which limits a successful prediction of monsoon's inter-annual variability. One of the main issues is the abrupt nature of the monsoon's onset. Although the regularity of the monsoon onset arrival is well known, the exact timing of the monsoon onset is difficult to forecast. Another challenge in the monsoon onset forecasting is the fact that the transition to monsoon not only takes place abruptly for each region of the subcontinent, but it also propagates in space and time.

Several earlier studies have indicated that the transition to strong convection, including the transition to the Indian Monsoon, exhibits properties of the critical transitions (Neelin et al., 2009; Peters et al., 2009). In particular, it has been shown that many of the climatic variables exhibit a threshold behavior at the onset of the monsoon, such as precipitation, vertically integrated water vapor, relative humidity etc. (Holloway and Neelin, 2009; Soman and Krishna Kumar, 1993; Fasullo and Webster, 2003). According to Ananthakrishnan and Soman, 1990, the onset of monsoon is not a transition from a regime of no rain to rain, it's a transition from sporadic rainfall to spatially organized and temporally sustained rainfall. Having these facts in mind, in Chapter 3 of my thesis, I propose a novel conceptual model which allows to explain as the abrupt nature of the monsoon's onset in a chosen region of the Indian subcontinent, as well as the spatial variability of the onset of monsoon. This model views the transition to monsoon as a spatio-temporal critical transition, and, based on the catastrophe theory, explains the main properties associated with monsoon onset and advance. In addition, I will show an example of how the parameters for

this conceptual model can be estimated for a chosen region of the Indian subcontinent directly from the observational data. The obtained results significantly add to the understanding of the mechanism of abrupt transition to monsoon and can be used for the forecasting of the monsoon timing, which I show in Chapter 4 of this dissertation.

1.2.4. Predictability of the Indian Monsoon

The prediction of the Indian monsoon strength and timing is one of the key questions about the Indian Monsoon. In this thesis the question of predictability of the monsoon timing, in particular, the onset and withdrawal of monsoon, is discussed. The forecasting of the monsoon timing is made on different time scales ranging from short (up to 4 days prior to the onset) to long-range forecasts (more than a month in advance) (Alessandri et al., 2014; Shukla and Mooley, 1987; Das et al., 2002; Goswami et al., 2010), using projections of the General Circulation Models (GSMs) and statistical forecasting based on the observational data (Goswami et al., 2006; Prasad, 2005; Yang et al., 2008). Despite enormous progress in the forecasting of the monsoon onset and withdrawal, there are certain limitations in the prediction of the transition to monsoon associated with internal natural variability of the monsoon and the intricate connection of the monsoon to other climatic phenomena and external factors, which are not fully understood. For example, it has been shown that the influence of the El-Niño - Southern Oscillation is connected with the Indian Monsoon in a complex nonlinear fashion, affecting the monsoon timing and decreasing its accurate forecasting (Webster et al., 1998). Therefore, the prediction skills of the monsoon timing are needed to be improved.

In Chapter 4 of this thesis, I address the question of long-range forecasting of the monsoon onset and withdrawal by using the results obtained in Chapter 3 on the critical nature of the transition to monsoon. I propose a novel method of the long-range forecasting of the monsoon onset and withdrawal in the Eastern Ghats region of the Indian subcontinent, as the arrival of monsoon to this region marks the full arrival of monsoon to the Indian subcontinent. Recent studies focus on the forecasting of monsoon onset over Kerala - a region on the western coast of the Indian subcontinent. However, the forecast in Kerala region is tingled with uncertainties due to the "bogus" of "false" monsoon onsets, caused by the mesoscale convective system coming from the Arabian Sea (Flatau et al., 2001). The forecasting scheme for monsoon onset in the Eastern Ghats, introduced in this thesis, on one hand proposes a qualitatively new approach for the forecasting of monsoon timing, and on another hand, it can be used as an additional forecast to the existing prediction scheme, as usage of both forecasts can improve the forecasting of monsoon onset propagation over the Indian subcontinent.

1.3. Arrangement of this thesis

According to the state-of-the-art knowledge about the Indian Monsoon presented in the outline above, there are three main research questions about the monsoon: 1)

When will the monsoon come? 2) Where? 3) How strong will it be? The aim of this dissertation is to address each of these questions, partially answering to the following issues related to them. In particular, the spatial structures (2) of monsoon and its strength (3) are studied from the perspective of extreme rainfall events, while the propagation of monsoon onset (2) and its predictability (1) are discussed from the view of understanding of the mechanism of abrupt transition to monsoon and the forecasting of the monsoon onset over the Indian subcontinent.

This dissertation is arranged as follows. In Chapter 2, extreme rainfall over the Indian subcontinent, which is the main cause of floods and landslides, is discussed. Due to the seasonality of the monsoonal rainfall, the spatial structures of the extreme rainfall events and extreme rainfall synchronicity undergo seasonal changes. Using the methodology of climate networks and a nonlinear similarity measure - event synchronization - for uncovering the evolution of the synchronicity of extreme rainfall during the pre-monsoon, monsoon and post-monsoon seasons, the key regions for synchronization of extreme rainfall events over the Indian subcontinent will be revealed. It will be shown that synchronicity of the extreme rainfall during the monsoon season depends to a large extent as on the large-scale monsoon circulation, as well as on the intricate interplay between the interaction of the monsoon circulation and the non-monsoonal precipitation pattern, caused by the westerlies. Among the key regions detected in this thesis, some of them were known and used by climatologists for the analysis of extreme rainfall during the monsoon season, while one specific region, determined using network approach - North Pakistan- was not previously recognized as a key region influencing the extreme rainfall over the Indian subcontinent. In this thesis, it will be shown that it is important to include North Pakistan in the analysis of extreme rainfall over the Indian subcontinent in order to capture the influence of the non-monsoonal precipitation pattern on the extreme rainfall events during the monsoon season.

Chapter 3 of this thesis focuses specifically on the transition from the pre-monsoon to the monsoon season - *onset of monsoon*. The onset of monsoon and its propagation over the Indian subcontinent is a spatio-temporal, abrupt transition. Although the main factors governing the onset of monsoon are known, there is a lack of understanding of the mechanism of abrupt monsoon transition and how this transition propagates through the Indian subcontinent, which makes it hard to predict. In this thesis, for the first time, the inter seasonal transition to monsoon is viewed from a dynamical systems perspective. Based on the catastrophe theory, a new mechanism of abrupt monsoon transition will be proposed and the main factors, responsible for "heterogenity" of the monsoon onset over the Indian subcontinent, will be revealed. The proposed mechanism allows not only to deepen the understanding of the variability and spatial propagation of monsoon onset, but also to reveal the indicators of the abrupt transition to monsoon in order to improve the existing forecasting of the monsoon timing, which is discussed in Chapter 4, based on the results obtained in this chapter.

Chapter 4 addresses the question of predictability of the monsoon timing, in particular, long-range forecasting of the monsoon onset and withdrawal dates. Based

on results from Chapter 3, time series analysis of near-surface air temperature and relative humidity at the transition to monsoon and precursor of the critical transition, the tipping elements of monsoon will be identified - as geographic regions of critical behaviour prior to the onset of monsoon. Consideration of the tipping elements of monsoon as coupled reference regions for the analysis of the observational data, reveals the indicator of the monsoon onset and withdrawal. A novel method for prediction of the monsoon timing is proposed, which yields a long-range forecasting scheme for early prediction of the onset and withdrawal dates of the monsoon in a given year in advance. The proposed method is compared to the existing long-range forecasting scheme and its advance in the early forecasting of monsoon timing is show.

The final Chapter 5 presents a summary of the main findings in this thesis, points out the contribution of this thesis to the present knowledge about the Indian Monsoon and gives recommendations for possible future work.

Chapter 2.

Extreme rainfall event synchronisation

This chapter is devoted to the identification of the spatial structures of extreme rainfall over the Indian subcontinent and their seasonal evolution. We employ a complex network approach to determine the topology and evolution of the network of extreme precipitation that governs the organization of extreme rainfall before, during, and after the Indian Summer Monsoon (ISM) season. We construct networks of extreme rainfall events during the ISM (June–September), post-monsoon (October–December), and pre-monsoon (March–May) periods from satellite-derived (Tropical Rainfall Measurement Mission, TRMM) and rain-gauge interpolated (Asian Precipitation Highly Resolved Observational Data Integration Towards the Evaluation of Water Resources, APHRODITE) data sets. The structure of the networks is determined by the level of synchronization of extreme rainfall events between different grid cells throughout the Indian subcontinent. Through the analysis of various complex-network metrics, we describe typical repetitive patterns in North Pakistan (NP), the Eastern Ghats (EG), and the Tibetan Plateau (TP). These patterns appear during the pre-monsoon season, evolve during the ISM, and disappear during the post-monsoon season. These are important meteorological features that need further attention and that may be useful in ISM timing prediction. This chapter is based on the associated publications P1, P2 and P3, and the following sections will closely follow these publications. Supplementary figures for this chapter can be found in appendixes A and B.

2.1. Introduction

Understanding the structure of the spatial heterogeneity of extreme rainfall during the ISM plays a crucial role in the daily life and prosperity of the Indian population. Spatial rainfall distribution and especially the distribution of extreme rainfall events is a significant question for Indian agriculture and economy, as extreme rainfall is a common cause of floods on the Indian subcontinent. It is therefore essential to track the origins and dynamics of the extreme events. In this study, we find such origins in the topology of networks of extreme rainfall events during the ISM, and the periods before and after the monsoon.
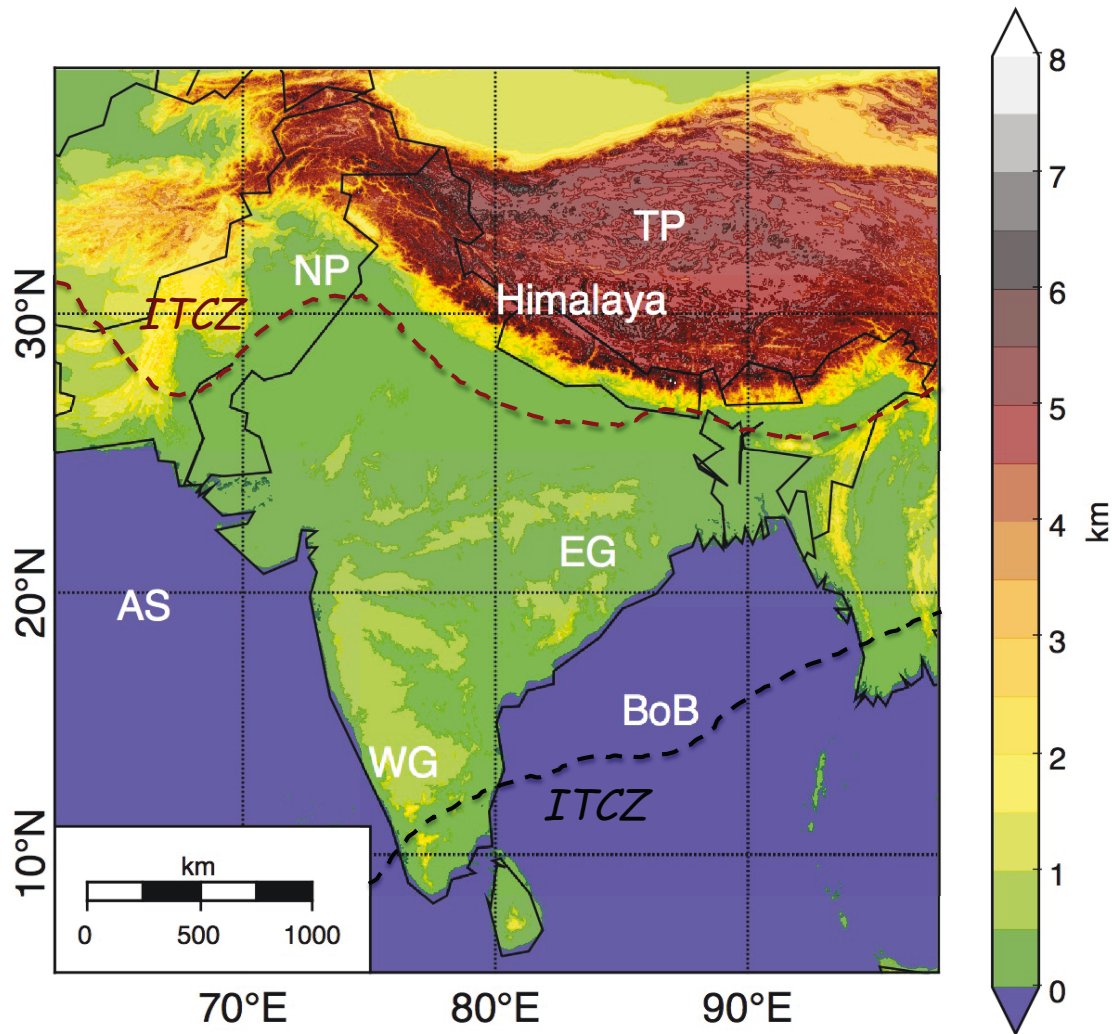
Figure 2.1.: Regional overview of the Indian subcontinent. Major topographic and political features referred to in the text are labeled in white (Himalaya, Tibetan Plateau (TP), North Pakistan (NP), Eastern Ghats (EG), Western Ghats (WG), Arabian Sea (AS), Bay of Bengal (BoB)), and the background image is based on the Shuttle Radar Topography Mission (SRTM30) gridded digital elevation model, which is available at GEBCO (). Intertropical Convergence Zone (ITCZ) shown schematically for monsoon season (red) and post-/pre-monsoon seasons (black).

2.1.1. ISM, pre-monsoon and post-monsoon seasons of the Indian subcontinent

Changes in precipitation over the Indian subcontinent during the year can be divided into three phases: the pre-monsoon season (March–May), the main rainy season (the Indian Summer Monsoon (ISM) season; June–September), and the post-monsoon

season (October–December). During the Indian Summer Monsoon season, the Indian subcontinent receives more than 80 % of its annual rainfall across the region (Bookhagen and Burbank, 2010). During the post-monsoon season, the strongest rainfall covers the southern tip of India and most of Sri Lanka. Pre-monsoon months (March–May) are characterized by light rainfall over the Himalaya, the southwestern part of India, and Myanmar (Burma) (see Fig. 2.1).

The ISM is driven by heating of the high-altitude Tibetan Plateau that leads to a near-surface low-pressure system that attracts moist air from the surrounding oceans, especially the Bay of Bengal (Gadgil, 2003; Webster et al., 1998). On large scales, the ISM is linked to the seasonal heating of land masse and interacts with the westerly jet stream. An important interaction occurs when the Somali jet stream crosses the Arabian Sea, changing the direction of ocean currents, and when colder water wells up from lower ocean layers, causing a decrease in temperature. Additionally, a low-pressure trough where the southern and northern trade winds meet, a border known as the Intertropical Convergence Zone (ITCZ), moves north. As a result, tropical storms, depressions, cyclones, squall lines and daily cycles become more erratic and thus less predictable. On the eastern peninsula, the differential heating between the Bay of Bengal and the surrounding land masses (including the Tibetan Plateau) constitutes the moisture source of monsoonal rain. These combined factors create a low-pressure "monsoon trough" to the south and parallel to the Himalayan mountains. It is this trough's fluctuations that largely influence when monsoonal rains start and stop, generally considered active and break phases (Krishnan et al., 2000; Gadgil, 2003).

October–December is a period during which the southern part of the Indian peninsula and Sri Lanka receive a major amount of their yearly rainfall. This season is also widely known as the Northeast Monsoon (NEM), winter monsoon (Rao, 1999), or post-monsoon season, which we use in this paper (Singh and Ranade, 2010), as it refers to a reversal of wind direction. Although differential heating and the resultant thermal circulation are responsible for both the ISM and post-monsoon seasons, the two monsoon seasons differ substantially in several respects (Wang, 2006). First of all, the heat source region of the post-monsoon season is much closer to the equator (Krishnamurti, 1971), where the effect of the Earth's rotation is diminished. Also, the circulation of the post-monsoon season encompasses a larger meridional domain, such that the tropical region has a strong interaction with the extratropical region. During the post-monsoon season, the ITCZ moves south, and jet streams return to their winter locations. The westerly jet stream splits into two: the northern jet stream runs north of the high-elevation Tibetan plateau and continues eastward above China; the southern jet stream runs to the south of the Himalaya. The area of maximum heating moves south to Indonesia, and low-pressure cyclones migrate into the Pacific Ocean. During the post-monsoon season, rainfall across northwestern India, Pakistan, Bangladesh and Nepal is caused by winter westerlies. Precipitation during the winter months is crucial for agriculture, particularly for the rabi crops.

The pre-monsoon season is usually determined to be the period before the ISM (March–May), and is characterized by changes in the temperature and pressure gradi-

ents, as well as wind direction – from predominantly northwesterly to southwesterly winds. During this season, climatologists try to predict the onset, strength, and internal variability of the developing ISM. In this study, we focus on special features of the ISM and pre-monsoon seasons, including spatial distribution of the extreme precipitation, temperature and pressure, which determine the coming ISM season.

2.1.2. Climate networks as a tool for ISM analysis

Various approaches exist for studying Indian monsoon dynamics, such as numerical modeling using, for instance, Atmospheric General Circulation Models (AGCMs) (Krishna Kumar, 2005; Waliser et al., 2003), statistical analysis of observational or reanalysis data (Revadekar and Preethi, 2012; Rajkumari and Narasimha, 1996), or recurrence analysis to detect regime transitions [associated publication P7, Marwan et al., 2009; Marwan and Schinkel, 2013] or coupling directions with intersystem recurrence networks (Feldhoff et al., 2013).

The application of complex network theory to analyze different climate phenomena is a new but rapidly growing area of research, where a number of studies have been carried out recently (Donges et al., 2009b; Donges et al., 2009a; Malik et al., 2010; Malik et al., 2011; Tsonis and Roebber, 2004; Tsonis et al., 2006; Tsonis et al., 2008; Tsonis et al., 2010; Gozolchiani et al., 2008; Gozolchiani et al., 2011; Yamasaki et al., 2009; Paluš et al., 2011; Barreiro et al., 2011; Deza et al., 2013b; Deza et al., 2013a; Martin et al., 2013; Tirabassi and Masoller, 2013). While most of these studies are focused on global climate networks of temperature fields and precipitation (Donges et al., 2009b; Donges et al., 2009a; Tsonis and Roebber, 2004; Tsonis et al., 2006; Gozolchiani et al., 2011; Yamasaki et al., 2008; Yamasaki et al., 2009; Scarsoglio et al., 2013), others consider smaller, regional networks that focus on a specific climate phenomenon of interest, such as El-Niño (Tsonis and Swanson, 2008; Gozolchiani et al., 2008), Atlantic Meridional Overturning Circulation (Feng et al., 2014), Rossby waves (Wang et al., 2013), continental rainfall in Germany (Rheinwalt et al., 2012), the South American Monsoon System (SAMS) (Boers et al., 2013), and the Indian Summer Monsoon (Malik et al., 2010; Malik et al., 2011; Rehfeld et al., 2012). In the work by Rehfeld et al. (2012) on Indian Summer Monsoon (ISM) dynamics, a paleoclimate network approach has revealed a strong influence of the ISM on the East Asian Summer monsoon during the late Holocene period, but with varying strength according to the warm vs. cold epochs. In Malik et al. (2010) and Malik et al. (2011), it was demonstrated that by combining the climate network approach with the event synchronization method, it is possible to identify regions that receive rainfall only during the most active phase of the Indian Summer Monsoon. Also, identification of the structure and organization, and in particular the spatial discontinuity of the rain field, was shown, and a predictability scheme for the synchronization of extreme rainfall was introduced. These studies were based on data sets covering only the land area and only for the Indian political boundaries. Since the time that these studies were published, new high-quality data sets have become available for larger regions, including rainfall over the ocean, which we employ in this work.

Table 2.1.: Properties of the data sets. APHRODITE: interpolated rain-gauge data (Yatagai et al., 2009). TRMM 3B42V7: satellite-derived data (Huffman et al., 2007). NCEP/NCAR: reanalysis data (Kalnay et al., 1996).

Properties	APHRODITE	TRMM	NCEP/NCAR
Period	Jan 1951–Dec 2007	Jan 1998–Dec 2012	Jan 1949–Dec 2012
Geographical coverage	(62.5–$97.5°$ E, 5–$40°$ N)	(62.375–$97.125°$ E, 5.125–$39.875°$ N)	(62.5–$97.5°$ E, 5–$40°$ N)
Spatial resolution	$0.5° \times 0.5°$	$0.25° \times 0.25°$	$2.5° \times 2.5°$
Temporal resolution	Daily precipitation	3 hourly, resampled to daily precipitation	Daily temperature and pressure anomalies, seasonal mean of winds
Number of grid points	4900	19 600	196

The question of the spatial structure and organization of present-day extreme rainfall during the pre-monsoon and post-monsoon periods, however, remains open. Additionally, the spatial scale and teleconnections of regions that receive extreme rainfall causing floods over the Indian subcontinent and Sri Lanka during the pre-monsoon, monsoon, and post-monsoon seasons have not yet been revealed. In this paper, we aim to explore the seasonal evolution of the synchronization of extreme rainfall events over the Indian subcontinent and Sri Lanka. In order to address this aim, we first construct and analyze climate networks of extreme rainfall during three seasons: pre-monsoon, ISM, and post-monsoon. Second, we reveal the dominant patterns of synchronized extreme rainfall events over the Indian subcontinent, which occur before the monsoon, develop during the monsoon season, and disappear after the monsoon. Third, we compare dominant patterns with wind fields to establish a linkage to atmospheric processes.

2.2. Data

We use observational satellite data from 1998 to 2012 from the Tropical Rainfall Measuring Mission (TRMM 3B42V7) (Huffman et al., 2007; TRMM, 2007), with a spatial resolution of $0.25° \sim 25$ km and a temporal resolution of 3 h aggregated to daily data. We have extracted data for the South Asian region (62.375–$97.125°$ E, 5.125–$39.875°$ N; see Table 2.1 and Fig. 2.1). This data set is the most recent precipitation data product available. It has a high spatial resolution and covers both land and sea. By the time of this study, however, there are only 15 years of data.

To confirm the significance of the results of this study, we analyze reanalysis gridded daily rainfall data for a time period of 57 years (1951–2007) (Asian Precipitation Highly Resolved Observational Data Integration Towards the Evaluation of Water Resources, APHRODITE) (Yatagai et al., 2009). This data set forms a reliable reanalysis product; however, it is given only for the land masses, excluding the ocean. We have extracted the data for the same region (62.5–$97.5°$ E, 5–$40°$ N)
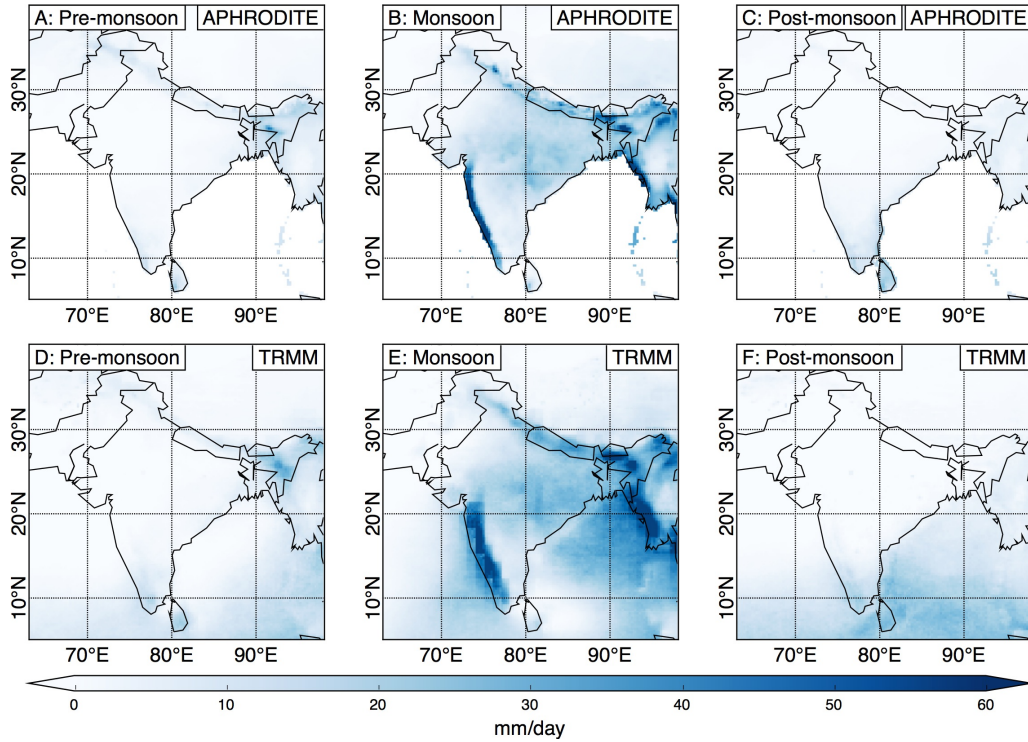
Figure 2.2.: 90-th percentile of daily rainfall amounts for the pre-monsoon (MAM), monsoon (JJAS), and post-monsoon (OND) periods for the APHRODITE (top) and TRMM (bottom) data sets using the same color scale.

with a resolution of $0.5° \sim 56\,\text{km}$ (APHRO-V1003R1) (see Table 2.1). This data set was used previously in Malik et al. (2010) and Malik et al. (2011) to study the spatial variability of the extreme Indian rainfall during the ISM period using the method of Event Synchronization (ES). In this study, we compare results with previous findings for the ISM season and determine geographic patterns of extreme precipitation over the Indian subcontinent during the pre-monsoon, monsoon, and post-monsoon seasons. We compare geographic patterns based on precipitation data sets with patterns of temperature and pressure networks derived from reanalysis gridded daily data provided by the National Center for Environmental Prediction and the National Center for Atmospheric Research (NCEP/NCAR) (Kalnay et al., 1996; NCEP/NCAR, 2015). In addition, we compare our results with wind fields using reanalysis gridded seasonal mean wind data, also provided by NCEP/NCAR (Kalnay et al., 1996; NCEP/NCAR, 2015). The spatial resolution of the data is 2.5°. The data are extracted for (roughly) the same region as for the APHRODITE data (see Table 2.1), and contain both land and ocean points in the considered region.

Network construction

Step 1. Apply a threshold to time series of each grid point (*i* and *j*) to obtain extreme event series
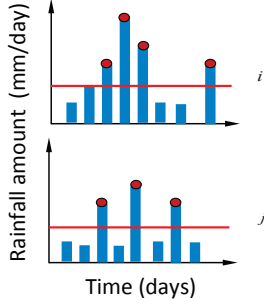
Step 2. Event synchronization – use time lags to compare individual events between two grid points

Step 3. Construct the network by creating links between points with the highest synchronization values

$$A_{ij} = \begin{cases} 1, & if \quad Q_{ij} > \theta_{ij}^{Q} \\ 0, & else. \end{cases}$$

Q_{ij} – is a correlation matrix

θ_{ij}^{Q} – is a threshold

A_{ij} – is an adjacency matrix
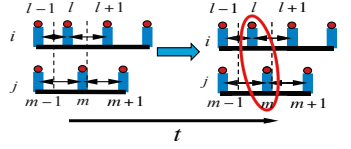
Time lag between grid points *i* and *j* :

$$\tau_{lm}^{ij} = \min\left\{ t_{l+1}^{i} - t_{l}^{i}, t_{l}^{i} - t_{l-1}^{i}, t_{m+1}^{j} - t_{m}^{j}, t_{m}^{j} - t_{m-1}^{j} \right\}/2,$$

$$J_{ij} = \begin{cases} 1, & if \quad 0 < t_{l}^{i} - t_{m}^{j} < \tau_{lm}^{ij}, \\ 1/2, & if \quad t_{l}^{i} = t_{m}^{j}, \\ 0, & else. \end{cases} \qquad c(i|j) = \sum_{l=1}^{s_i} \sum_{m=1}^{s_j} J_{ij},$$

$$Q_{ij} = \frac{c(i|j) - c(j|i)}{\sqrt{(s_i - 2) \cdot (s_j - 2)}},$$

local extremes
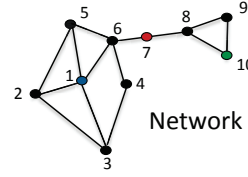
Network

Figure 2.3.: Schematic illustration of the network construction using event synchronization (ES) method. i and j are grid cites between which the sychronicity of extreme rainfall events is calculated, l and m – events that are compared, τ_{lm}^{ij} – a minimum time lag between the chosen pair of grid sites. Node 1 in the network has high degree (4), node 7 has small degree (2), but high betweenness, as all shortest paths from nodes $1, 2, 3, 4, 5, 6$ to nodes $8, 9, 10$ go through the node 7. For definition of network measures see Table 2.3.

2.3. Methods

We consider separately time series of rainfall events, temperature and pressure fields for three time periods: (i) pre-monsoon, (ii) ISM, and (iii) post-monsoon. The pre-monsoon period (**M**arch, **A**pril, **M**ay – MAM) is defined as the period from 1 March to 31 May for each year, and consists of 92 days per year. This number multiplied by the number of years in the data set gives the length of the time series for each node in the MAM period. The monsoon period (JJAS) is defined as the period from 1 June to 30 September for each year, and consists of 122 days per year. The post-monsoon period (OND) is defined as the period from 1 October to 31 December for each year, and consists of 92 days per year. The time series at each node for the JJAS and OND periods are computed in the same manner as for the MAM period.

Event Synchronization (ES)

Considering rainfall time series, it is important to choose an appropriate method to infer similarity of dynamics between different geographical sites. Rainfall time series are not as smooth and continuous as those for temperature or pressure fields, but

often contain a high-frequency component. In this study, we use ES as a method for climate network construction from precipitation data, as proposed in Malik et al. (2010). This method has advantages over other time-delayed correlation techniques (e.g., Pearson lag correlation), specifically for studying precipitation data, as it allows us to define extreme event series of rainfall, depending on the kind of extreme, and uses a dynamic time delay. The latter refers to a time delay that is adjusted according to the two time series being compared, which allows for better adaptability to the region of interest. Another advantage of this method is that it can also be applied to a non-Gaussian and event-like data sets.

We begin by extracting an event series, which is merely a time series that includes only the highest daily rainfall amounts, which we call "extreme events". In the realm of hydrology and climate sciences, extreme rainfall events are days that receive rainfall amounts that exceed the 90th percentile for all days in the time series at a given grid point (see Fig. 2.2). This threshold thus gives a unique amount of rainfall per day for each grid site. Only the daily rainfall events that are above this threshold for a given site are considered to be extreme rainfall events, and are what make up an event series.

To determine the synchronization between two grid points, let us consider two grid sites, i and j. An event l that occurs at a grid site i at time t_l^i is considered to be synchronized with an event m that occurs at a grid site j at time t_m^j within a time lag $\pm\tau_{lm}^{ij}$ if $0 < t_l^i - t_m^j < \tau_{lm}^{ij}$, where $\tau_{lm}^{ij} = \min\{t_{l+1}^i - t_l^i,\ t_l^i - t_{l-1}^i,\ t_{m+1}^j - t_m^j,\ t_m^j - t_{m-1}^j\}/2$. Here, $l = 1, 2, \ldots, s_i$, $m = 1, 2, \ldots, s_j$, where s_i and s_j are the number of events at the ith and jth grid sites. Then, for each grid site, we count the number of times when an event occurs at j after i: $c(i|j) = \sum\limits_{l=1}^{s_i} \sum\limits_{m=1}^{s_j} J_{ij}$, and vice versa: $c(j|i)$. Here, J_{ij} is an event that happens at place j after place i within the time lag $\pm\tau_{lm}^{ij}$:

$$
J_{ij} = \begin{cases} 1, & \text{if } 0 < t_l^i - t_m^j \leq \tau_{lm}^{ij}, \\ 1/2, & \text{if } t_l^i = t_m^j, \\ 0, & \text{else.} \end{cases} \tag{2.1}
$$

We then define *the strength of synchronization*

$$
Q_{ij} = \frac{c(i|j) + c(j|i)}{\sqrt{(s_i - 2)(s_j - 2)}} \tag{2.2}
$$

between events at different grid sites i and j, and normalize it to be $0 \leq Q_{ij} \leq 1$. Here, $Q_{ij} = 1$ means complete synchronization, and $Q_{ij} = 0$ is the absence of synchronization. After repeating this procedure for all pairs $(i \neq j)$ of grid sites, we obtain a correlation matrix. In this case, the correlation matrix for precipitation data is a square, symmetric matrix, which represents the strength of synchronization of the extreme rainfall events between each pair of grid sites. Visualization of the network construction is shown in Figure 2.3.

Table 2.2.: Details of network construction and thresholding. Extreme rainfall event networks: the average number of events per grid point during the considered period (MAM, JJAS, or OND), the mean number of synchronized events, and the maximal number of synchronized events. Temperature and pressure networks: thresholds of the Pearson correlation for the MAM, JJAS, and OND periods.

Data	MAM	JJAS	OND
TRMM			
Avg. number of events	126	175	120
Avg. number of synchronized events	21	34	24
Max. number of synchronized events	114	162	111
APHRODITE			
Avg. number of events	517	693	517
Avg. number of synchronized events	104	132	107
Max. number of synchronized events	489	655	486
NCEP/NCAR: thresholds			
Temperature	0.19	0.15	0.21
Pressure	0.5	0.5	0.5

Pearson correlation

In order to compare spatial patterns of extreme rainfall with spatial patterns of temperature and pressure fields, we also construct networks for these fields using NCEP/NCAR data. First, we remove the seasonal cycle by subtracting the long-term daily mean from the daily gridded temperature (pressure) data. We then use a zero-lag Pearson correlation coefficient as a measure of similarity between the nodes, as, for example, in Donges et al. (2009b).

Network construction

Applying a certain threshold or link density, we yield an adjacency matrix

$$A_{ij} = \begin{cases} 1, & \text{if } Q_{ij} \geq \theta_{ij}^{Q}, \\ 0, & \text{else.} \end{cases} \tag{2.3}$$

Here, θ_{ij}^{Q} is a chosen threshold (see Sect. 2.3), and $A_{ij} = 1$ denotes a link between the ith and jth sites, and 0 denotes otherwise. The adjacency matrix represents a climate network, and complex network theory can subsequently be employed to reveal properties of the given network (see Table 2.3).

In this study, we use an undirected network; i.e., we do not consider which of the two synchronized events happened first, to avoid the possibility of misleading directionalities of event occurrences at grid sites that are topographically close.

Table 2.3.: Network measures. N – total number of nodes, D_j – degree of a node j, B_v – betweenness of a node v, L_{ij} – geographical link length between nodes i and j, ALL$_i$ – average geographical link length of a node i, MLL$_i$ – maximal geographical link length of a node i, $\sigma_v(i,j)$ – the number of shortest paths between nodes i and j passing through node v, $\sigma(i,j)$ – total number of shortest paths between i and j, α_{ij} – angular geographical distance, R – radius of the Earth, 6371.009 km.

Degree, D_i	Betweenness, B_v	Average geographical link length, ALL$_i$	Maximal geographical link length, MLL$_i$
$D_i = \dfrac{\sum_{n=1}^{N} A_{ij}}{N-1}$	$B_v = \sum\limits_{i \neq j \neq v \in \{V\}}^{N} \dfrac{\sigma_v(i,j)}{\sigma(i,j)}$	$\mathrm{ALL}_i = <L_{ij}>_j =$ $= <\alpha_{ij}\, A_{ij}\, R>_j$	$\mathrm{MLL}_i = \max(L_{ij})_j =$ $= \max(\alpha_{ij}\, A_{ij}\, R)_j$

Thresholding

To include only statistically significant correlations, we choose the 5 % strongest correlations and construct climate networks. We use 5 % as our threshold, since it satisfies both necessary conditions: a high correlation and a sufficient number of extreme events for comparison. Details of network construction and thresholding are given in Table 2.2.

For temperature networks, the thresholds of the Pearson correlation coefficient are 0.19, 0.15, and 0.21 for the pre-monsoon, monsoon and post-monsoon seasons, respectively, and for pressure networks, 0.5 – for all three seasons. It is important to note that pressure correlations over the Indian subcontinent are much higher than temperature correlations (see Table 2.2). The longer time period of the APHRODITE data set allows us to infer statistically significant correlations of the extreme rainfall synchronization in the long term, and similarities between the APHRODITE and TRMM data sets show the permanent pattern of the extreme rainfall synchronization

In this study, we use gridded data sets to construct networks of extreme precipitation, temperature and pressure fields. It is important to note, however, that climate networks derived from gridded data sets are affected by the spatial sampling of these data. Specifically, spatial sampling has an effect on network measures. This important issue is discussed in associated publication P2 and in the Appendix A of this thesis, where the effect of spatial sampling on the network measures is illustrated on the ISM climate network derived from NCEP/NCAR daily temperature anomalies using the method discussed in Sect. 2.3. This study has shown that spatial sampling of gridded NCEP/NCAR data does not qualitatively change network measures for the Indian region.

Network measures

In this study, we compare networks of the pre-monsoon, monsoon and post-monsoon periods using four network measures: degree, betweenness, average link length and

maximal link length. Analytical definitions of the network measures are presented in Table 2.3.

The *degree* of a node (i.e., the geographical site) i in the network gives the number of links connected to node i.

The shortest path between two nodes is the way to go from one node in the network to another using a minimal number of links. For given nodes i and j in the network, $\sigma(i,j)$ shortest paths exist. If a large fraction of the shortest paths from a node i to a node j pass through a certain node v, $v \neq i, j$, then node v is an important mediator for transport through the network, and we would consider this node to have a high *betweenness*. In this study, extreme rainfall event transport is related to the propagation of the extreme rainfall over the subcontinent. *Note*: the interpretation of betweenness in this study is that it indicates the extreme event pathways through the network of extreme rainfall. As a result, patterns with high betweenness can play a crucial role in understanding the mechanism of extreme event transport over the Indian subcontinent (see Sect. 2.4).

The *average geographical link length ALL_i (maximal geographical link length MLL_i)* of a node i is the average (maximum) geographical distance of that node's links.

2.4. Seasonal evolution of spatial patterns of extreme rainfall

First, we determine general features that correspond to the chosen time period, the so-called "dominant" patterns of the entire time period, by comparing climate networks for the pre-monsoon, ISM and post-monsoon periods using the TRMM data. Second, we present a visualization of the links of the dominant patterns of ISM during the three seasons, and analyze the seasonal evolution of these patterns. In order to understand which atmospheric processes cause synchronization of extreme rainfall events, we compare the visualization of links of these patterns with wind fields. Third, we compare the results of the network analysis for the APHRODITE and TRMM data sets. Finally, we build networks from the temperature and pressure fields over the Indian peninsula for three seasons, and compare the structure of these networks with dominant patterns of the ISM extreme rainfall.

2.4.1. TRMM

Network measures

Figure 2.4 shows the degree, betweenness and the average geographical link length of the networks for the TRMM data (see Tables 2.1 and 2.3).

- *Degree*: during the pre-monsoon period, there are five regions with a high degree: (i) Western Ghats (WG) and the Arabian Sea, (ii) North Pakistan (NP), (iii) the Himalaya, (iv) Eastern Ghats (EG) and the Bay of Bengal, and (v) the Tibetan Plateau (TP). The regions (i) and (iii) have an especially high

Figure 2.4.: Common network measurements for the three time periods based on the TRMM data: pre-monsoon (MAM), monsoon (JJAS), and post-monsoon (OND). From top to bottom: degree, betweenness, average geographical link lengths.

degree during the pre-monsoon season. During the monsoon season, the highest degree is in NP, EG and TP, while during the post-monsoon season, it is in the Himalaya, TP and NP.

- *Betweenness*: high betweenness is observed for the pre-monsoon, monsoon and post-monsoon seasons for the same regions, as specified above with a high degree.

- *Average and maximal geographical link lengths*: comparatively long links can be found in the Arabian Sea and the Bay of Bengal during the pre-monsoon period; in NP, TP, EG and the Himalaya during the monsoon season; and in TP and the Himalaya during the post-monsoon period.
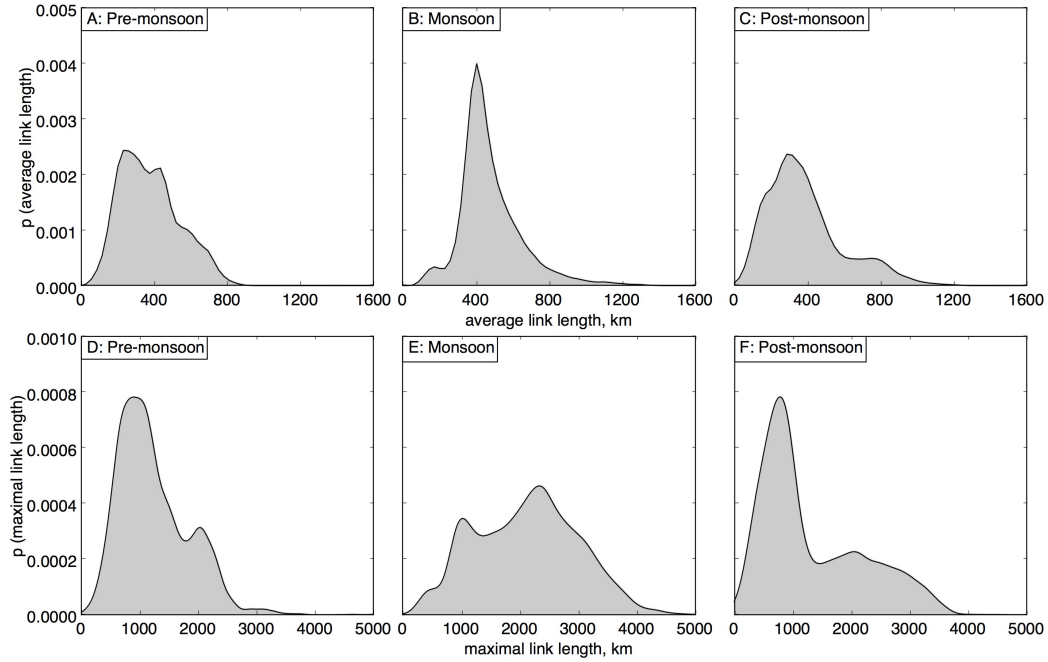
Figure 2.5.: Average and maximal link length distributions for the three time periods based on the TRMM data: pre-monsoon (MAM), monsoon (JJAS), and post-monsoon (OND).

Examining the distributions of the link lengths of the TRMM data yields some interesting behavior (see Fig. 2.5). There are two peaks in the distributions of the average link length of the pre- and post-monsoon seasons, at about $250\,\mathrm{km}/450\,\mathrm{km}$ and $300\,\mathrm{km}/800\,\mathrm{km}$, respectively, while the monsoon season has a pronounced single peak, at around $450\,\mathrm{km}$. More specifically, the maximum of the average link length distribution shifts from $250\,\mathrm{km}$ up to $450\,\mathrm{km}$ and back down to $300\,\mathrm{km}$ between the three seasons. We also calculate the average link length over the whole region, and find a distance of $484\,\mathrm{km}$ for the monsoon season, compared to the shorter 382 and $390\,\mathrm{km}$ for the periods before and after the monsoon, exemplifying a trend toward longer links during the monsoon period. It is also worth noting the long tail of the monsoon season distribution, when compared with those of the pre- and post-monsoon seasons. The maximal link length distributions are also shown in Fig. 4, and are bimodal in all three seasons.

Employing the network measures outlined above, we look into the role of hubs (super nodes) in the organization of the spatial structure of the pre-monsoon, monsoon, and post-monsoon periods. We define the hubs of a network as the $10\,\%$ of grid points with the highest degree, betweenness, and average link length. We infer seven main patterns that have either a high degree, betweenness, or average link length during at least one of the three time periods (see Table 2.4). Three of these patterns are believed to be dominant during the ISM. First, the NP region shows a high degree,

Table 2.4.: Hubs of the extreme rainfall networks. Columns are hubs in degree, betweenness, and average link length. "+" – the network measure in the given region is in the top 10 % for the given period. "−" – lower than the top 10 %. The order of "+" or "−" means the season: pre-monsoon, monsoon, and post-monsoon, respectively. For example, the intersection of first row and first column (North Pakistan (NP) and degree) – "$+/+/+$" – means that one can observe a high degree in NP during the pre-monsoon, monsoon, and post-monsoon seasons, respectively.

Geographical location of pattern	Degree, D_i	Betweenness, B_v	Average geographical link length, ALL_i
North Pakistan, NP	$+/+/+$	$-/+/-$	$-/+/-$
Tibetan Plateau, TP	$+/+/+$	$-/-/-$	$-/+/+$
Eastern Ghats, EG	$+/+/+$	$-/+/-$	$-/+/-$
Himalaya	$+/-/+$	$+/-/+$	$-/+/+$
Western Ghats, WG	$+/-/-$	$+/-/-$	$+/-/-$
Arabian Sea, AS	$+/-/-$	$+/-/-$	$+/-/-$
Bay of Bengal, BoB	$+/-/-$	$+/-/-$	$+/-/-$

betweenness, and average link length during the monsoon season, indicating a large number of long connections in this region during this time. The high betweenness of the NP region shows its importance in the synchronization of extreme rainfall events over the Indian subcontinent specifically during the monsoon period . The EG and TP regions also have a large number of long connections during the monsoon season, with TP showing a similarly large number in the post-monsoon season as well. These regions, therefore, play an important role in the organization of the structure of extreme rainfall event synchronization, primarily during the monsoon season. Using a similar analysis for the other time periods, we uncover the main patterns in the networks of extreme rainfall event synchronization for each season: (i) pre-monsoon season: WG, the Himalaya – over the land, and the Arabian Sea and the Bay of Bengal; (ii) monsoon: NP, EG and TP; (iii) post-monsoon: the Himalaya and TP.

We find three dominant patterns for the ISM season: NP, EG and TP. These patterns are characterized by a high degree, high betweenness (except for TP), and the longest average geographical link lengths during this season. They are specific signatures of the ISM, which start to form in the pre-monsoon season, and disappear during the post-monsoon season. Therefore, these regions deserve special attention for understanding the spatial structures of the synchronization of extreme rainfall events during the monsoon season, and we highlight them in the analysis that follows. In the next section, we focus on the links of the dominant patterns of ISM, and compare their changes during the three seasons.

Link visualization

In the previous section, dominant patterns for the ISM were described: NP, TP and EG. This section focuses on the seasonal evolution of these patterns and their connections with other areas on the Indian subcontinent. From each of these patterns,

we choose 153 nodes, and extract and integrate all links that belong to these patterns. This so-called "link visualization" is shown in Fig. 2.6.
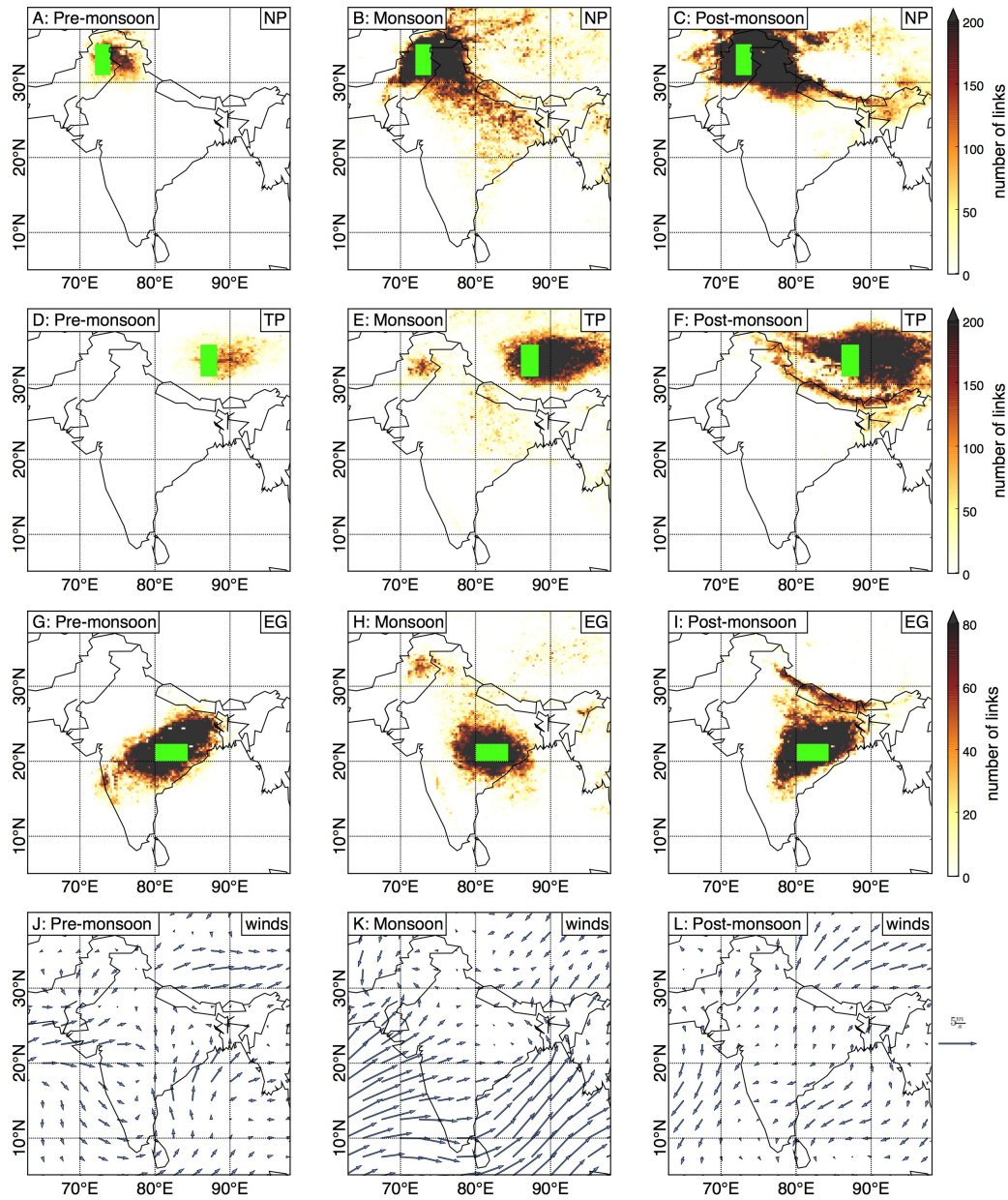
Figure 2.6.: Links between a set of 153 reference grid points and other grid points, and the surface wind vector mean between 1998 and 2012. From top to bottom: North Pakistan (NP), Tibetan Plateau (TP), Eastern Ghats (EG) (TRMM) and the surface wind vector mean (NCEP/NCAR).

Links stemming from the NP pattern show local synchronization of extreme rainfall

events during the pre-monsoon season. This phenomenon is not surprising, given the mountainous terrain of the region. During the ISM, however, long-range connections appear; extreme rainfall events in the NP region synchronize with events in TP, the Himalaya, EG and Burma (Fig. 2.6). These clusters are of great interest for further research, as they appear only during the ISM season, and are possibly linked to monsoonal trends in wind strength (see Sect. 2.4.3). The post-monsoon season sees a decrease in the number of connections to points in the NP region, but maintains connections to TP and the Himalaya.

The TP pattern also shows local synchronization of extreme rainfall events during the pre-monsoon season. Once again, this coincides with the topography of the region that prevents rainfall from synchronizing with other regions. However, the TP has many links to both the NP and EG regions during the ISM. These connections are long range and, possibly, caused by large-scale atmospheric processes such as ISM winds and Western Disturbances (Madhura et al., 2015). During the post-monsoon season, the connections are more locally clustered within the TP, and there are also a lot of connections between TP and the Himalaya.

The EG pattern shows the most intricate behavior of extreme rainfall event synchronization: the shape of the pattern varies noticeably from season to season. During the pre-monsoon season, extreme rainfall events are synchronized within the EG region, and with the WG region and the Arabian Sea. During the ISM, there are three main clusters of synchronized extreme rainfall that are connected to the EG region: NP, TP and WG. During the post-monsoon season, the synchronization resembles that of the pre-monsoon season (see Fig. 2.6), with additional connections to the Himalaya. This feature has a climatological interpretation, since the Himalaya receive heavy rainfall during the post-monsoon season.

2.4.2. Data set intercomparison: TRMM vs. APHRODITE

Network measures

In this section, we compare 15-year satellite-derived TRMM data with 57-year reanalysis APHRODITE data using networks of extreme rainfall (see Table 2.1). The reason for comparison of these two data sets is discussed in Sect. 4.2.2. Figure 2.7 shows the degree, betweenness and the average geographical length of the networks for the APHRODITE data (see Tables 2.1 and 2.3). We find that geographic patterns of networks derived from the APHRODITE data show strong differences in comparison to the TRMM data.

- *Degree*: during the pre-monsoon season, areas in WG and Burma have a low degree according to the APHRODITE data set, and a high degree for the TRMM data set. The EG region, marked by a high degree for TRMM during the monsoon season, shows a low degree for APHRODITE. The post-monsoon season also has some discrepancy, with low and high degree in the NP pattern for the APHRODITE and TRMM data sets, respectively. There are, however, some similarities as well, such as the existence of hubs in NP, TP and the

Himalaya for pre-monsoon, NP and TP for monsoon, and the Himalaya for post-monsoon.
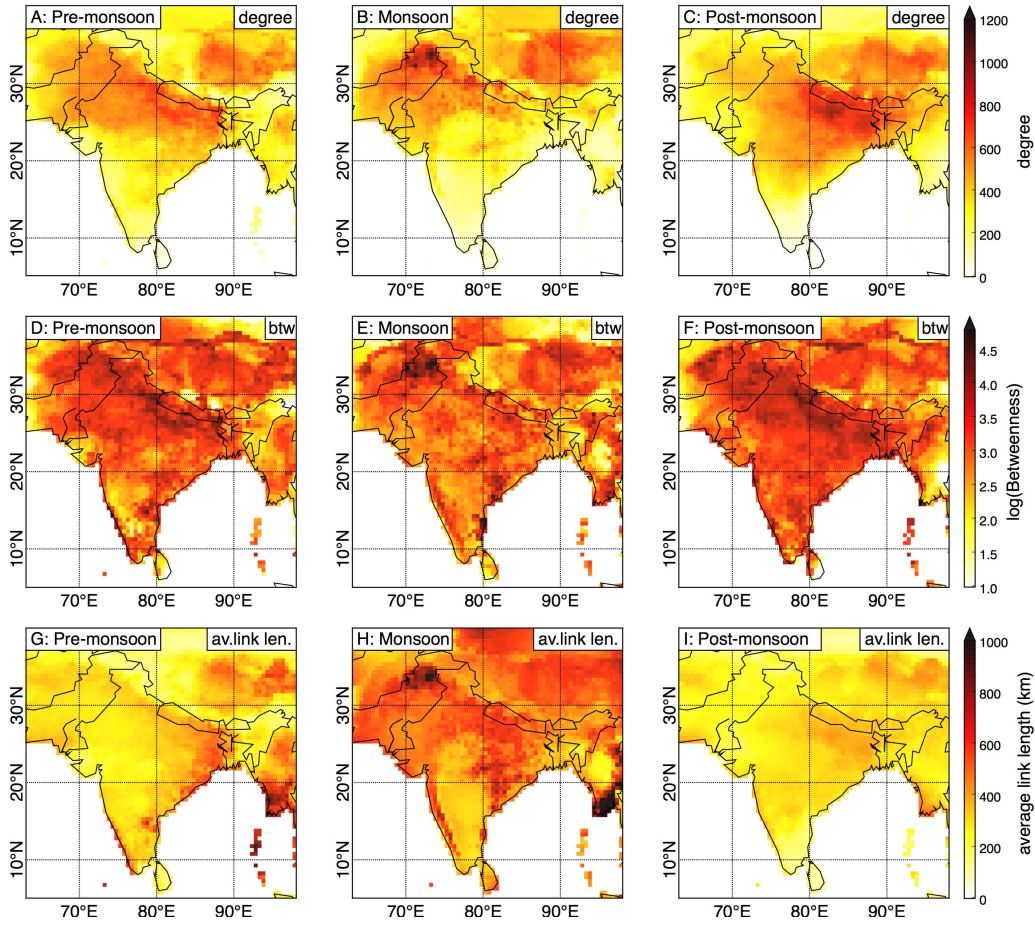
Figure 2.7.: Common network measurements for the three time periods based on the APHRODITE data: pre-monsoon (MAM), monsoon (JJAS), and post-monsoon (OND). From top to bottom: degree, betweenness, average geographical link lengths.

- *Betweenness*: the betweenness hub for APHRODITE during the pre-monsoon period is in the Himalaya. This corresponds to the highest rainfall over the Himalaya during the pre-monsoon season and the beginning of the monsoon formation over WG, EG and Burma (see Fig. 2.2). During the ISM, TRMM finds that the areas with high betweenness are in NP and EG, while in the post-monsoon season, the high betweenness shifts to the Himalaya and WG. In all three seasons, the TRMM data set agrees with the APHRODITE data set as far as identifying areas of high betweenness goes (see Figs. 2.4 and 2.7). The lack of APHRODITE data over the ocean does not affect the betweenness of the network, besides coastal areas.

- *Average geographical link length*: the longest links during the pre-monsoon season for the TRMM data can be found in the Arabian Sea and the Bay of Bengal, but in TP and EG for the APHRODITE data. During the ISM, the APHRODITE data show new patterns that appear in NP and Burma, while the pattern in WG disappears. The post-monsoon season sees a shift in the longest link lengths, and reveals three main patterns: the eastern Himalaya, TP and Burma, the first two of which coincide with the TRMM data.

It is important to note that similarities in the spatial patterns obtained from 0.25° resolution TRMM data with patterns obtained from 0.5° resolution APHRODITE data allow us to conclude that the obtained patterns are reliable, and do not depend on the resolution of the data.

Link visualization

In this section, we compare the seasonal evolution of the connections of patterns for the APHRODITE and TRMM data sets. Similarly to Sect. 2.4.1, we choose 45 points from the APHRODITE data set and obtain Fig. 2.8, which is an analog to Fig. 2.6 for the TRMM data.

Connections to the NP region do not qualitatively change from season to season for APHRODITE, unlike for TRMM. The NP pattern from the APHRODITE data set has a larger region of synchronized rainfall during all three seasons (see Figs. 2.6 and 2.8). The pre-monsoon season shows many links between NP and the eastern Himalaya for APHRODITE, but not for TRMM. During the monsoon season, there are no long-range connections to TP in APHRODITE, as there are in TRMM. For the post-monsoon season, the connections are clustered locally, unlike the TRMM pattern, which also includes links to the Himalaya.

The TP region in APHRODITE shows a different spatial distribution of links than in the TRMM data (see Figs. 2.6 and 2.8). The APHRODITE TP region does not show strong seasonal changes in the connections. The pre-monsoon season reveals connections to the eastern Himalaya, and the ISM shows no synchronization of extreme rainfall with NP, both of which are contrary to the TRMM data. Moreover, during the post-monsoon period, the APHRODITE data set displays a wider range of connections than the TRMM data do.

The EG pattern from the APHRODITE data also differs from the pattern obtained from the TRMM data. In the pre-monsoon season, connections extend to the Himalaya for APHRODITE, but not for TRMM. The ISM season uncovers two main clusters - NP and Burma - where extreme rainfall is synchronized with the EG region, while the TRMM data set has additional links to WG and TP. Also, there is no synchronization of extreme rainfall events in the area between the NP and EG regions from both the APHRODITE and TRMM data. During the post-monsoon season, events are synchronized locally, and not with the Himalaya, unlike the pattern derived from TRMM (see Figs. 2.6 and 2.8).
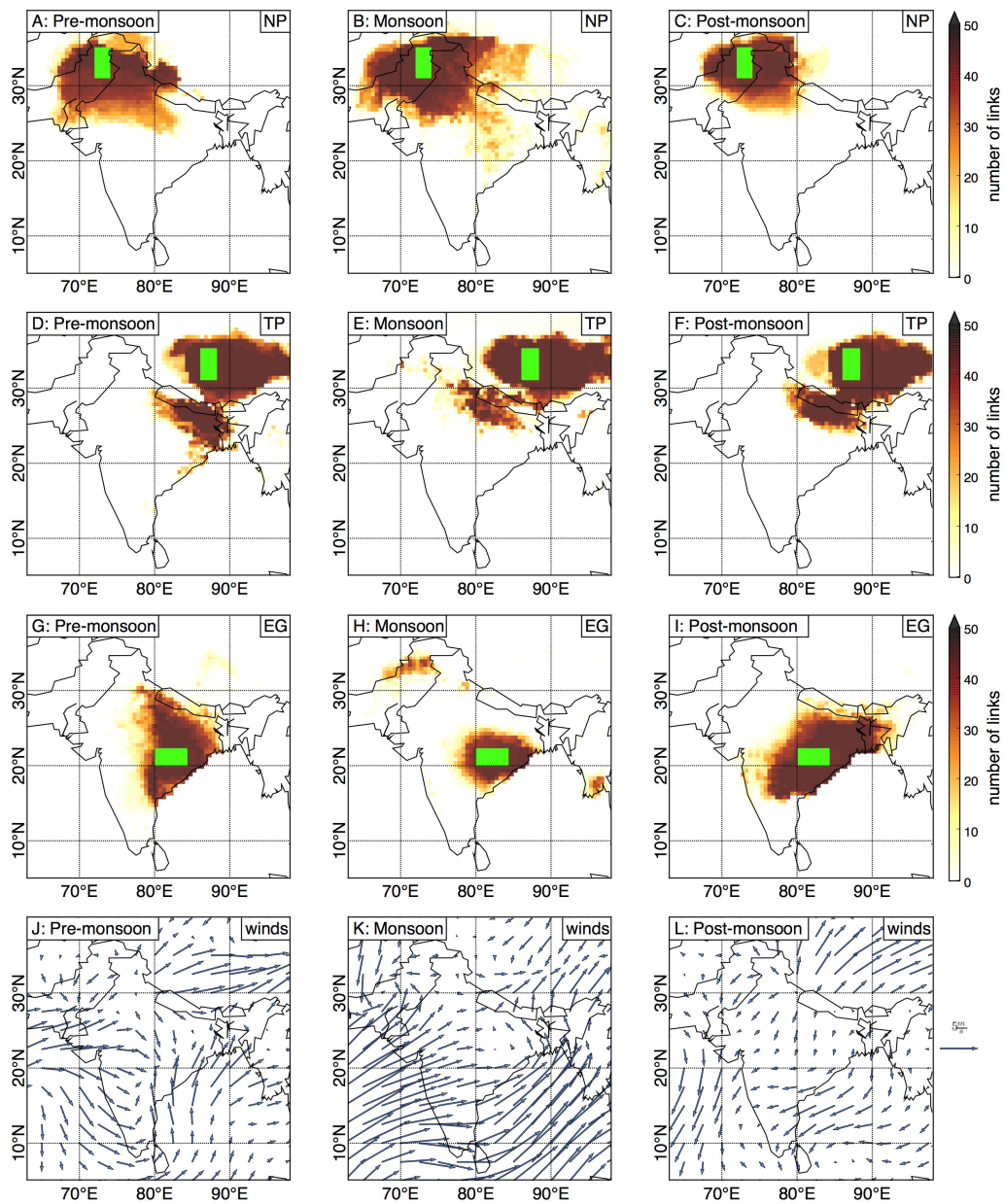
Figure 2.8.: Links between a set of 45 reference grid points and other grid points and the surface wind vector mean between 1951 and 2007. From top to bottom: North Pakistan (NP), Tibetan Plateau (TP), Eastern Ghats (EG) and the surface wind vector mean (NCEP/NCAR data).

2.4.3. Comparison of network structures of TRMM and APHRODITE with surface vector mean wind fields

Here, we compare the mean surface wind fields for the three time periods – pre-monsoon, ISM and post-monsoon – with the patterns obtained previously from the network analysis (see Sects. 2.4.1 and 2.4.2, Figs. 2.6 and 2.8).

The directionality of the winds over the Indian subcontinent partially explains the synchronization of extreme rainfall events within the patterns in NP and TP during the pre- and post-monsoon periods. These patterns follow the topography that prevents the rainfall from synchronizing with other locations across the subcontinent: NP is a low-elevation area, bounded by mountains in the northwest, north and northeast directions; TP is a high-elevation plateau, bounded by the Himalaya in the southwest. The TRMM data show a strong resemblance to the changing winds across the three seasons (see Fig. 2.6), while the APHRODITE data show no significant changes (see Fig. 2.8).

The shape of the APHRODITE EG region during the pre- and post-monsoon seasons, however, matches the wind direction, whereas the TRMM data in the same region cannot be explained fully from the wind field. During the pre-monsoon season, the APHRODITE data set shows a spread from south to north, following the winds. The post-monsoon pattern also corresponds to the wind direction: from northeast to southwest. The noteworthy observation is that during the pre-monsoon season, the spatial pattern in NP coincides with the divergence of the surface vector mean winds, while the EG spatial pattern coincides with the convergence of surface vector mean winds for both the APHRODITE and TRMM data. During the monsoon season, surface vector mean winds change dramatically, and the NP spatial pattern coincides with wind convergence, while during the post-monsoon season, the NP spatial pattern coincides with wind divergence.

The ISM season shows a difference between rainfall event synchronization and wind fields, in both data sets. As mentioned above, there are connections between NP and EG, but not in the area between these two regions. This seems to indicate that winds are not the cause of this synchronization. However, this phenomenon may be caused by the topography of these regions and the influence of two branches of the ISM: the Bay of Bengal branch that transports moisture and interacts with the wind systems from the Arabian Sea branch.

2.4.4. Comparison of patterns of extreme precipitation with patterns obtained from temperature and pressure fields

In this section, we analyze the seasonal evolution of climate networks over the Indian subcontinent. We compare networks of extreme rainfall (analyzed in previous sections) with networks of temperature and pressure fields (see Figs. 2.9 and 2.10).

- *Temperature network: degree*: a temperature network obtained from the NCEP/NCAR data (see Sect. 2.1, Table 2.1) for the pre-monsoon season exhibits degree hubs in NP/Afghanistan, TP and the southern part of the
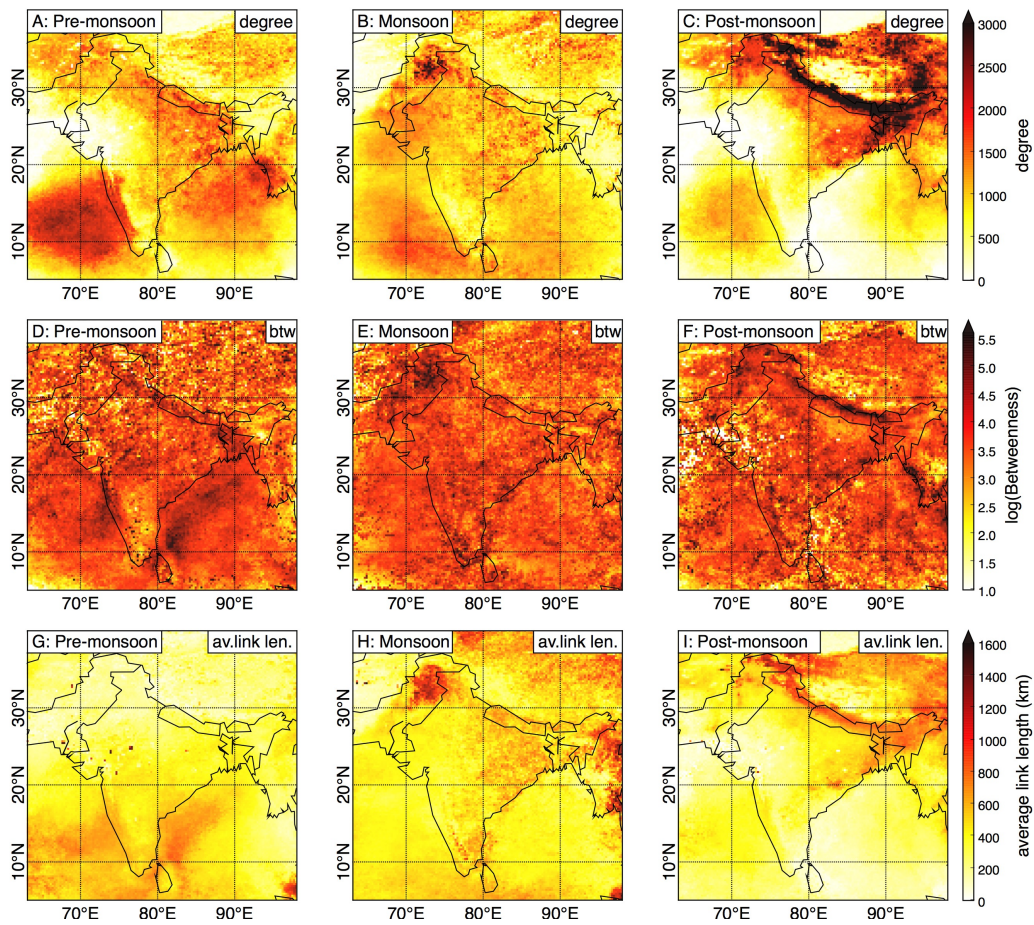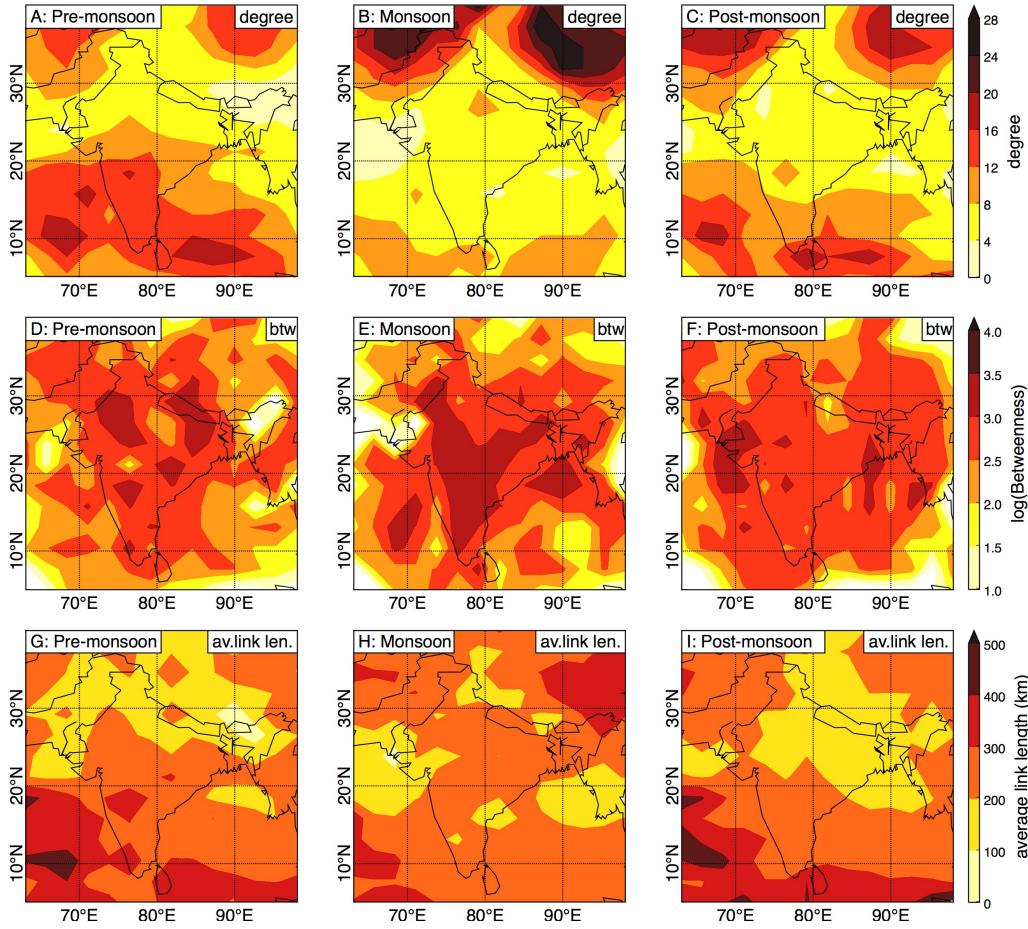
Figure 2.9.: Common network measurements for the three time periods based on the NCEP/NCAR data for the pre-monsoon (MAM), monsoon (JJAS), and post-monsoon (OND) temperature networks. From top to bottom: degree, betweenness, average geographical link lengths.

Indian peninsula, including Sri Lanka (see Fig. 2.9). During the ISM season, only two of the previously identified patterns appear – NP/Afghanistan and TP. The post-monsoon season has the same hubs as during the pre-monsoon season.

- *Temperature network: betweenness*: betweenness hubs of the temperature networks do not show a distinctive structure. They appear to be located in central India, and do not change qualitatively throughout the three seasons.

- *Temperature network: average link length*: during the pre-monsoon period, average link length hubs appear in the southern parts of the Indian peninsula, the Bay of Bengal and the Arabian Sea. The ISM hubs appear in NP/Afghanistan,
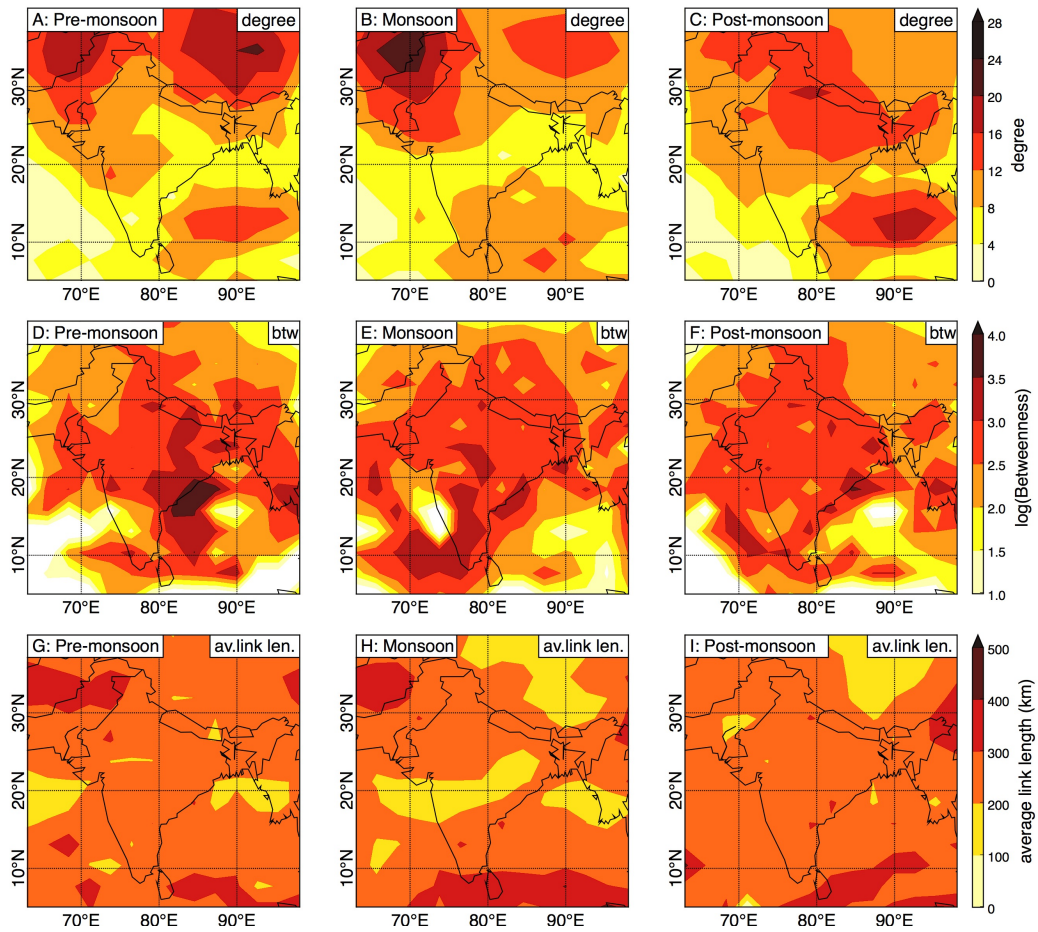
Figure 2.10.: Network measurements for the three time periods: pre-monsoon (MAM), monsoon (JJAS), and post-monsoon (OND) pressure networks. From top to bottom: degree, betweenness, average geographical link lengths (NCEP/NCAR data).

TP, and in the southern Arabian Sea. As with degree, the post-monsoon season hubs match those of the pre-monsoon season.

- *Temperature network vs. extreme rainfall network*: during the pre-monsoon season, coincidence of the degree and the average link length hub of the temperature network with the WG and Arabian Sea hub of the extreme rainfall network (high degree, betweenness and the average link length) emphasizes the role of the Arabian Sea in controlling extreme rainfall over the western coast of the Indian subcontinent. During the ISM, the NP and TP hubs of the temperature network coincide with hubs of the extreme rainfall network, and the long average link length of the TP in the temperature network points out the importance of the TP in the distribution of the temperature gradient over the Indian subcontinent, which creates a pressure gradient and affects

the distribution of the extreme rainfall through wind systems. During the post-monsoon season, the effect of the NP and TP hubs on the temperature and extreme rainfall synchronization networks weakens. While temperature changes during the post-monsoon season are governed mostly by the surface air temperature of the Arabian Sea and the Bay of Bengal (see Fig. 2.9), extreme rainfall synchronization during this season is controlled by TP and the Himalaya (see Figs. 2.4 and 2.6). The important issue of annual and decadal evolution of the temperature networks over the Indian subcontinent is discussed in the associated publication P3 and in the Appendix B of this thesis.

- *Pressure network: degree*: the pressure network constructed based on data from NCEP/NCAR shows pre-monsoon degree hubs in the regions of NP, Afghanistan, TP, the Bay of Bengal and Sri Lanka (see Fig. 2.10). These hubs maintain their locations during the ISM season and, additionally, the Bay of Bengal hub extends across the southern tip of India. During the post-monsoon season, the hubs combine to form one large hub over the central and northern parts of India and the Bay of Bengal.

- *Pressure network: betweenness*: the betweenness does not show well-defined patterns across all seasons, except for the EG hub during the pre-monsoon season. Difficulties in the pattern determination on the betweenness maps may be due to the relatively small number of nodes in this network.

- *Pressure network: average link length*: the hubs of the average link length, although not very distinguished, are still observable in NP, Afghanistan and along the 5–10° N belt over Sri Lanka. They appear during the pre-monsoon season, do not change across the ISM, and cover the whole region, except for TP during the post-monsoon season.

- *Pressure network vs. extreme rainfall network*: during the pre-monsoon season, NP, TP and Bay of Bengal spatial patterns of the pressure network coincide with the spatial patterns of the extreme rainfall network. During the monsoon season, low pressure over TP affects extreme rainfall locally on the plateau, and over the Himalaya. The NP hub in the pressure network during the pre-monsoon and monsoon seasons most likely affects extreme rainfall over the Indian subcontinent through the influence of Western Disturbances, which intensify the monsoon activity over the northern part of the Indian subcontinent. During the post-monsoon season, however, hubs of the extreme rainfall network are much more localized over the Himalaya, while pressure network hubs extend over the Indian subcontinent and the Bay of Bengal. This feature could be explained either by the low resolution of the pressure data, or by higher frequency variability of the extreme rainfall.

Comparison of the hubs of temperature and pressure networks with dominant patterns of the network of extreme precipitation over the Indian peninsula and Sri Lanka

shows that the NP and TP regions can be characterized as dominant patterns (hubs) of the ISM and post-monsoon temperature network, while the regions of EG and WG are more closely linked to the pre-monsoon season. On the other hand, NP and TP are dominant patterns of the pre-monsoon and ISM pressure network.

2.5. Discussion

In this study, we compare the spatial structures of synchronized extreme rainfall events for the rain-gauge interpolated (APHRODITE) data set (Yatagai et al., 2009), which was used in previous studies (Malik et al., 2010; Malik et al., 2011), with recent satellite-derived Tropical Rainfall Measurement Mission (TRMM) data set (Huffman et al., 2007; Bookhagen and Burbank, 2010) that covers a larger spatial domain, including the Indian Ocean. We have shown that there are many similarities regarding the synchronization of extreme rainfall events between these two data sets over the land (see Sects. 2.4.2 and 2.4.2). Taking into account the longer time period of the APHRODITE data set, we argue that patterns obtained for TRMM that coincide with patterns from APHRODITE are robust for the time period from 1951 to 2012. However, there are differences between the two data sets as well, namely the high-degree TRMM patterns in WG and Burma, which are not reflected in the APHRODITE data. The fact that these differences are in coastal areas allows us to assume that they are caused by a lack of APHRODITE data over the oceans, especially since the high-degree behavior comes primarily from connections to the surrounding bodies of water.

Based on our complex network analysis, we have revealed three dominant spatial patterns in the network of extreme precipitation during the ISM (Sect. 3.1): North Pakistan (NP), Eastern Ghats (EG), and the Tibetan Plateau (TP); and two main spatial patterns for the pre- and post-monsoon seasons: Western Ghats (WG) and the Himalaya. All of these patterns coincide with the topography of the Indian peninsula, and four of them – EG, WG, TP, and the Himalaya – play a governing role in the onset and spatial organization of the ISM extreme rainfall (Wang, 2006; Pai and Nair, 2009; Malik et al., 2010; Malik et al., 2011). However, we show that the NP pattern also strongly influences the network of extreme rainfall over the Indian subcontinent, and should be taken into account when studying the ISM dynamics.

The EG, WG, TP and Himalaya patterns are known as areas that influence the ISM dynamics, mostly because of the intricate topography of these regions that forces orographic lifting and high rainfall amounts. The Western Ghats are the first highlands of the Indian subcontinent encountered by the ISM winds. The mountains rise abruptly from the western coastal plains of the subcontinent, creating an orographic barrier for the monsoonal winds. The WG, together with the Himalaya, is the main cause of the substantial orographic precipitation all across the Indian subcontinent during the ISM season (Bookhagen and Burbank, 2010). During the winter season, however, it is the Eastern Ghats that create an orographic barrier for the rainfall during the post-monsoon season. The Tibetan Plateau is another

important region during the winter months, as precipitation in the region is caused by winter westerlies. It was shown that persistent warming on the Tibetan Plateau for the last three centuries coincides with intensification of the ISM, and the cool/warm epochs in TP also coincide with a weak/strong ISM (Feng, 2005). Our results from temperature, pressure, and extreme precipitation networks confirm the important role of the above-mentioned regions in the ISM dynamics.

The formation of the NP pattern during the ISM is caused by the topography of the region that, together with the ITCZ and the Arabian Sea branch of the ISM, promotes the formation of wind convergence in this region. This can explain why the NP region is characterized by both high degree and high betweenness: the convergence of surface winds is caused by the low pressure in the NP area. The high degree, betweenness, and average link length that we have observed in NP supports the theory that it is not the differential heating of the land and sea that is the governing mechanism of the ISM, but the monsoonal winds along with the Himalaya that act as a high shield that stops Siberian dry and cold air from penetrating the Indian subcontinent (Webster et al., 1998; Chakraborty, 2002; Sinha et al., 2013; Boos and Kuang, 2010). Additionally, rainfall in the NP region is mostly caused not by the monsoonal rainfall, but by Western Disturbances, which transport moisture from the Caspian Sea to the low-pressure area of the NP. In this study, we have shown that the NP region influences extreme rainfall synchronization across a large area of the Indian subcontinent. We suggest that since this region reflects Western Disturbances and influences extreme rainfall over most of the Indian subcontinent, it can serve as an indicator region for the interaction between the ISM system and Western Disturbances. Therefore, it might deserve careful consideration as one of the key regions, along with the EG (because of their connection), for the analysis of the ISM interaction with Western Disturbances, as well as for the analysis of floods in Pakistan.

We also observe several common features in the networks of extreme precipitation, temperature and pressure fields during the three seasons, as well as unique features for each season. Common features of the networks of extreme precipitation are a high degree and betweenness over NP and EG during the ISM, and a high average link length in NP, EG, TP and the Himalaya also during the ISM, confirming their role in ISM dynamics. In particular, we find that the Himalaya play more than just the role of an orographic barrier, blocking ISM winds from blowing rainfall into China, Afghanistan, and Russia. For the temperature and pressure networks, the common features are a high degree over both NP and TP (see Table 2.4).

Each of the three considered seasons also has its unique features, such as different long-range directions of the extreme rainfall synchronization that coincide with the main winds during the chosen season, or the dominant role of the NP pattern during the ISM. Our results can be explained as follows: the common patterns in the networks for the three seasons are caused by permanent properties of the underlying system, such as topography and geography, while the evolution of these patterns is caused by seasonal factors and, in particular, monsoonal activity. Patterns of synchronization of extreme rainfall events during the ISM and post-monsoon seasons appear due to

monsoonal southwesterly winds during the ISM and northeasterly winds during the post-monsoon season.

2.6. Conclusion

In this study, we have revealed the topology of extreme precipitation networks during the pre-monsoon, Indian Summer Monsoon, and post-monsoon seasons.

We have shown that the network of the Indian Summer Monsoon has three essential spatial domains: North Pakistan (NP), Eastern Ghats (EG), and the Tibetan Plateau (TP). These patterns are characterized by a high degree, high betweenness (except for TP), and the longest average geographical link lengths during this season. They start to form in the pre-monsoon season, and disappear during the post-monsoon season. The large number of connections and the long average link length of the NP, TP and EG regions during the ISM season imply that these regions strongly affect extreme rainfall event synchronization all over the Indian subcontinent. Also, the average and maximal link lengths of these regions are significantly increased in comparison to the pre-monsoon and post-monsoon periods.

The areas of the Eastern Ghats and the Tibetan Plateau were previously known as areas that influence the ISM dynamics due to the intricate topographies of these regions. We found that the NP pattern also plays an important role in the extreme rainfall organization during the ISM, because it is strongly influenced by Western Disturbances, and may serve as a key region for inferring interaction between the ISM system and Western Disturbances. It is important to note that, during the pre-monsoon season, the pattern in NP coincides with the area of divergence of the surface vector mean winds, while the EG pattern coincides with the convergence of the surface vector mean winds. During the ISM, this relationship between NP and EG patterns and winds reverses: NP coincides with wind convergence, while EG lies in the path of the Bay of Bengal monsoonal wind branch.

During the pre-monsoon season, the main patterns of the network of extreme rainfall event synchronization are Western Ghats and the Himalaya over the land, and the Arabian Sea and the Bay of Bengal. The Tibetan Plateau has the biggest influence on the network of extreme precipitation over the Indian peninsula and Sri Lanka during both the ISM and post-monsoon periods. We infer that the Tibetan Plateau pattern influences not only the ISM, but also pre-monsoon and post-monsoon dynamics. Also, it has been argued in the literature that this region influences the ISM rainfall dynamics (Feng, 2005; Wang, 2006; Rajagopalan and Molnar, 2013).

Therefore, the patterns detected in the NP, TP and EG regions are important for extreme rainfall synchronization during the ISM, while the patterns in WG and Himalaya mostly influence the synchronization of the extreme rainfall during the pre-monsoon season, and also, in the case of the Himalaya, during the post-monsoon season.

We found that tracking the topology of networks of extreme rainfall events during the ISM and the periods before and after the monsoon might help to reveal the origins

of the extreme rainfall events in the region. Currently, the Western Ghats pattern, or more specifically the Kerala region, is commonly used by climatologists for the prediction of the onset of the ISM (Pai and Nair, 2009). However, the observation of several patterns in several regions simultaneously could ultimately prove to be more effective for forecasting. We suggest that our findings be used for determining the timing of the ISM by tracking the evolution of the dominant patterns described above. In Chapters 3 and 4 of this thesis will be shown that obtained patterns, in particular, Eastern Ghats and North Pakistan, play an important role during the transition to monsoon - monsoon onset. In addition, in chapter 4 of this thesis will shown that these patterns can be used for the prediction of monsoon onset and withdrawal.

Chapter 3.

Mechanism of spatio-temporal abrupt transition to monsoon

In this chapter, the issue of the spatial and temporal propagation of the monsoon onset is discussed. The onset of monsoon is an abrupt spatio-temporal transition whose mechanisms are not fully understood. Here, using reanalysis observational data of near-surface air temperature, it is shown that a threshold behavior, which is clearly observed in the time series of climatic variables at the transition from the pre-monsoon to the monsoon, corresponds to the well-defined critical transition of the cusp catastrophe type. In this chapter, it is demonstrated that a set of critical conditions of the monsoon onset corresponds to the boundary of a cusp region in the parameter space. Based on these facts, a novel conceptual model of a spatio-temporal abrupt transition to monsoon is proposed, and values of the parameters of the model describing this transition are estimated directly from the observational data. This chapter is related to the associated publication P4 and the following presentation will closely follow its content.

3.1. Introduction

The mechanism of abrupt onset of monsoon has been the subject of recent studies, where it was shown that abrupt onset is caused by the large-scale shift of the regional circulation pattern over the Indian subcontinent (Gadgil, 2003; Goswami et al., 2010), related to the establishment of deep convection zones over the Bay of Bengal and Arabian Sea (Soman and Krishna Kumar, 1993), and is conjugated with an abrupt increase of the relative humidity and vertically integrated zonal moisture transport (Sikka and Gadgil, 1980; Rao, 1976; Fasullo and Webster, 2003). However, there is a lack of understanding how the conditions for abrupt transition to monsoon propagate across temporal and spatial scales. In particular, the forecast of the monsoon onset most awaited by farmers should not only contain the onset date over the southern part of the Indian subcontinent (as it is currently forecasted), but should also include the information of the monsoon onset propagation in time over the Indian subcontinent. Preferably, the best detailed monsoon onset forecast should be presented in a form of map of the onset of monsoon dates over the subcontinent - or *advance of monsoon* similar to Figure 3.1, which shows the map of the average onset dates of monsoon propagation over the Indian subcontinent, but for a chosen year and in advance.
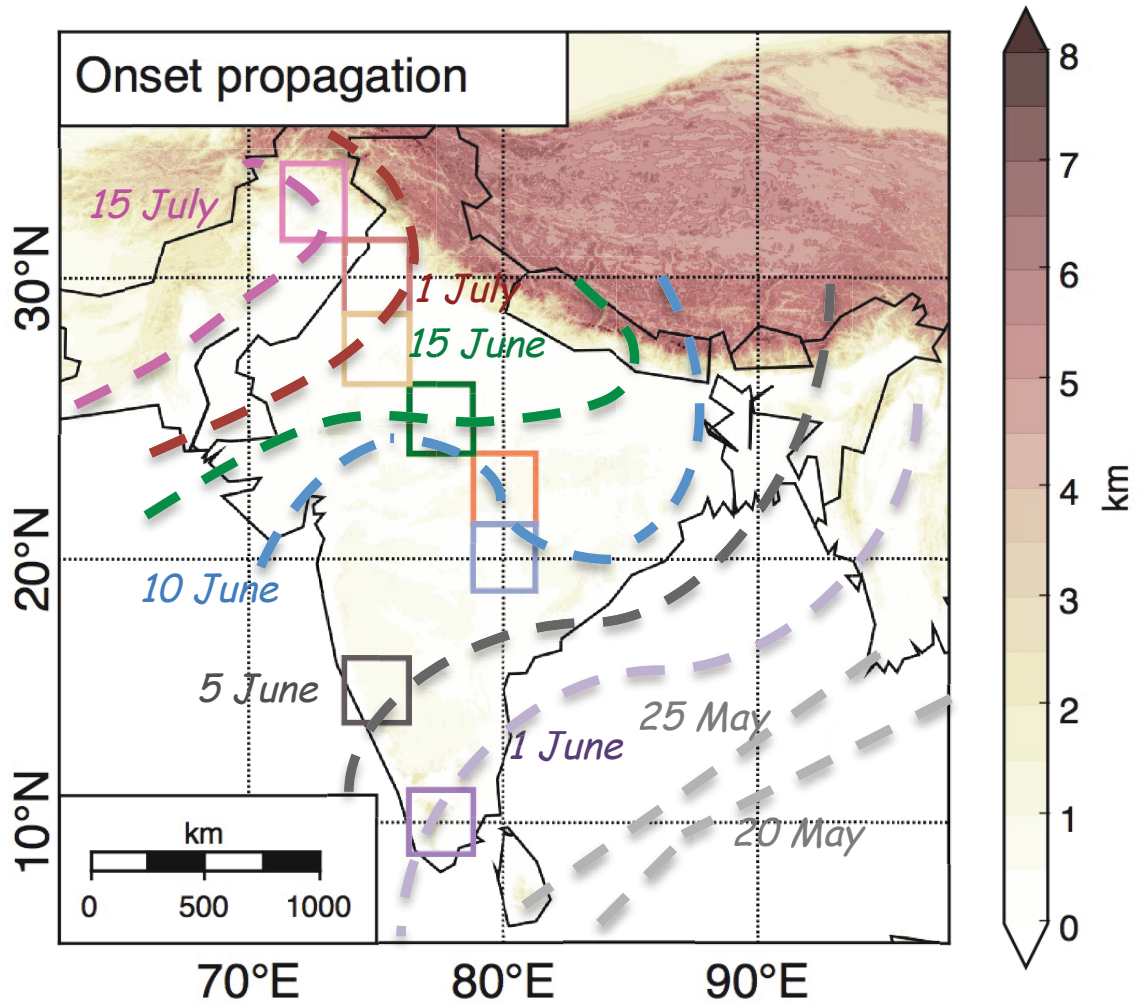
Figure 3.1.: Topography and propagation of the monsoon onset (long-term average) through the Indian subcontinent. Dates and lines of similar color indicate the onset of monsoon over the boxes with the same color. The map is reproduced from the Indian Meteorological Department website $http://www.imd.gov.in$.

This kind of forecast would fully satisfy the inhabitants of the Indian subcontinent. However, providing such forecast remains a great scientific challenge, as not all the mechanisms of transition to monsoon are understood and factors, responsible for this transition, revealed.

The main concern of this chapter is to reveal crucial factors governing the spatial and temporal propagation of monsoon onset and the instabilities that accompany the onset of monsoon, rather than identifying the interactions between the monsoon and the atmosphere, ocean, land surface, and the sun. First, we appraise observational data to characterize the equilibria in near-surface air temperature over the Indian subcontinent near the date of monsoon onset for various regions of the Indian subcontinent. Then, based on the results, we derive a conceptual model of the spatio-temporal propagation of the transition to monsoon. Finally, we estimate the parameters of the conceptual model from observational data, discuss features of monsoon onset propagation that this model explains and possible applications of this model for derivation of the spatio-temporal annual forecast of the monsoon onset.

3.2. Data

Although the monsoon onset is a result of complex interactions of several atmospheric processes, in order to reduce complexity, we consider a footprint of this process on the near-surface atmospheric layer. We analyze a near-surface atmospheric layer through the near-surface air temperature (1000 hPa) using reanalysis data (NCEP/NCAR) for the period 1951-2014, with a resolution 2.5°. The choice of near-surface air temperature as a climatic variable to describe the transition to monsoon is caused by three major facts: 1) air temperature has less uncertainty in comparison to other climatic variables, in particular precipitation, therefore, allows for a more reliable description of the transition to monsoon, 2) it is a continuously changing variable (unlike precipitation), which makes it easier to analyze and model, 3) it does contain an imprint of the abrupt transition to monsoon, as will be shown later in this chapter.

3.3. Monsoon onset is an abrupt transition from pre-monsoon to monsoon: observations

The fact that the transition to monsoon takes place abruptly makes it difficult to forecast. Another important feature of monsoon onset is that it propagates through the Indian subcontinent with varying characteristics. In order to describe this transition by taking into account both spatial and temporal propagation of monsoon onset, it is crucial to reveal the key features of this transition from observational data. In this section, we analyze near-surface air temperature over the Indian subcontinent in order to show that the transition to monsoon can be viewed as a critical transition. This representation of the transition to monsoon would allow to describe this transition qualitatively using dynamical system theory, which we will discuss later in this chapter.
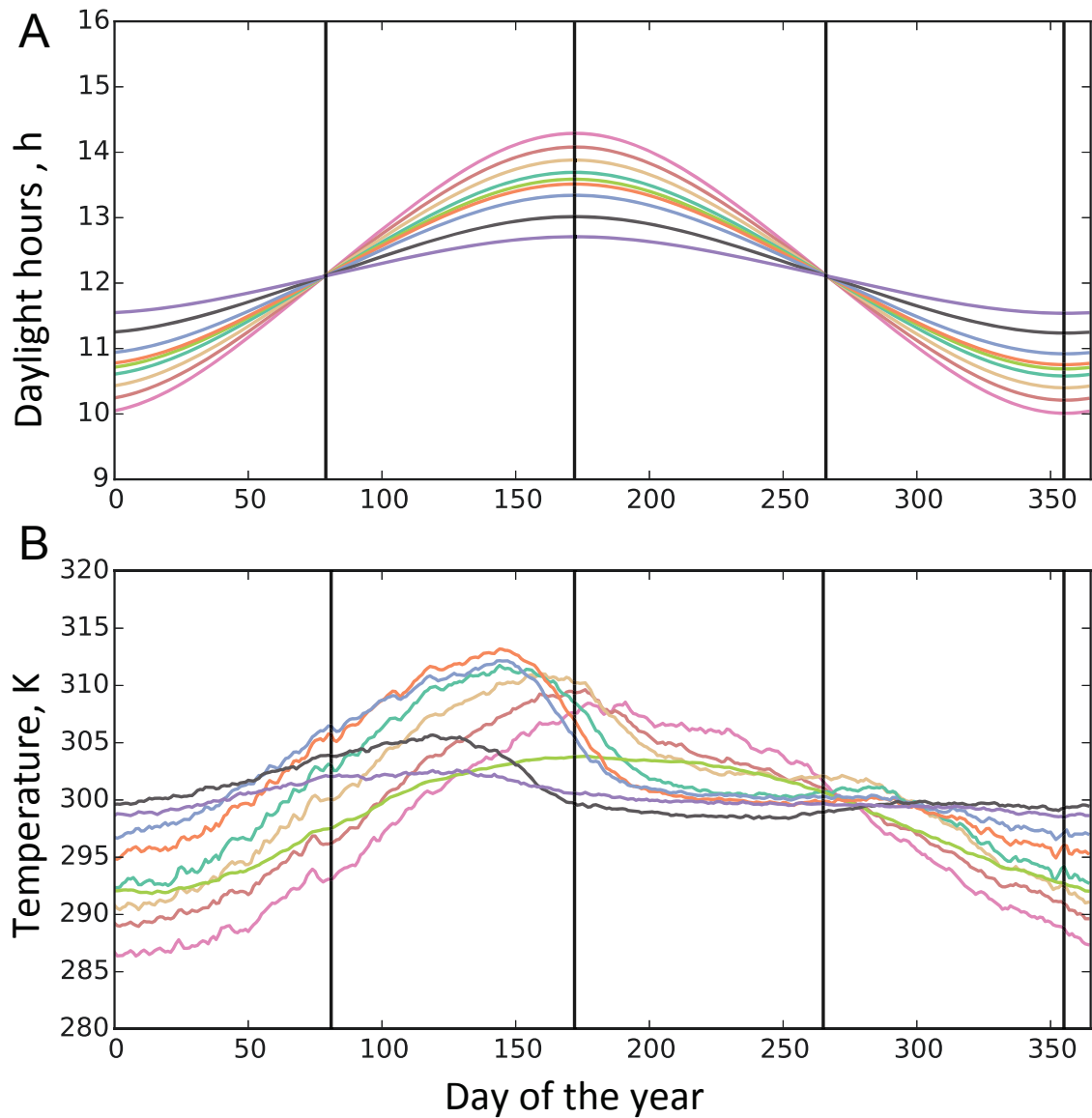
Figure 3.2.: A) Time series of near-surface air temperature (T) depending on the day (DOY) of the year for different geographical locations shown on Figure 4.2 A). B) Dependence of daylight hours (or the length of the day) on the day of the year (DOY), black lines mark - spring equinox, summer solstice, autumnal equinox and winter solstice,respectively. At the equinoxes, the Intertropical Convergence Zone (ITCZ) crosses the equator, at summer solstice - it is in its most northern position – above the blue and orange boxes (23N°). $< IS >$ - means average value over the Indian subcontinent. *Important to note*, that while daylight hours increase at the transition to monsoon - monsoon onset, the air temperature at the onset of monsoon decreases.

Figure 3.3.: Monsoon loop: Dependence of near-surface air temperature at 1000 hPa on the length of the day, black dotted lines correspond to winter solstice, spring equinox, summer solstice and autumnal equinox (marked with grey lines), respectively. At the equinoxes, the Intertropical Convergence Zone (ITCZ) crosses the equator, at summer solstice - it is in its most northern position – above the blue and orange boxes (23N°) from the Figure 3.1.

The spatial propagation of monsoon onset over the subcontinent shown in Figure 3.1 is associated with movement of the Intertropical Convergence Zone (ITCZ) northward onto the Indian subcontinent due to seasonal changes in the Sun's declination. It affects the length of the day during the year and amount of solar radiation received by the Earth's surface. Figure 3.2 shows changes of the length of the day for the regions of the Indian subcontinent marked with boxes on Figure 3.1. At the same time, the near-surface temperature in each region of the Indian subcontinent (averaged for the period 1951–2014) changes, following the slow changes in the length of the day (see Figure 3.2 A), B)) and the amount of incoming solar energy varies considerably with latitude. After the spring equinox, however, while the length of the day continues to increase, the temperature begins to saturate, until it reaches its maximum before the onset of monsoon. The transition to monsoon takes place abruptly for each year (see Figure 3.5). Analysis of near-surface air temperature shows that after the monsoon onset in a chosen region, the temperature decreases until around 300 K - the temperature of the monsoon (T_{mon}) - and holds almost constant until the end of the monsoon season. Therefore, it is possible to identify the existence of monsoon state in the observed air temperature. The abrupt transition to monsoon state after the temperature reaches the maximum value reveals the existence of the pre-monsoon state, from which this transition takes place.

The annual regularity of the monsoon onset, advance and withdrawal allow us to consider the transition to monsoon as a periodic, abrupt (in the sense of onset) transition. Having this in mind, together with the link between the changes in the near-surface air temperature and incoming solar radiation, depending on the length of the day, we plot the dependence of the temperature on the length of the day in Figure 3.3. It shows that in a region, which exhibits monsoon, the relation between the temperature and the length of the day has the form of a "loop", which we call the "monsoon loop". However, in a region where there is no monsoon (e.g. North Pakistan, marked by the pink line), instead of the "monsoon loop" the closed curve of an ellipse shape is observed. Hence, the nature of changes in temperature is quite different from the region, which exhibits the transition to monsoon from one that does not. We find that the regions lying on the axis of monsoon propagation, which coincides with the monsoon trough, - between the Eastern Ghats (blue line) and North Pakistan (pink line) - have the most pronounced characteristic features associated with the monsoon: i) gradual increase of the near-surface air temperature during the pre-monsoon season, ii) existence of a monsoon state - almost constant temperature during the monsoon season, iii) abrupt transition to this state, iv) withdrawal of monsoon marked by the beginning of a decrease of the near-surface air temperature.

The magnitude of the transition between the identified earlier pre-monsoon and monsoon states can be defined as a temperature difference between the maximum temperature value of the chosen geographical region (T_{max}) and the temperature of its monsoon state (T_{mon}), see Figure 3.2 B). It is important to note that the magnitude of the transition from the pre-monsoon to monsoon depends on the geographical location, in particular, on the latitude (see Figure 3.4). The transition with the largest magnitude is observed in the region marked with orange, which coincides with
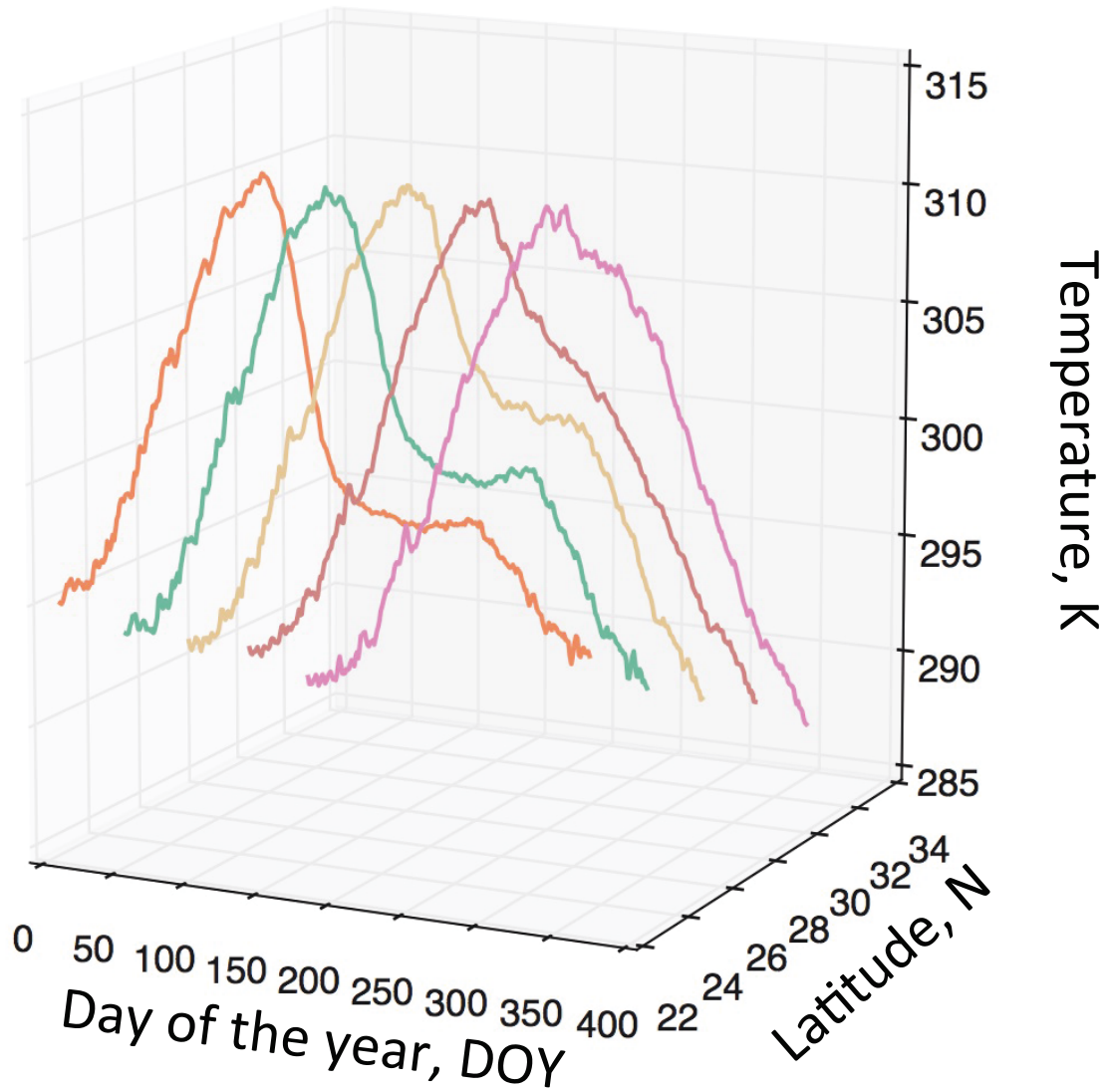
Figure 3.4.: Time series of near-surface air temperature at 1000 hPa (T) depending on the day of the year (DOY) and geographical location (see marked boxes on Figure 3.1).
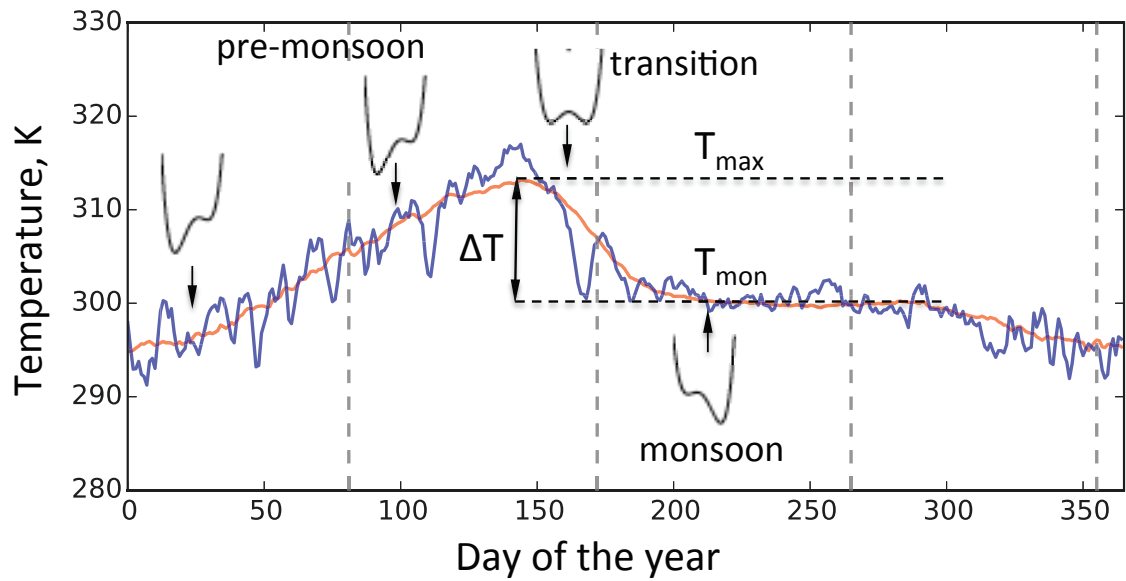
Figure 3.5.: Time series of near-surface air temperature (T) depending on the day (DOY) of the year for (80°E, 22.5°N) – orange region on Figure 4.2 A). $\Delta T = T_{max} - T_{mon}$ - temperature difference between the monsoon and pre-monsoon states. Chosen region experiences the largest transition to monsoon in comparison to others, as it has the largest ΔT. Onset of monsoon in this region coincides with the summer solstice – as ITCZ is located at this moment near 23N°. Potential energy profiles $U(T)$ (black) correspond to different states of the chosen near-surface air parcel: pre-monsoon, transition potential, where transition from the pre-monsoon to monsoon takes place, and monsoon.

the hottest place on the Indian subcontinent during the summer (23.5°N - Tropic of Cancer). Moving along the axis of monsoon propagation (perpendicular to the line of the onset of monsoon in Figure 3.1), the magnitude of transition decreases, until it ceases to exist in the North Pakistan (marked by the pink line), and there is no observed transition to monsoon in this region.

Although the transition to monsoon varies depending on the considered region (timing of the transition differs, as well as the magnitude), there are common features in the time series of temperature, which allow us to clearly distinguish two states of the atmospheric surface layer near the onset of the monsoon date: pre-monsoon state (characterized by maximum values of temperature - T_{max}) and stable monsoon state (characterized by constant temperature - T_{mon}). The changes of the near-surface air temperature in a chosen region are illustrated in Figure 3.5 on an example time series from the region with the largest magnitude of the transition from the pre-monsoon to monsoon: the mean time series for the period 1951-2014 is shown with an orange line, while the time series for 2013 - with a blue line. It is seen that the transition for year 2013 (as well as other years - not shown here) is abrupt, while the averaging of the time series for the period of time 1951-2014 results in a more smooth transition. Therefore, we are able to conclude that the spatial transition to monsoon has two main control parameters: first - associated with the speed of transition itself or with time (see Figure 3.4, (T, Day of the year) projection), and second - connected with the magnitude of transition or latitude (see Figure 3.4, (T, Latitude) projection)).

Summarizing the analysis of observational data, let us point out the main features of the spatially organized transition to monsoon: i) bistability or existence of two states: pre-monsoon and monsoon, ii) an abruptness of transition, iii) changes in the magnitude of transition of temperature for areas in the Indian subcontinent along the axis of monsoon propagation.

3.4. Conceptual model of abrupt transition to monsoon

3.4.1. Derivation of the model

According to our observations described above, the near-surface air temperature varies around one of the two states: pre-monsoon and monsoon. Let us describe the state of a near-surface air parcel over the fixed region of the Indian subcontinent (one of the boxes on Figure 3.1) at a certain day by internal variable T – near-surface air temperature. We proceed the building up of the conceptual model of changes of the near-surface air parcel, by considering it as a nonlinear dynamical system that can possess two states, with shifts between these different states. A one-dimensional conceptual model for this system is given by following equation:

$$\frac{dT}{dt} = -U'(T) + W(t), \tag{3.1}$$

where $U(T)$ - is a potential function, $W(t)$ - is the noise forcing the system.

It is generally known that the number of minima in the potential energy profile $U(T)$ in the nonlinear system determines the number of equilibrium states. Taking into account the temporal asymmetry of fluctuations in observable time-series of the near-surface air temperature (see Figure 3.5), it is reasonable to assume that two observable steady states are not equivalent energetically. Hence, the potential energy profile $U(T)$ with two asymmetric minima has the form:

$$U(T) = \frac{1}{4}T^4 + \frac{1}{2}uT^2 + vT. \tag{3.2}$$

When the control parameters v and u are fixed, the system settles into an equilibrium state where the variable T minimizes (locally) the function $U(v, u, T)$. The equilibrium surface has equation:

$$\frac{dU}{dT} = T^3 + uT + v = 0. \tag{3.3}$$

For $u \geq 0$ it has one minimum: $U_{min} = 0$ at $T = 0$, and for $u < 0$ there are two negative minima: if $v = 0$ - two minima are equal to $T = \pm\sqrt{-u}$, if $v \neq 0$ - the system has two distinct stable equilibria. We consider the case when the parameter v changes from a negative to a positive value: if $v = 0$ - the stability of one of the equilibria is lost, a sudden jump to an alternative state occurs. Figure 3.5 shows how a shape of the potential profile $U(T)$ changes in correspondence with changes of the near-surface air temperature of an air parcel over the chosen region of the Indian subcontinent.

To implement such a sudden jump to an alternative state (from the pre-monsoon to monsoon), let the parameter v be linearly dependent on time, and take negative values v_0 for $t < t_0$ and positive ones for $t > t_0$. Such behavior is demonstrated, e.g., by the function:

$$v(t) = v_0 + \epsilon(t - t_0), \tag{3.4}$$

where the coefficient ϵ characterizes here the rate of the change of the control parameter. We require the rate (ϵ) to be slow compared to the response time of the system.

To reproduce changes in the magnitude of the transition to monsoon, which were observed in time-series of air surface temperature at increasing latitude (see Figure 3.4), let us use different values of parameter u. However, only negative values of the parameter $u < 0$ allow us to describe changes of the temperature between the two states. Positive values of parameter u correspond to the potential of the system with only one stable state, and not two - as observed in the data.

To account for both features observed in the data: a sudden jump of the temperature (abrupt transition to monsoon - onset) and changes in magnitude of the transition in

the system, we have to require not just the first derivative, but the second derivative of the potential function to be also zero:

$$\frac{d^2U}{dt^2} = u + 3T^2 = 0. \tag{3.5}$$

Eliminating T from equations (3.5) and (3.3), we can draw the bifurcation set in a control space:

$$27v^2 = -4u^3. \tag{3.6}$$

In the one-dimensional case, the model (3.1) turns to one ordinary differential equation for T with a slowly varying time-dependent bifurcation parameter, $v(t)$, as given below:

$$\frac{dT}{dt} = -\frac{dU(T, u, v(t))}{dT} + W(t) = -(T^3 + uT + v(t)) + W(t), \tag{3.7}$$

$$v(t) = v_0 + \epsilon t, \tag{3.8}$$

where u is a negative constant, $\epsilon > 0$ is a positive constant, and the initial conditions are $T(0) = T_0$, and $v(0) = v_0$. The v parameter is called the "asymmetry parameter", while the u parameter is called the "splitting" parameter (Poston and Stewart, 1989).

The proposed model corresponds to the cusp-catastrophe (see Figure 3.6). In the next subsection, we will describe the main characteristics of the cusp-catastrophe, which we compare with our observations. It is important to note, that we consider the current version of the model of abrupt transition to monsoon as conceptual in nature. It is not concerned with the underlying mechanism of the near-surface air temperature changes, but only describes specific features of its dynamics.

3.4.2. Main properties of the cusp catastrophe model: fold, pitchfork and dynamical bifurcations

Catastrophes are bifurcations between different equilibria, or fixed point attractors (Thom, 1989). They are classified based on the number of control parameters that are simultaneously varied. If there are two control parameters, it is called a *"cusp"* catastrophe. Cusp catastrophe is one of the simplest bifurcations leading to local bistability and hysteresis. Some characteristics of the cusp catastrophe have been found in geomorphic processes on the Earth's surface, such as landslides, debris flows, and river sediment transport (e.g., Henley, 1976; Graf, 1979; Chappel, 1983; Henley, 1983; Qin et al., 2001). In this section, we describe the characteristics of the cusp catastrophe, which we observe in time-series of near surface air temperature during
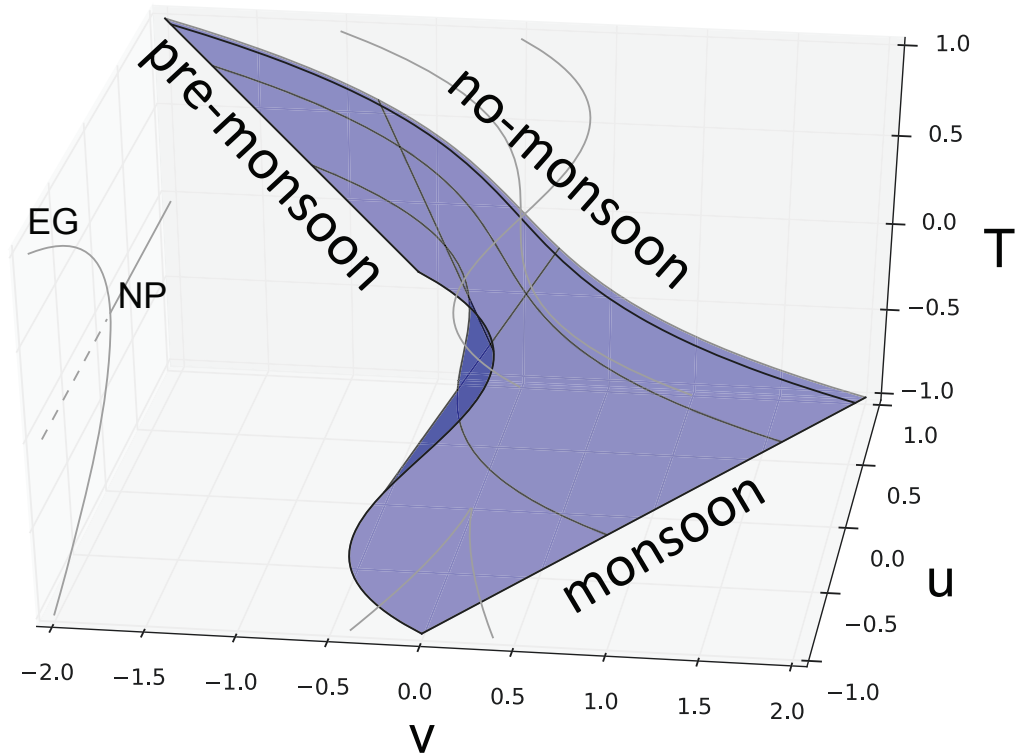
Figure 3.6.: Cusp catastrophe model describing the transition to monsoon. Qualitative description of the transition from the pre-monsoon to monsoon is shown as a cusp catastrophe. T is a near-surface temperature, u and v – parameters, where u is associated with the location of the region along the axis of monsoon, and v is connected with the upcoming ITCZ or insolation received by the region, changing in time. In the vicinity of onset, it corresponds to the observational data shown on Figure 3.4. (T,v) plane shows projections of the T changes with v – corresponds to the observational data shown on Figure 3.4; (T,u) plane shows projections of the number of possible states: u<0 – pre-monsoon and monsoon states (temperature from the boxes blue through light red - see Figure 3.4), u>0 – only one - pre-monsoon state (pink box or NP, see Figure 3.1).

the transition to monsoon. Cusp catastrophe bifurcation is characterized by two bifurcations in two projections: (T, v) and (T, u). Let us consider them separately, the abrupt transition corresponds to the onset of monsoon.

Fold bifurcation. In the (T, v) projection, the model exhibits a *fold bifurcation*. Dependence of steady state solutions for T on the value of parameter v is called a *bifurcation diagram*. For the fixed value of the parameter u, the bifurcation diagram for the fold bifurcation is shown in Figure 3.6 - (T, v) projection and in Figure 3.7 with black line. Starting from the negative v and moving to the positive v, the system follows the upper stable branch, and after $v_c = \frac{2}{3\sqrt{3}} u^{3/2}$, the stable upper branch loses stability, and the system abruptly changes its state to another (lower) stable branch. The abrupt transition to monsoon for a chosen region of the Indian subcontinent (with fixed u) in observational data corresponds to the (T, v) projection of the cusp catastrophe model, the upper branch – to the pre-monsoon state of the near-surface air temperature, the lower branch – to the monsoon state.

Pitchfork bifurcation. The (T, u) projection of the cusp catastrophe model exhibits a *supercritical pitchfork bifurcation*: for positive values of u ($u > 0$), there is one stable equilibrium at $T = 0$. For $u < 0$, there is an unstable equilibrium at $T = 0$, and two stable equilibria at $T = \pm\sqrt{u}$. In observational data, this transition through the pitchfork bifurcation corresponds to an occurrence of two states: pre-monsoon and monsoon at $u < 0$ for the regions of the Indian subcontinet lying on the axis of monsoon propagation from the orange to the pink box (see Figures 3.1, 3.4), while $u > 0$ corresponds to the existence of only one state in the regions where the monsoon does not reach (at latitudes higher than $32.5°N$).

The condition of the cusp catastrophe (eq. 3.6) divides the parameter plane (Figure 3.6, (u, v) projection) into two regions. Inside the wedge, there are three equilibria: two stable and one unstable. Outside the wedge, there is a single equilibrium, which is stable. If we approach the cusp point from inside the wedge, all three equilibria merge together. The origin of the cusp catastrophe $(u, v) = (0, 0)$ corresponds to the state of the near-surface air temperature in the North Pakistan region at the moment when the monsoon reaches the region and disappears. The parameter u decreases ($u < 0$) along the axis of monsoon propagation from NP to EG (see Figure 3.6). The parameter v slowly grows with time and passes a critical value v_c at the onset of monsoon in each of the considered regions from NP to EG. The change in time of a parameter v leads to delayed phenomena described in the next section.

Dynamical bifurcation. The important feature of our conceptual model is a slowly varying time-dependent bifurcation parameter $v(t)$, which passes through the critical value v_c (a bifurcation point). This feature considerably affects the stability of the system: it makes the system non-autonomous, and its evolution completely transient. If one starts from $v_0 < 0$ and increases the parameter v, after passing through the critical point v_c, the system remains for a considerable time on the unstable state and only after some time undergoes a rather quick transition to another stable state (see Figure 3.7). There is still an effective fold bifurcation, but it is delayed. In the case of a fold bifurcation, the transition from one state to another
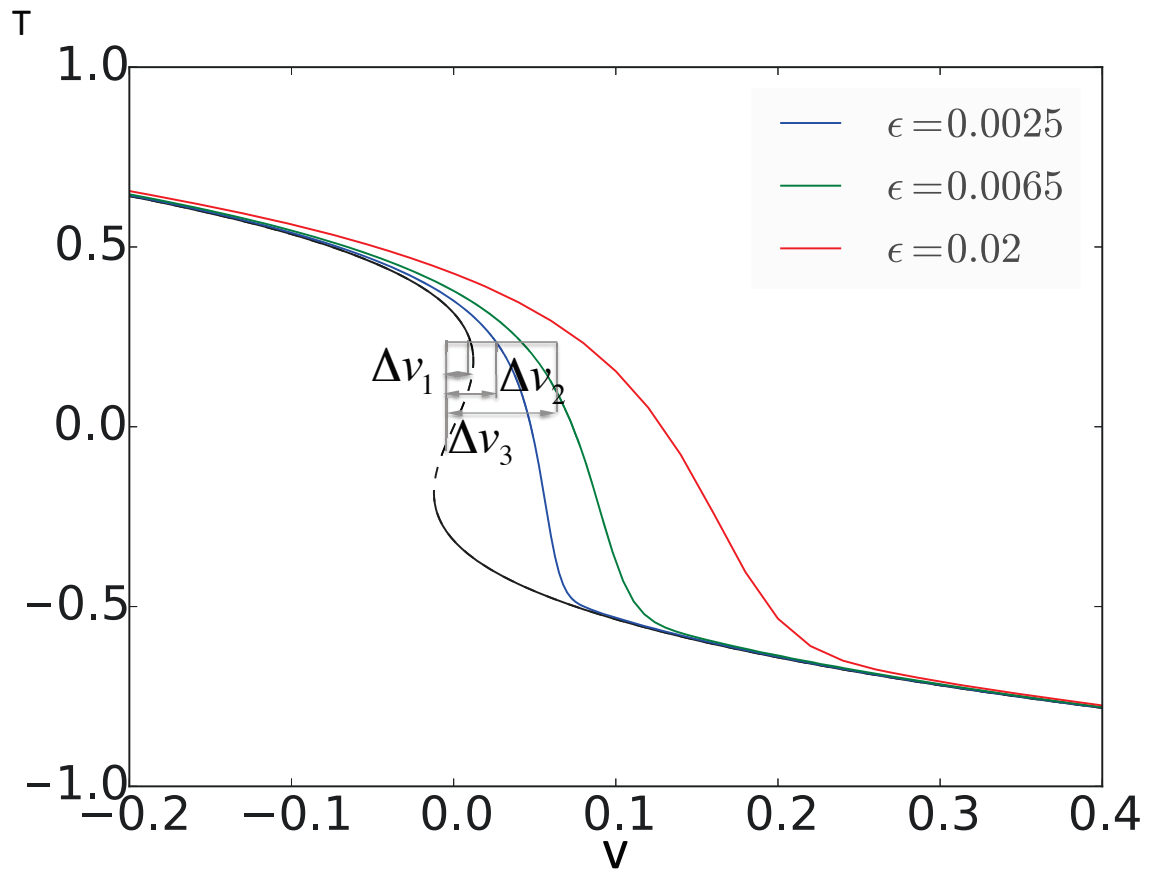
Figure 3.7.: Dynamical bifurcation in fold bifurcation. Bifurcation diagram (black) (eq. 3.10) and solution of the differential equation $\frac{dT}{dt} = -(T^3 + uT + v(t))$, $v(t) = v_0 + \epsilon t$: slow transition through the bifurcation point, $\epsilon = 0.0025$ (blue), fast transition through the bifurcation point, $\epsilon = 0.0065$ (green), very fast transition through the bifurcation point, $\epsilon = 0.02$ (red). Δv_1, Δv_2, Δv_3 - difference of parameter v between the stable state parameter value, and changing in time with given rate parameter v.

one overshoots the critical value v by the amount $\epsilon^{2/3}$ (Majumdar et al., 2013). The higher is passing rate ϵ, the more distinct is the delayed bifurcation phenomenon. In the next section, we take this feature into account in the estimation of the parameter v in the cusp model from observational data.

Pre-bifurcation noise amplification

Some physical phenomena can be explained only by taking into account fluctuations (Ebeling and Sokolov, 2005). Spontaneous fluctuations underlie the most amazing and ubiquitous phenomena such as noise-enhanced phase synchronization in excitable media, noise-enhanced phase coherence in stochastic resonance (Neiman et al., 1998; Neiman et al., 1999). Noise-enhanced phenomena might be good indicators of impending the critical transitions. In particular, the phenomenon of pre-bifurcation growth of fluctuations is used as a precursor of tipping points in geophysical studies. (e.g.Lenton, 2011). This phenomenon was known in the theory of nonlinear oscillations since the 1930's, and, in particular, in Wiesenfeld, 1985, unlimited growth of fluctuation in the immediate vicinity of the bifurcation point was shown. However, in Surovyatkina et al., 2005, the nonlinear saturation of the fluctuation variance in the vicinity of the bifurcation point was revealed. In particular, it was estimated that away from the bifurcation point the variance of fluctuations is proportional to the noise variance. At the approaching the bifurcation point, the variance of fluctuation increases, and in the immediate vicinity of the bifurcation point the linear growth of fluctuations is replaced by the nonlinear saturation. In the saturation regime, the fluctuation variance is proportional to the standard deviation of the external noise. The nonlinear saturation occurs in the range of parameters proportional to the standard deviation of noise. The growth of fluctuations depends on the distance to the bifurcation point. It is important to note, that in the case of a dynamic bifurcation, there is a delicate balance between the noise and rate-dependent phenomena. A strong noise at a low rate can induce a rapid transition to another stable state. However, at higher rates, the effect of noise amplification is less pronounced, and the result of the bifurcation transition depends on the larger extend on the rate of change of the parameter. In Chapter 4 of this thesis, we use the phenomenon of pre-bifurcation noise amplification for the detection of tipping elements in the spatially organized system of monsoon.

Summarizing this section, it is important to note that we consider such a model as conceptual in nature. It is not concerned with the underlying mechanism of the near-surface air temperature changes, but only describes its dynamics. We emphasize that the cusp catastrophe model exhibits two types of critical transitions: the pitchfork bifurcation and the saddle-node bifurcation. The first type of critical transition is associated with the spatial characteristics of transition to monsoon: the existence of monsoon onset in a given region of the Indian subcontinent. Analysis of the time-series of near-surface air temperature reveals that the transition to monsoon ceases to exist near the North Pakistan region ($u_{NP} \approx 0$), while in the Eastern Ghats region the transition to monsoon is the largest ($u_{EG} < u_{NP}$, $u < 0$). The second transition is associated with temporal characteristics of the abrupt transition to monsoon (monsoon onset) in a given region. At the onset of monsoon at a chosen region, the parameter $v \approx 0$. The detailed analysis of the observational data and

estimation of the cusp model parameters for various regions of the Indian subcontinent will be presented in the next section.

3.5. Advance of monsoon as a cusp catastrophe: estimating model parameters from observational data

In the previous section, we introduced the cusp catastrophe model for the description of a transition to monsoon by focusing entirely on the qualitative verification. The next step is to perform a quantitative evaluation of an actual match between a cusp catastrophe model and the near-surface air temperature data using the phenomenological fitting procedures. The main goal of the fitting is to reproduce features observed in data, using the model characteristic: bistability, an abrupt transition from pre-monsoon to monsoon states, changes in a magnitude of transition, rate-dependent and noise-dependent phenomena. It is indispensable for verification of the fact that a cusp catastrophe suits better for describing the observational data than other conceivable models derived from data, neither of which reproduces all these features.

Here, we show how to estimate the model parameters from observational data. As a first step, we introduce the following rescaling in oder to obtain values of T on the scale $-1 < T < 1$:

$$T = \frac{T_{obs} - T_c}{k}, \tag{3.9}$$

where T_{obs} is the observational near-surface air temperature from NCEP/NCAR data taken from one of the geographical regions presented in Figure 3.1(note, that the model description is valid only for the regions from the orange to the pink box), k - is a positive constant, which we require to be $k > (T_{obs} - T_c)$.

As a second step, we estimate the parameters u and v, and also a constant ϵ (rate of the varying parameter v):

1. The parameter u is obtained using the equilibrium condition (3.3). Taking into account that for $v = 0$ the value of variable $T = T_{max}$, we find parameter $u_1 = -T_{max}^2$. To confirm the previous estimate of u, we can also find a parameter u using condition (3.5), which requires the second derivative of the potential function $U(T)$ to be equal to zero. For a given value of u, it corresponds to the value of T for the onset of monsoon: T_{onset}. Recalling condition (3.6), we obtain $u_2 = -3T_{onset}^2$. The values of parameters u_1 and u_2 obtained from observational data coincide quite well. Therefore, the choice of estimation procedure of parameter u from the data should be determined by the given time series from which the estimate is made: in this case, when identification of T_{max} from the given time series has less uncertainty than the identification of T_{onset}, one should use the u_1 estimation, and vice versa.
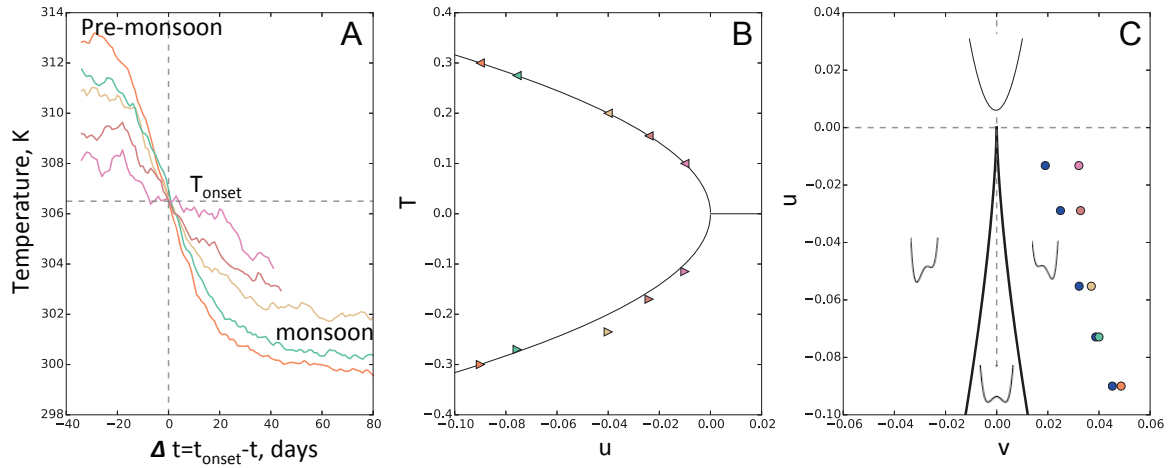
Figure 3.8.: Estimation of parameters from the observational data. A) Time series of near surface air temperature in respect to the onset date for a chosen region (see Figure 3.1), T_{onset} marks the onset of monsoon temperature, t_{onset} - day of monsoon onset. B) Pitchfork bifurcation reconstruction: triangles –rescaled values of temperature derived from data, values of parameter u calculated using eqs. 3.3 and 3.6. C) The cusp – in the parameter plane (u, v). The point $(u, v) = (0, 0)$ is the origin of two branches of the saddle-node bifurcation curve the (eq.3.11). Potential profiles (black) show the number of stable states. Inside the wedge, there are three equilibria: two stable and one unstable. Outside the wedge, there is a single equilibrium, which is stable. Black lines of cusp – are theoretical values of parameters u and v as if parameter v does not depend on time (bifurcation in a parameter space), blue points are theoretical results with accounted delay $\epsilon^{2/3}$ in bifurcation due to the change of parameter v in time (dynamical bifurcation in a parameter space) (See Figure 3.7), thereby, points situated on the distance from the right boundary of the wedge. Colored points are results of estimation for parameter u, which is shown in B), the parameter v is estimated by comparison of re-scaled observational data with model results (see Figure 3.9).

2. The parameter v is estimated from the condition (3.6), which defines the boundaries of a cusp region in a parameter space. Thus, having estimated parameter u from observational data, it is possible to estimate the value of parameter v as: $v_{theor} = \pm\sqrt{-4/27 * u^3}$. We call this estimate of a parameter v – theoretical estimate (v_{theor}), as it would be the value of a parameter v, if the parameter v would be time-independent: $v \neq v(t)$. However, in observational data the parameter v depends on time: $v = v(t)$. It results in a "delayed" transition to monsoon in the time series in comparison to the stable state solution, therefore, for the estimation of the "real" parameter v from the observational data, we have to account for the dynamical bifurcation effects (see Section 3.4.2 and Figure 3.7).

3. In order to obtain the estimate of the "real" time-dependent parameter v from the observational data, we use the phenomenological fitting procedure. We calculate the solution of our conceptual model (3.7) using values of parameter u estimated above. We choose the initial condition T_0 close to a locally stable equilibrium, which corresponds to the pre-monsoon state. Then, we choose the initial value of parameter v (v_0) so that $v_0 < \sqrt{-4/27 * u^3}$. The rate of change of the control parameter $v - \epsilon$ – we require to be small $\epsilon << 1$. Using different values of ϵ, we find the actual match between our conceptual model and the observational data. Results of the fitting procedure for two regions EG and NP are shown in Figure 3.9.

4. To examine the noise influence in the model and to compare fluctuations induced by noise in the model with those in the time series of observations, we use a stationary random process similar to white noise with different values of a variance of noise. Results are shown in Figure 3.9. As it is seen on the plots, during the transition to monsoon state, model fluctuations are well correlated with fluctuations of the time series.

Figure 3.8 C) shows representation of the states of the system on the parameter space (v, u). We compare the values of analytical estimations of parameter v (black line) with values of parameters corresponding to the dynamical bifurcation (blue circles), and values of parameters derived from observations (orange, green, beige, red, and pink circles). Parameter v for observational data was estimated by marking the monsoon onset date in the time series. We found that the set of critical conditions of the monsoon onset corresponds to the boundary of a cusp region in parameter space (colored circles fit well to the blue circles) (see Figure 3.8 C)). The results are fully consistent with observations.
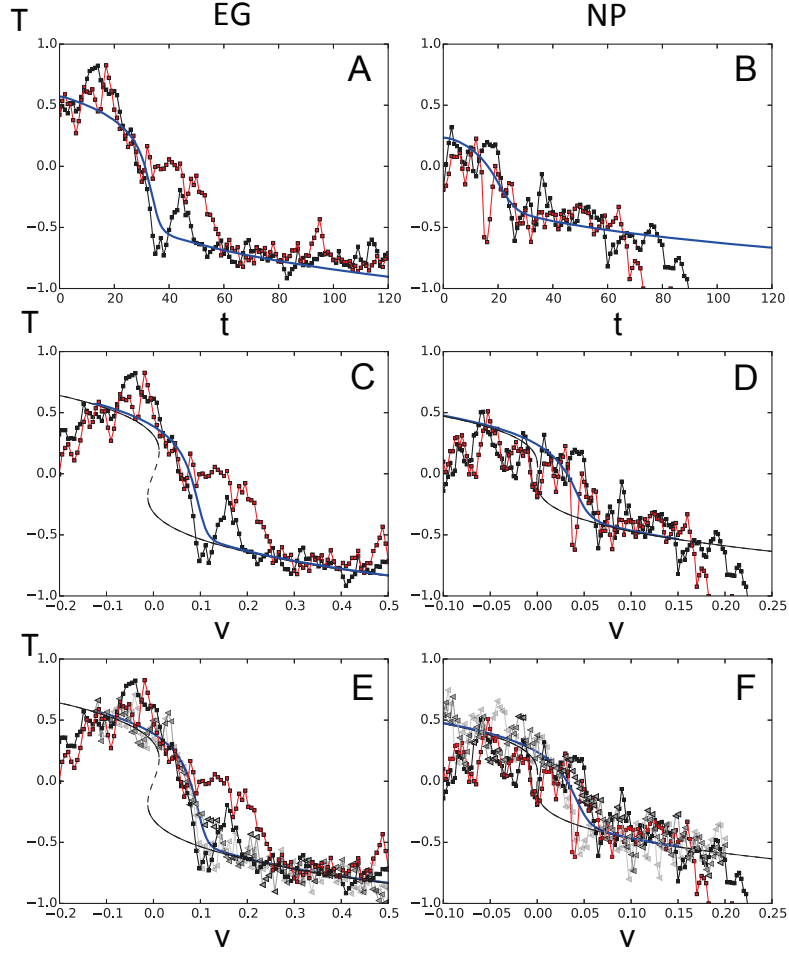
Figure 3.9.: Estimation of model parameters from the observational data: A), C), E) for the Eastern Ghats region (EG) from the orange box on Figure 3.3 A); B), D),F) for the North Pakistan region (NP) from the pink box on Figure 3.3 A). T is a re-scaled near-surface temperature ($\frac{T_{EG}-307.7}{9.8}$, $\frac{T_{NP}-309}{9.8}$), in order to have it on the scale of the cusp catastrophe model. Red and black curves correspond to time series from 2013 and 2014, respectively for the A), C) D), and for 2013 and 2011 for B), D), E). t - is a time in respect with the drop of the near-surface air temperature (onset of monsoon in this place), v - is a parameter of the cusp catastrophe model associated with time, re-scaled time for the time series from A) was performed as follows: $-0.1294 + (T - 130) * 0.0065$ - for 2013, $-0.1294 + (T - 140) * 0.0065$ - for 2014, where 0.0065 is a speed of the changing parameter $v - \epsilon$, 130 and 140 - are days of the year when the drop of the temperature started, and -0.1294 - is v_0, and initial value of v. Similar, for the NP region (B), C), D), re-scaling of t to parameter v: $(T - 198) * 0.0025 - 2011$, $(T - 212) * 0.0025 - 2014$. Blue curve on A) shows the fitted model to the data (red and black), this curve is a solution of the ODE associated with the cusp catastrophe model: $\frac{dT}{dt} = -(T^3 + uT + v(t))$, where $v(t) = v_0 + \epsilon t$. Here, parameters u and v are estimated for the EG and NP as shown on Figure 3.8. Black curve - bifurcation diagram - a set of steady state solutions for each value of parameter v of the cusp catastrophe model. Dark and light grey curves obtained by adding the Gaussian noise to the cusp catastrophe model: $\frac{dT}{dt} = -(T^3 + uT + v(t)) + W(t)$. For EG: $\sigma_W^2(2013) = 0.52$, $\sigma_W^2(2014) = 0.67$; for the NP: $\sigma_W^2(2011) = 0.63$, $\sigma_W^2(2013) = 0.66$.

3.6. Contribution of the model to understanding of the mechanism of abrupt transition to monsoon

We have presented the cusp catastrophe model of abrupt transition to monsoon derived from near-surface air temperature time series. The current version of the model has obviously proven to be able to reproduce the following specific features of Indian monsoon: i) bistability or existence of two states: pre-monsoon and monsoon, ii) an abruptness of transition, iii) changes in a magnitude of transition of temperature for areas in the Indian subcontinent along the axis of monsoon propagation.

Admittedly, the model does not provide a physical mechanism of transition to monsoon, thus, conclusions about the underlying dynamics are somewhat limited. Another limitation of the model is the designation of control factors. Further research should be done to bring the model to the physical principals of the monsoon transition in the near-surface air characteristics. On the other hand, the abstract nature of our model might be regarded as an advantage as it is based on observational data. This new information on critical transitions in near-surface air temperature will add more light to the problem of the abrupt transition to monsoon.

3.7. Conclusion

The proposed conceptual model of the transition to monsoon based on a cusp catastrophe describes the mechanism of the abrupt spatio-temporal propagation of monsoon onset. A formulation of a detailed and accurate model to predict the exact timing of the transition to monsoon for each year and chosen location is prevented by the limited knowledge of the complex feedbacks in the atmosphere affecting the monsoon. Although the proposed mechanism of an abrupt transition to monsoon onset does not provide a forecast for the advance of the monsoon over the Indian subcontinent, it opens the possibility to use the properties of the cusp catastrophe in an indirect forecasting of the advance of the monsoon in the given year. This assumption raises the question: how do we expose such catastrophic changes when they are thoroughly interconnected across temporal and spatial scales before the transition? And can we somehow anticipate the transition and predict when it will happen?

The knowledge about the two types of the critical transitions taking place with the advance of the monsoon: one on temporal, another one on spatial scale, allows us to use precursors of such a critical transition depending on the type of the critical transition, for prediction of the timing of the critical transition. This question will be further considered in Chapter 4 of this thesis, where the variance of fluctuations prior to the critical transition is used to identify the tipping elements of monsoon and predict the timing of the critical transition to monsoon.

The present approach advanced our understanding of predictability of the abrupt transition, which propagates across temporal and spatial scales. We have shown that there are two stable equilibrium states in the monsoon dynamics: pre-monsoon and

monsoon. The onset of monsoon is an unstable equilibrium state, which explains an abrupt nature of the transition from the pre-monsoon to monsoon. We find that the transition from the pre-monsoon to monsoon for the regions of the Indian subcontinent laying on the axis of monsoon propagation correspond to a critical transition of a cusp catastrophe type. Main properties of a cusp catastrophe correspond to regularities in observational data.

The main advantages of the proposed model in comparison to the existing explanations of the abrupt transition to monsoon are: i) it describes and explains not only temporal transition to monsoon in a certain region of the Indian subcontinent, but also spatial propagation of monsoon onset along the axis of monsoon, ii) it demonstrates how to expose catastrophic changes in the state of the system when they are interconnected across temporal and spatial scales in the case when the model can not accurately anticipate the transition, and opens the possibility to predict spatial and temporal propagation of the critical transition.

Chapter 4.

Tipping elements of the Indian Monsoon: prediction of onset and withdrawal

Forecasting the onset and withdrawal of the Indian summer monsoon is crucial for life and prosperity of more than one billion inhabitants of the Indian subcontinent. However, accurate prediction of monsoon timing remains a challenge, despite numerous efforts. Here, we present a method for prediction of monsoon timing based on a critical transition precursor. We identify geographic regions - tipping elements of the monsoon - and use them as observation locations for predicting onset and withdrawal dates. Unlike most predictability methods, our approach does not rely on precipitation analysis, but on air temperature and relative humidity, which are well represented both in models and observations. The proposed method allows to predict onset and withdrawal dates more than two weeks and a month earlier than existing methods, respectively. In addition, it enables to correctly forecast monsoon duration for some anomalous years, often associated with El-Niño-Southern Oscillation. This chapter is based on the associated publication P5, and some of the following sections will closely follow the presentation in that study. Supplementary figures for this chapter can be found in appendix C.

4.1. Introduction

The prediction of the Indian summer monsoon (hereafter monsoon) timing is a vital question for the Indian subcontinent and significantly affects agricultural planning and the Gross Domestic Product of the country, which is determined of up to 22 % by agriculture (Wang et al., 2009; Goswami et al., 2010; Subash and Gangwar, 2014). A slight deviation of the monsoon timing manifested as delay (or early arrival) may lead to drastic droughts (floods) causing damages to infrastructure, losses of crops and livelihoods of the population. The onset of monsoon takes place abruptly and its predictability for more than two weeks in advance, as well as early predictability of withdrawal, remains an important concern.

Various prediction attempts for monsoon onset and withdrawal dates (OD and WD) have been made for different time scales from short (up to 4 days) and medium (4–10 days) range forecasts using Numerical Prediction Models (IMD, 2015; NCMRF,

2015; Das et al., 2002; Durai and Roy Bhowmik, 2014) to extended (10-30 days) and long-range forecasts (sub-seasonal, 30+ days) (IMD, 2015; Shukla and Mooley, 1987; Das, 1987; Munot and Kumar, 2007; Yang et al., 2008; Goswami and Gouda, 2010; Alessandri et al., 2014). Forecasting methods have so far been mostly based on statistical model approaches, which include averaged values of zonal asymmetric temperature anomaly (Prasad, 2005), sea surface temperature, mean sea level pressure (IMD, 2015; Goswami et al., 2006; Wang et al., 2009), tropospheric moisture build-up over areas south of the Indian peninsula (Taniguchi and Koike, 2006; Joseph P.V. and K, 2006), vertically integrated moisture budget (hydrologic onset and withdrawal index or HOWI) (Fasullo and Webster, 2003), moist static energy (Rajagopalan and Molnar, 2014), outgoing long-wave radiation (OLR) and wind fields (Wang et al., 2009; Puranik et al., 2013).

The Indian Meteorological Department (IMD, 2015) provides a forecast of monsoon OD for Kerala 21 days in advance with an accuracy ± 4 days with 10% deviation. However, there are certain difficulties in the existing forecasting methods, in particular, of "bogus" (false) monsoon onsets mostly related to non-monsoonal atmospheric circulation systems (Flatau et al., 2001). In addition, the methodology used for forecasting of WD, which determines the length of the monsoon season, has certain issues and limitations, in particular, predicting a WD earlier than September 1 or forecasting of late WD (IMD, 2015). These limitations require the improvements of the prediction skills for monsoon onset and withdrawal dates (Webster, 2013).

In this study, we propose a novel method for forecasting monsoon onset and withdrawal by identifying tipping elements of the monsoon. The notion of a *tipping element* in Earth system was introduced by Lenton et al. (2008). According to the definition, the tipping element is a component of the Earth system that may pass a tipping point - a critical threshold at which a small perturbation can qualitatively change the state of the Earth system (Lenton et al., 2008).

The global monsoon system has been argued to be one of the tipping elements of the Earth. Here we show that the Indian monsoon exhibits a periodic and abrupt transition on inter-annual time scale: the monsoon onset. We furthermore show that the Indian monsoon has its own tipping elements - geographic regions which exhibit a critical behaviour before the monsoon onset. We coin these geographic regions *tipping elements of the monsoon.*

We use the tipping elements of the monsoon as optimal observation locations or reference points (RPs). Based on the analysis of time series of near surface air temperature (T) and relative humidity (rh), we create a long-range ($>$30 days) forecasting scheme for monsoon onset and withdrawal dates, which overcomes previously identified forecasting difficulties, such as the "bogus" onset of 2002, and abnormally late withdrawal in 2008. Our approach exhibits two major differences to existing methods: i) Unlike most predictability methods, we do not rely on the analysis of precipitation time series, which are often poorly measured and modelled (Fasullo and Webster, 2003). Instead, we use near surface air temperature (T) and relative humidity (rh), which are well represented in both measurements and models and show clear indicators of the upcoming monsoon onset (Soman and Krishna Kumar,
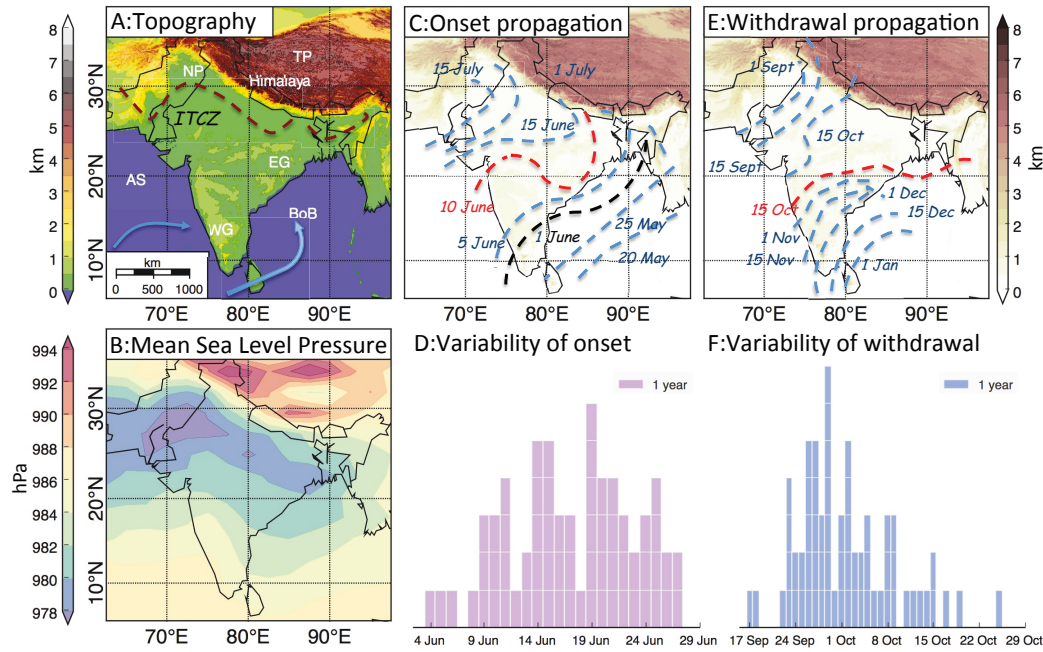
Figure 4.1.: A) Topography of the Indian subcontinent with key features of the Indian Summer monsoon: Himalaya, Tibetan Plateau (TP), North Pakistan (NP), Eastern Ghats (EG), Western Ghats (WG), Arabian Sea (AS), Bay of Bengal (BoB), Intertropical Convergence Zone (ITCZ) [Amante, 2009]. Blue arrows indicate near sea-level wind direction; B) Composites of mean sea level pressure (June-September, 1951-2014 based on NCEP/NCAR data); C) and E) Schematic representation of the long-term average propagation (since 1951, based on (IMD, 2015)) of the advance and withdrawal of monsoon over the Indian subcontinent (northern limit of monsoon). Dashed black line shows averaged monsoon onset for the Kerala region forecasted by IMD, and dashed red line for the Eastern Ghats (the region of main interest in this study); D) and F) show histograms of onset and withdrawal dates for the Eastern Ghats region (1951–2014).

1993); ii) Our approach allows to adjust the prediction scheme for abnormal years, often associated with El-Niño-Southern Oscillation.

4.2. Climatic Setting, Data, and Methods

4.2.1. Climatic Setting

The ISM is driven by several factors, including temperature and pressure gradients between land and ocean (Krishnamurti and Ramanathan, 1982), latent heat release during the monsoon season (Choudhury and Krishnan, 2011), associated migration of the Intertropical Convergence Zone (ITCZ) (Saha and Saha, 1980; Gadgil, 2003),

and the high elevation of Himalayan mountain peaks resulting in orographic shielding (Boos and Kuang, 2010), which establish an area of deep convection over the Indian subcontinent (Joseph et al., 1994; Ananthakrishnan and Soman, 1990) (Fig. 4.1 A, B).

The monsoon is characterised by a sudden onset associated with an abrupt and large-scale shift of the regional circulation pattern over the Indian peninsula (Gadgil, 2003; Goswami et al., 2010). In particular, a few days before monsoon onset outgoing long wave radiation (OLR) shows deep convection over the Bay of Bengal and Arabian Sea, relative humidity increases abruptly in the vertical direction before onset of monsoon (Soman and Krishna Kumar, 1993)), and vertically integrated zonal moisture transport increases (Sikka and Gadgil, 1980; Rao et al., 2005; Fasullo and Webster, 2003). A withdrawal of monsoon occurs gradually, and is caused by a southward movement of the ITCZ, resulting in an anticyclonic flow over northern and central India, a displacement of the moist marine air with dry continental air and, leading to a deceleration of the low-level westerly flow, followed by a reduction of rainfall over the Indian subcontinent. The movement of the northern limit of monsoon during the onset and withdrawal of the ISM and its variability are shown on (Fig. 4.1, C, D,E, F)).

4.2.2. Data

We use daily values of near surface air temperature (T) (at 1000 hPa), relative humidity (rh) (at 1000 hPa), and wind fields at 700 hPa from two reanalysis gridded daily data sets: ERA40, provided by the European Center for Medium-range Weather Forecasts (ECMWF) (Uppala et al., 2005) for the period 1971-2002, and NCEP/NCAR, provided by the National Center for Environmental Prediction and the National Center for Atmospheric Research (Kalnay et al., 1996) for the period: 1951-2014. The spatial resolution of both data sets is 2.5°. We have extracted data for the monsoon region (62.5–97.5° E, 5.0–40.0° N; see Fig. 4.1)), which results in 15*15=225 gridded points. OD and WD of monsoon are taken from Singh and Ranade, 2010 and the IMD (IMD, 2015). ENSO years were classified based on the Oceanic Nino Index (ONI) (*http* : //*ggweather.com/enso/oni.htm*).

Choice of the onset date (OD) of the Indian monsoon

The Indian Meteorological Department (IMD) considers the onset of the monsoon date - as the onset date over the southern tip of the Indian subcontinent (Kerala) region (Figure 1, C), black dotted line). However, there are some difficulties in determining the onset of the monsoon date for this region, mainly due to "bogus" (false) monsoon onsets. In order to avoid this uncertainty in the definition of the correct day of monsoon onset over Kerala, in this study, we use as the onset date over the Eastern Ghats (EG) region as the monsoon onset date (OD) (Figure 4.1 C, red dotted line). Most importantly, arrival of the monsoon to the EG marks the full arrival of the monsoon onto the Indian subcontinent, as the northern position of the

Intertropical convergence zone (ITCZ) during the monsoon is located near the EG (23.5N).

Choice of data for prediction scheme

Holloway and Neelin (2009) among other studies have shown that column water vapor w (vertically integrated specific humidity) is a good proxy for transition to the strong convection – onset of precipitation. In Holloway and Neelin (2009), and other parametric models of precipitation called convective parameterizations, precipitation occurs when w reaches a certain critical saturation value $w_c(T)$, which depends on the critical temperature T_{crit}. While vertically integrated climate variables are harder to measure with desired accuracy for prediction of the onset and withdrawal dates, values of the near-surface air temperature (T) and relative humidity (rh) are better represented in models, experiments, and observations (Mishra et al., 2014; Kim et al., 2015). In this regard, we choose T and rh for the prediction of the onset and withdrawal dates of the monsoon. In addition, we also determine T_{crit} for our method - which is equal to T_{sat} (see Table 4.1).

4.2.3. Methods

We propose a novel approach for predictability of monsoon OD and WD, which consists of three main steps: i) We identify *tipping elements of the monsoon* using a precursor of critical transitions, that indicates the proximity of the system to a critical threshold – the phenomenon of pre-bifurcation growth of fluctuations (Surovyatkina et al., 2005). The tipping element is a geographic region, which shows the maximal growth of the variance of fluctuations (σ^2) prior to the monsoon onset; ii) We choose the tipping elements of the monsoon as optimal observation locations or reference points (RPs) for targeted observations, and by analyzing time series within these RPs, we establish a causal relationship between them and derive an indicator of monsoon onset and withdrawal; iii) We introduce a prediction scheme for onset and withdrawal dates, based on trends of T and rh in the RPs.

i) Tipping elements of the Indian monsoon

We calculate σ^2 of T and rh for each grid point for a window length of $w = 7$ days prior to the OD, d days before onset date of monsoon in a given year y as following:

$$\sigma^2(x,d,w,y) = < [x(t^*(y) - d - k) - \bar{x}(t^*(y) - d - k)]^2 >_w = \tag{4.1}$$

$$= \sum_{k=1}^{w} \frac{[x(t^*(y) - d - k) - \sum_{i=1}^{w} \frac{x(t^*(y)-d-i)}{w}]^2}{w} \tag{4.2}$$

where $x(t)$ is a time series, w the length of the time window, d the number of days prior to OD, y a given year, and $t^*(y)$ the OD in the given year y.
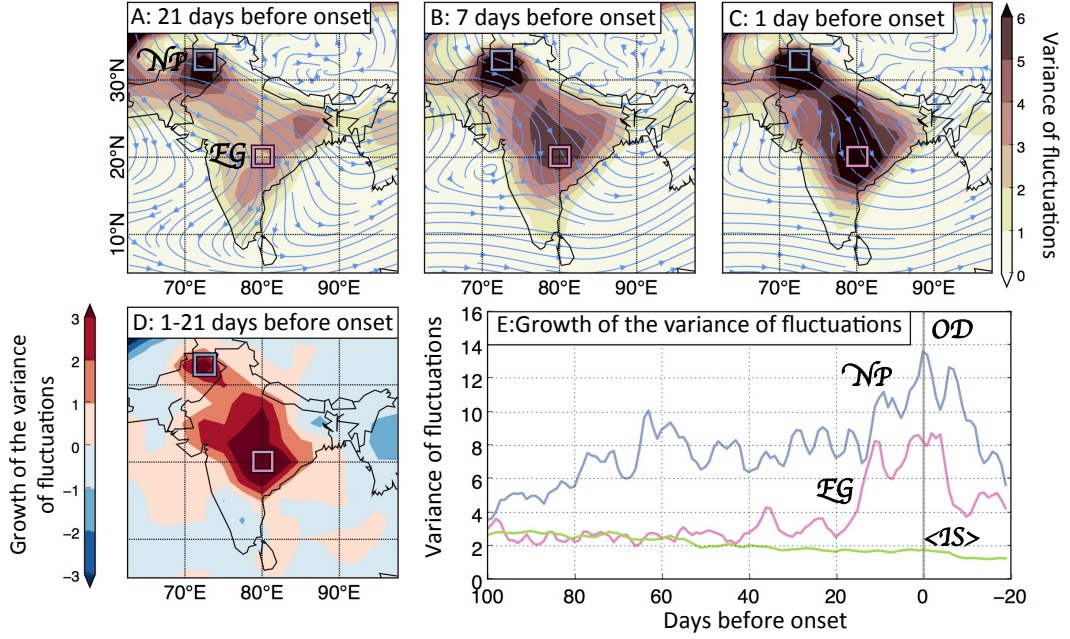
Figure 4.2.: Pre-monsoon growth of the variance of fluctuations (σ^2) of the weekly mean values of near-surface air temperature (T) 21 days, 7 days and 1 day before the monsoon onset at the Eastern Ghats: A, B and C. D=C-A. Composites are for the period 1971-2001 and were calculated from the ERA40 reanalysis data set, 700 hPa winds are indicated by the blue lines. Two boxes refer to RPs: North Pakistan, NP (blue) and Eastern Ghats, EG (pink). E - growth of the variance of fluctuations in NP (blue), EG (pink), and averaged over the Indian subcontinent ($< IS >$) at approaching onset date of the monsoon (OD).

For detection of most common positions of the RPs, we average σ^2 over the whole range of years:

$$\sigma^2 = \sigma^2(x, d, w) = < \sigma^2(x, d, w, y) >_y = \sum_{y=1}^{Y} \frac{\sigma^2(x, d, w, y)}{Y} \qquad (4.3)$$

where Y is the total number of years.

Our result uncovers that the Eastern Ghats and the North Pakistan regions (marked by pink and blue boxes) experience the highest growth of σ^2, while approaching the critical transition to monsoon onset (see Figure 4.2). An analysis of σ^2 of rh while approaching the OD shows similar results (see SI, 4.3).

Determining the geographic regions of critical behavior or the tipping elements of the Indian monsoon is supported by several facts. First, in associated publication P1 (Stolbova et al., 2014) and Chapter 2 of this thesis using climate network analysis of extreme precipitation over the Indian subcontinent during the pre-monsoon, monsoon
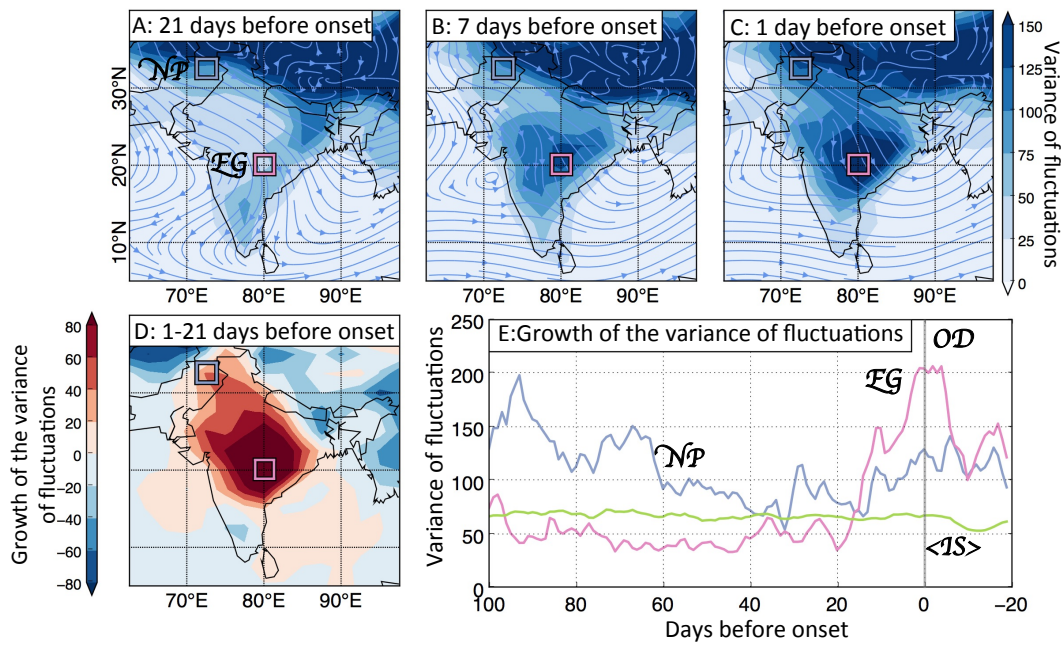
Figure 4.3.: Pre-monsoon growth of the variance of fluctuations (σ^2) of the weekly mean values of near-surface relative humidity (rh) 21 days, 7 days and 1 day before the monsoon onset at the Eastern Ghats: A, B and C. D=C-A. Composites are for the period 1971-2001 and were calculated from the ERA40 reanalysis data set, 700 hPa winds are indicated by the blue lines. Two boxes refer to RPs: North Pakistan, NP (blue) and Eastern Ghats, EG (pink). E - growth of the variance of fluctuations in NP (blue), EG (pink), and averaged over the Indian subcontinent ($< IS >$) at approaching onset date of the monsoon (OD).

and post-monsoon seasons it was shown that only during the monsoon season the EG and NP experience the synchronization of the extreme rainfall. This is caused by the establishment of the monsoon trough, which connects these regions. Second, from a meteorological perspective, it is not so surprising that the EG and NP regions exhibit highly developed instability in observables on the eve of the monsoon onset. The maximum northern position of the ITCZ runs through the EG, and therefore, it coincides with hottest place on the Indian subcontinent (around latitude 23.4N, see Figure 4.4). The topography of the EG creates a favorable condition for the formation of a low-pressure system, and when ITCZ reaches the EG, two branches of monsoon merge: Arabian Sea and Bay of Bengal. At the same time, high pressure in NP and its intricate topography bounded by the Himalaya, create favorable condition for the developing anticyclone. Altogether, it creates a general wind pattern, in which the center of the monsoon cyclone is near the EG, while the center of the anticyclone - is in the NP region. As a consequence, we observe the maximum growth of σ^2 in the centers of the cyclone and the anticyclone systems. Third, the collision of the
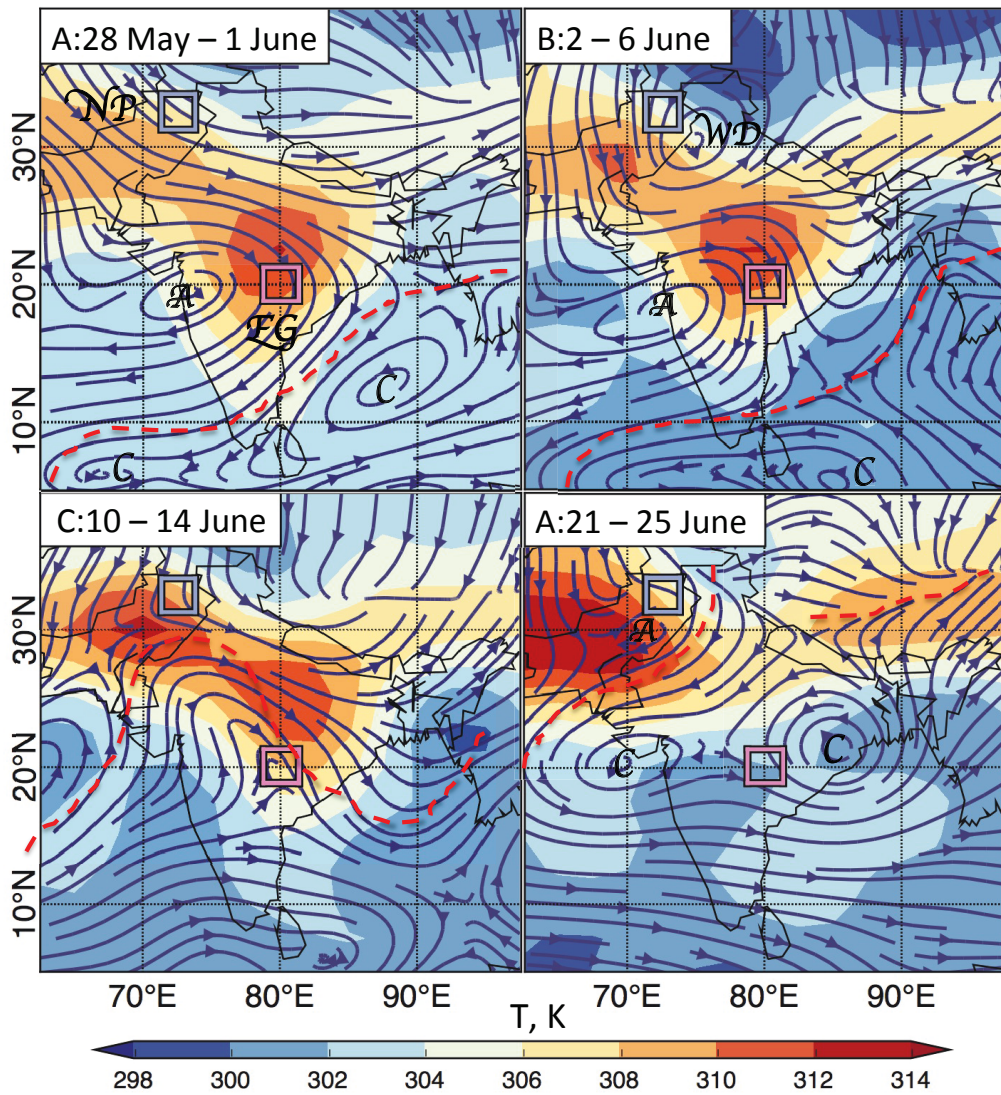
Figure 4.4.: Streamline analysis of the mean resultant winds at 700 mb over the Indian region during the period: A) 28 May - 1 June 2015, B) 2-6 June 2015, C) 11-15 June, D) 21-25 June 2015. Onset of monsoon over the EG is on 13th June in 2015. C denotes cyclonic circulation associated with the equatorial trough of low pressure, and A - anticyclonic circulation associated with 'warm high' above surface 'heat low' over India, WD is referred to the Western Disturbances, associated with subtropical Westerlies. Northern Boundary of Monsoon is indicated by a red dashed line and is identified with the Intertropical Convergence Zone. Color shows near-surface air temperature (T), averaged over the mentioned periods, 2015.
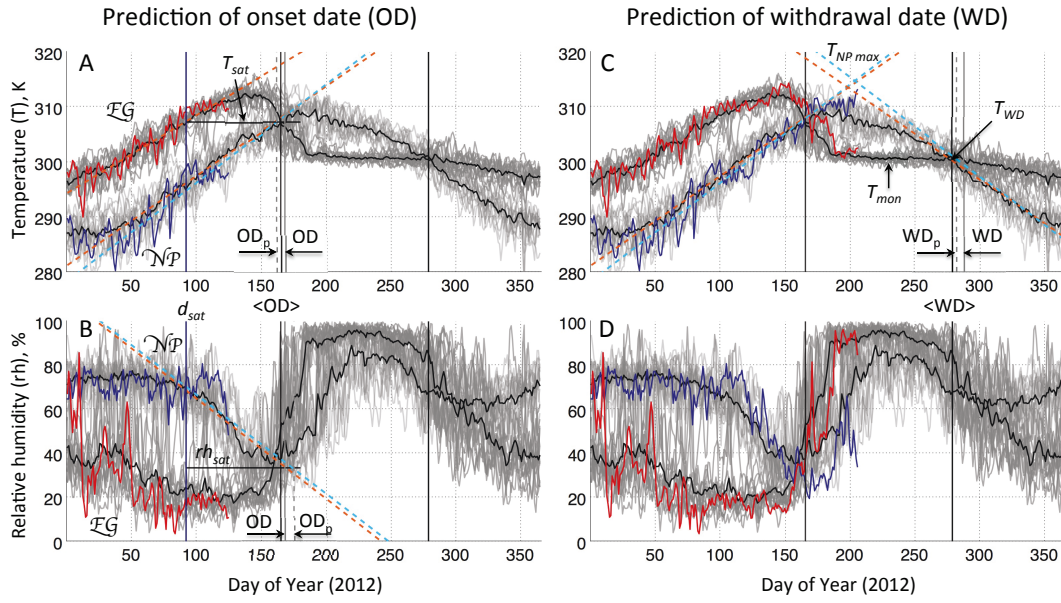
Figure 4.5.: Prediction of onset date (OD) and withdrawal date (WD): case study 2012. Left: prediction of the onset date (OD); right: withdrawal date (WD) of monsoon in the EG. A, C: air temperature at 1000 hPa; B, D: relative humidity at 1000 hPa. Time series from reference points: 14-year mean (black) and 2012 values for NP (blue) and the EG (red). Grey lines show time series from the NP and EG for the training period of 14 years. Saturation temperature T_{sat} (A) and saturation humidity rh_{sat} (C) are marked by horizontal black solid lines ($T_{sat} = T_{onset}$, T_{onset} and rh_{sat} calculated as intersection of mean time series for the training period from the EG and NP), and day of the saturation (d_{sat}) (when temperature in the EG in 2012 reaches T_{sat}) - with dark blue. Orange line indicate trends to the mean time series in the NP and EG for the training period, light blue - trends for 2012. Black solid lines indicate mean values of the OD ($<OD>$) and WD ($<WD>$) for the training period. Dotted grey lines correspond to the predicted onset (OD_p) and withdrawal dates (WD_p), while solid grey lines - to actual onset and withdrawal dates for 2012.

anticyclone located in NP and the developing low pressure system associated with the monsoon, marks the onset of monsoon in the EG. Therefore, fluctuation in NP and the EG show indicators of this collision.

These factors combined allow us to identify EG and NP as tipping elements of the monsoon and choose them as optimal observation locations or reference points (RPs) for comparative analysis aiming to predict monsoon onset and withdrawal.

ii) Identification of the OD and WD with a time series analysis for the RPs.

We analyze the time series of T and rh in the RPs. We find that there is an important relation between the two tipping elements of the monsoon: the Eastern Ghats (EG) and North Pakistan (NP). The intersection of the average time series in the RPs for the period from 1951–2014 takes place twice. At both times, it coincides with the mean values of the OD and WD as determined by the IMD within the EG with a standard deviation of ± 5 days (see Figure 4.5). We observe that yearly variations in the intersection also occur within a few days of monsoon onset at the EG (see Figure C1, Appendix C). This allows us to equalize temperatures in the tipping elements of the monsoon, and derive a prediction scheme for forecasting the OD and WD of monsoon in the EG.

iii) Prediction schemes for the OD and WD of monsoon.

We develop a prediction scheme for forecasting the OD and WD with reanalysis data for the period from 1951–2014. As a training period, we use 14 years of data prior to the year when a prediction is made. For the sensitivity analysis of the prediction scheme to the length of the training period we refer to the Figure S4, SI. We illustrate the performance of this prediction scheme for OD and WD with a case study for 2012 (see Figure 4.5) (parameters used for calculation of the estimated OD and WD dates are presented in the Table 4.1).

Our first step is to make a qualitative prediction of the OD. We perform a linear time-series trend estimation for the two RPs and compare these with trends of the mean time series of the training period. The slopes of the trends for the RPs provide an estimation of an early, normal, or late monsoon arrival: greater than average slope of T will lead to an earlier than usual OD, and vice versa. Trends of rh in the RPs in comparison with the average trends for the training period add up to the predictability of the OD: higher than average values of rh lead to a late OD, and vice versa. In addition, the tendency of expected early (late) intersection of the time series of rh from the RPs usually leads to an earlier (later) than normal OD.

The analysis of the mean time series from the RPs shows that the OD coincides with the date when T in EG and in NP become equal (see Figure 4.5). Therefore, for the forecasting of OD, we need to predict when T for EG will drop abruptly and meet T for NP. However, during the pre-monsoon period T for EG is in a nonlinear saturation mode (when T reaches maximum on 145 DOY) and it is a challenge to predict how close the system is to a critical threshold and when an abrupt transition will occur. At the same time period, T in NP gradually increases and can be approximated by a linear trend. Hence, using the linear trend we can predict when T in NP will reach a certain value, which for EG is a critical threshold for the onset of the monsoon. The value of the critical threshold might be estimated using the average critical threshold from the training period (see SI).

We forecast the OD by identifying the time when the linear trend of T in NP reaches T_{sat}, which is characterised by monsoon onset temperature in the EG from

Table 4.1.: Parameters used for calculating monsoon onset and withdrawal date. $<$
$NP>$ and NP - characteristics related to the mean time series for the training
period and for year for which prediction is made from the NP, $<EG>$ and EG -
the same definition - for EG region, (x,y) - linear trend calculated for the period from
x to y day of the year (DOY), T_{sat} and rh_{sat}- temperature and relative humidity of
the intersection of the mean (during the training period) time series from NP and
EG, d_{sat} - day of saturation, when $T_{EG}(d_{sat}) = T_{sat}$ for the first time during the
pre-monsoon period, $T_{NP_{max}}$ - maximum temperature in the NP during the given
period of time, $T_{mon} = T_{WD}$, where T_{mon} is temperature of monsoon, T_{WD} - is
temperature of the mean withdrawal date, SV - saturation value, training period is
14 years.

	$<NP>$	$<EG>$	NP	EG	SV	DS
OD_T	(30,125) DOY	(30,100)	(30,125)	(30,100)	T_{sat}	$d_{sat} = f(T_{sat})$
OD_{rh}	(81,172) DOY	———	$(d_{sat},125)$	———	rh_{sat}	d_{sat}
WD_T	(30,125) DOY	———	$T_{NP_{max}}(195, 205)$	———	T_{WD}	———
			(30,125)			

the training period (see Table 4.1, C). When T in NP highly fluctuates during a year
and causes difficulties to correctly determine the trend, the trend from the training
period can be used for OD forecasting.

An additional way of estimating the OD of monsoon is using variations of the
relative humidity (rh) in the NP region. We estimate the OD by identifying the time
when the linear trend of the rh in North Pakistan reaches rh_{sat}, which is determined
by the intersection of rh from the EG and NP (see Figure 4.5 B and Table 4.1).

The prediction scheme of the WD is based on the symmetry of T changes in NP
during the year. Knowing the T in EG from the training period, the trend of NP in
the pre-monsoon period, and the maximum T in NP, we can estimate the trend of
the T decrease in the NP region. The WD is then estimated as the intersection of
the projected T decrease in NP and the T in the EG during the monsoon season (see
Figure 4.5 C). Variation of rh are too high for WD prediction and the intersection
of the rh time series usually takes place one month later than the actual WD (see
Figure 4.5 D). Thus, we do not attempt to predict the WD based on rh.

4.3. Results and Discussion

4.3.1. Performance of the predictability schemes.

The performance of the proposed prediction scheme is shown in Figure 4.6. The
prediction is regarded successful if the time difference between the predicted OD and
the real one is less than a week (≤ 7 days) for the OD and ≤ 10 days for WD. The
proposed scheme based on T results in 74% of successful predictions of the OD on
day 125 of the year (DOY) (April 10-th) (based on rh in 70%). Predictability of the
OD using rh is lower than using T (70% versus 74%) mostly because of the high
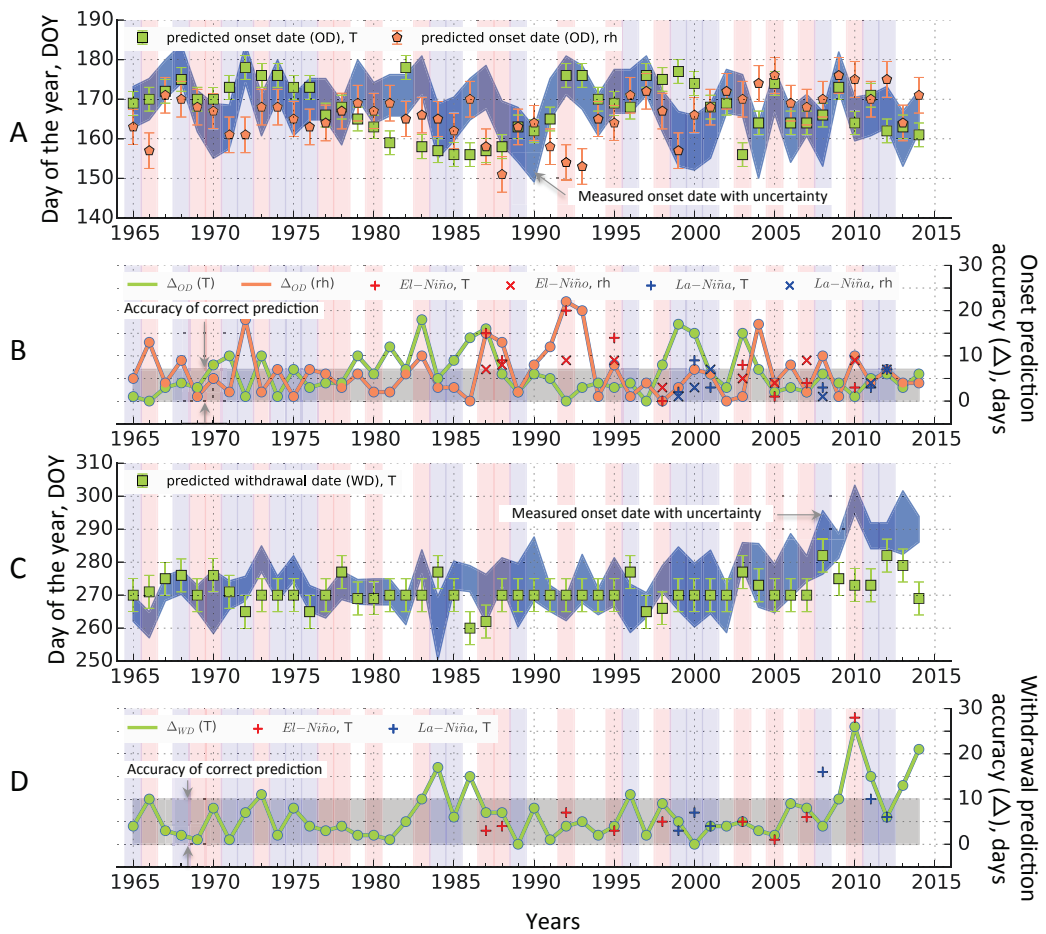
Figure 4.6.: Monsoon OD and WD prediction based on T (green) and rh (orange) and measured (dark blue) OD (A) and WD (C). Red and light-blue shading indicates pos. ENSO (El-Niño) and neg. ENSO (La-Niña) years. Also shown is the difference (Δ) between the real onset or withdrawal and predicted dates in days ($\Delta_{OD(T)}$: prediction based on temperature, $\Delta_{OD(rh)}$: on relative humidity). Grey shading indicates range of 7 days, within the prediction is considered accurate (B). The accuracy of prediction of the WD has a range of 10 days (grey shadow) (D). Markers "+" (T) and "×" (rh) show improved prediction based on the training period of 14 years only from preceding pos. (red) and neg. (blue) ENSO years (B and D). We observe a significantly improved prediction for La-Niña years.

variability of rh and the associated difficulties in approximating a linear trend. Still, in some cases, the OD prediction based on rh may be useful, if the prediction based on T fails. While other existing methods forecast the monsoon onset date over Kerala ranging from one month to two weeks prior to the onset date (at the end of April and on May 15-th), our approach allows to forecast the full arrival of monsoon onto

the Indian subcontinent from 30 to 50 days in advance, and on average two to three weeks earlier than existing methods. The main advantage of our method is that it not only allows a long-range forecasting of the full monsoon arrival onto the Indian subcontinent, but it also enables us to estimate the exact onset date, while other methods of long-range forecasting only give a qualitative forecast of early, normal or late monsoon arrival.

The prediction scheme for WD succeeds in 84% of years on 205 DOY (July 25-th). Our approach allows to predict WD more than a month earlier than existing forecasting systems, which do not attempt to predict the WD before 244 DOY (September 1st, http://www.imd.gov.in).

4.3.2. Anomalous years

Although, our prediction scheme works for most of the years, the proposed approach has certain limitations. They are associated with difficulties in estimating the trend of T and rh for some years. We refer to a year as anomalous when the proposed approach has difficulties to predict OD and WD. We identified three main reasons for the increased uncertainty in the forecasting of monsoon timing during these years.

First, increased uncertainty might be caused by difficulties in the correct determination of the "real" OD and WD in the EG (Wang et al., 2009). Second, increased uncertainty occur because of the difficulties in the trend estimation in NP because of high fluctuations of T and rh possibly due to intensification of the Western Disturbances in NP (Cannon et al., 2014) and - as a result - an increase in winter and pre-monsoon rains, caused by positive phases of North Atlantic Oscillation (NAO) and El-Niño Southern Oscillation (Syed et al., 2012). In particular, we observe an increased uncertainty in the forecasting of the OD based on rh for the years 1990–1993 and based on T for the years 1998–2000 (Figure 4.6), which might be associated with two regime shifts in the fog frequency during the pre-monsoon in the 1990-ies and from 1998–2006 (Syed et al., 2012; Cannon et al., 2014). Third, forecasting of monsoon timing meets certain difficulties because of the intricate relationship between the monsoon and ENSO. It has been shown that especially pos. ENSO years cause local anomalies in the spatial distribution of the atmospheric pressure, temperature and wind during the pre-monsoon (Byshev et al., 2012; Ludescher et al., 2014; Hlinka et al., 2014; Singh et al., 2000) and thereby affect estimation of trends.

Two thirds of the anomalous years are ENSO years. In particular, ENSO affects predictability of the OD: neg. ENSO years decrease the accuracy of prediction with respect to ENSO-neutral by 3% from 81% to 78%, and pos. ENSO years – by 6% to 75 % for the prediction scheme based on T (similar for rh). In particular, inaccurate prediction based on T is made for the following years: 1973, 1983, 1987, 1992 (pos. ENSO years); 1971, 1985, 1999, 2000 (neg. ENSO years); 1979, 1981, 1986 (ENSO-neutral years). For the prediction of the WD, anomalous years are: 1966, 1973, 1983, 1998, 2010 (pos. ENSO years), 1984, 2009, 2011 (neg. ENSO years) and 1986, 2014 (ENSO-neutral years). For these anomalous years a more thorough analysis is required, as T and rh in NP and EG do not exhibit typical behaviour.

We can improve the prediction quality by taking into account the ENSO state during the training period. Our prediction scheme based on the training period of 14 years with a separate analysis of pos., neg., and neutral ENSO years increases the forecast accuracy of WD up to 89% for pos. ENSO (9 years) and up to 83% for neg. ENSO years (see Figure 4.6 C). Forecast of the OD during the pos. ENSO years do not improve the accuracy of prediction, possibly due to the high fluctuations in NP causing problems with the trend estimation. In contrast, forecast for neg. ENSO years considerably improves the prediction of the OD, resulting in 83% of accurate predictions within 7 days (out of 6 years) based on T, and accurate predictions within 7 days for all years (out of 6 years) based on rh (see Figure 4.6 B).

In addition, there are some difficulties in estimating the WD for the last 5 years (see Figure 4.6 C, D). Data of determined post-factum withdrawal dates in EG (which we call real withdrawal dates and compare our results with), show an increase in the last decade (IMD, 2015). That is, the length of the monsoon is increasing. This observation might be caused by difficulties in the determination of the WD during these years, since T variations were more erratic. Alternatively, the change in WD may be related to a change in the monsoon state. Since our analysis is mostly based on the estimation of the WD using a training period (in the wider sense the state of the system), it seems that during the last several years the state of the system has changed. As a result, information only from the training period based on observation of the previous years is not sufficient for an accurate prediction of the WD in the last pentade. If we exclude the last 5 years from the prediction of the WD, we obtain an improved forecasting prediction skill up to 91%. Above mentioned issues, however, do not affect the accuracy of prediction of the OD during the last pentade, which remains high (5 out 5 accurate predictions based on T, and 4 out 5 - based on rh) (see Figure 4.6 A, B).

4.4. Conclusion

We have proposed a novel approach for Indian monsoon onset and withdrawal prediction based on a critical transition precursor - the pre-bifurcation growth of fluctuations. We have revealed two geographic regions (North Pakistan and the Eastern Ghats) of critical behavior that exhibit the largest growth of the variance of fluctuations prior to the onset of the monsoon. We call these regions *tipping elements of the monsoon* and treat them as coupled reference points to predict the onset and withdrawal dates of monsoon based on time-series analysis of near-surface air temperature and relative humidity.

Based on this approach, we have developed a prediction scheme for long-range (30+ days) forecasting of onset and withdrawal dates of the monsoon. The proposed scheme allows to predict onset dates two weeks earlier than existing forecasting methods, and in 74% of the considered years gives an accurate prediction with a range of 7 days. Also, our approach allows to predict the withdrawal date 20 days earlier than existing forecasting methods, and for 84% of the considered years it results

in an accurate prediction within 10 days difference from the real withdrawal date. In addition, the proposed approach allows to include information about the ENSO events in the forecasting scheme and notably improve the forecasting of monsoon timing during La-Niña years.

Because North Pakistan and the Eastern Ghats are regions of critical behaviour when the monsoon season approaches, we propose to improve observational data in these regions, especially, in Pakistan, where the number of stations is quite low.

Our approach can be used as an example for identification of tipping elements in spatially organized systems undergoing a critical or abrupt transition and using them for prediction of spatiotemporal abrupt transitions.

Chapter 5.

Conclusion

5.1. Contribution of this dissertation

The aim of this thesis was to advance the understanding of the Indian Monsoon – a large-scale climate phenomenon, which governs life and prosperity of almost 30% of the world's population. Although the monsoon arrives regularly every year, there is significant variability in the monsoon timing and strength. The importance of the monsoon is connected with the fact that it is strictly tightened with the agricultural year. One can start plowing only just before the monsoon arrives, so the sprouts of the future crops would have a chance to appear above the ground to greet the monsoon and receive awaited water for the growing. However, if the monsoon comes too early, it leads to flooding of the sprouts and therefore, losses of the crops. If the monsoon arrives unexpectedly late – droughts will destroy the sprouts and decrease the yields of crops. The strength of the monsoon in a certain year is of great importance as well, as for agriculture, as well as the main source of the drinking water on the Indian subcontinent. Finally, extremes of monsoonal rainfall are crucial for the population, as extreme rainfall events are the main cause of drastic floods on the Indian subcontinent, which lead to damages to infrastructure, losses of crops and livelihoods and cause multiple deaths.

There are three vital questions about the monsoon for inhabitants of the Indian subcontinent: 1) "when the monsoon will come?", 2) "how strong will it be?", 3) "where will it occur?". This dissertation was aimed to address each of these questions about the monsoon. In particular, the first part of this thesis was devoted to extreme rainfall events, their spatial structures and the evolution of these structures. The second part of this thesis focused on the problem of spatial and temporal propagation of monsoon and its mechanisms. It was aimed to fill the gap between the two mechanisms: abrupt transition to monsoon and the advance of monsoon over the Indian subcontinent, which are not yet fully understood. The third part of this thesis was concerned with the question of predictability of the monsoon timing, in particular, prediction of the full arrival of monsoon onto the Indian subcontinent.

The above mentioned questions addressed in this thesis were studied using modern methods of complex system science, including climate network theory, which was used for the analysis of the spatial structures of extreme rainfall; dynamical systems and catastrophe theories – were used to identify dynamical states in the monsoon system, regions of critical behavior, precursors of the upcoming monsoon onset, prediction of

monsoon timing and uncovering the mechanisms of advance of monsoon. The results obtained in the frame of this dissertation can be grouped into three main questions:

Extreme precipitation synchronization: spatial patterns and their evolution

An extreme rainfall rarely comes alone. When extreme rainfall occurs in a certain place, it is important to detect other regions, which are vulnerable for extreme rainfall, in order for inhabitants to prepare. Of course, depending on where the extreme rainfall occurs first, the configuration of the vulnerable regions changes. In order to detect the spatial structures of vulnerable regions as a function of location of an extreme rainfall event, we have employed a climate network approach. The nodes of the climate network represent geographic locations and links - synchronicity of the extreme rainfall events between these geographic locations. The networks were constructed from the high spatio-temporal reanalysis data and high-resolution satellite data for the three seasons of the Indian subcontinent: the pre-monsoon, monsoon and the post-monsoon season. We focused the analysis only on the 5 % of the strongest correlations between the pairs of geographic locations of the Indian subcontinent, yielding an undirected unweighted network. The fixed value of the link density in the constructed climate networks (5 %) for three seasons allowed us to track the evolution of the strongest connections between the geographic region of the subcontinent in terms of the extreme rainfall synchronicity.

Through the analysis of various complex-network metrics (such as degree, betweennes, and average link length), we describe typical repetitive patterns in North Pakistan and the Eastern Ghats which have a large influence on the spatial structures of the synchronization of extreme rainfall events over the Indian subcontinent, specifically during the monsoon season. While one of these regions – the Eastern Ghats – were previously known by climatologists as an area influencing the extreme rainfall events over the Indian subcontinent, the North Pakistan region had not yet been considered during the analysis of extreme precipitation over the Indian subcontinent mainly due to the lack of data in this region and the fact that the monsoon circulation does not reach this far North. However, our study has shown, that the North Pakistan area is crucial for the analysis of extreme rainfall events over the subcontinent.

This discovery was possible due to newly released observational satellite data and spatial analysis of the synchronicity of extreme rainfall events using the climate network approach. Having in mind that extreme rainfall events in North Pakistan are usually caused by non-monsoonal circulation pattern - Western Disturbances, and the evidence of the synchronization of extreme rainfall events between this region and Eastern Ghat region, receiving the extreme rainfall due to monsoon, shown in our study, we uncover the new way of interplay between the monsoon and Western Disturbances through the synchronicity of extreme rainfall events. The obtained results open a perspective to observe the interaction of monsoon with non-monsoonal pattern, caused by the Westerlies, in the North Pakistan region and, possibly, to improve the predictability of extreme rainfall occurrence over the Indian subcontinent.

Associated publications: Stolbova et al., Nonlinear Processes in Geophysics (2014, P1), Molkenthin et al., Nonlinear Processes in Geophysics (2014, P2), Tupikina et al., Nonlinear Processes in Geophysics (2014, P3), Donges et al., Chaos (accepted, 2015, P6).

Mechanism of advance of the Indian Monsoon

Despite the fact that many atmospheric processes governing the monsoon and its onset are well understood and described, there is still a lack of understanding of the mechanism of abrupt monsoon onset and its spatial propagation, which prevents successful forecasting of the advance of the monsoon every year. The second part of this thesis addresses this question from the perspective of the catastrophe theory.

The bifurcation theory has been applied in previous studies to explain the mechanism of abrupt monsoon transition, however, on millenial time scale; and the transition was described between the strong monsoon circulation and weak monsoon circulation during the Holocene. In Chapter 3 of this dissertation, for the first time the catastrophe theory has been applied to study the abrupt transition to monsoon on inter-seasonal time scale – the monsoon onset. Earlier studies of monsoon onset provided some evidence that the transition to monsoon or monsoon onset exhibit some properties of the critical transition, and in particular, threshold behaviour. In Chapter 3, using observational data it was shown that the transition to monsoon indeed can be considered as a critical transition, and advance of the monsoon along the axis of monsoon propagation corresponds to a well-defined critical transition of the cusp-catastrophe type. The advance of the transition to monsoon was shown to be controlled by the two parameters: v - parameter, depending on time and associated with the inclination of the sun, thus, net radiation flux, which causes the abrupt transition to monsoon in time for the certain region; and u - parameter depending on the latitude of the geographical region where the monsoon onset takes place. The values of these parameters for the Indian monsoon were estimated directly from the data, and thus, allowing not only a qualitative description of the mechanism of advance of monsoon, but also a quantitative one. The main advantage of the proposed dynamical model of the cusp catastrophe for the advance of the monsoon is that it not only allows to explain the temporal transition to monsoon in a chosen region of the Indian subcontinent, but also, for the first time, explains the spatial propagation of the monsoon onset and its ceasing in the northern part of the Indian subcontinent. The proposed conceptual model enhances the understanding of the mechanism of the abrupt spatio-temporal transition to monsoon onset, and opens perspectives for the spatio-temporal forecast of the advance of monsoon over the Indian subcontinent.

Associated publication: Stolbova et al. (submitted, 2015, P4).

Prediction of onset and withdrawal dates of the Indian Monsoon

The discovery of the mechanism of advance of the Indian Monsoon onto the Indian subcontinent in Chapter 3 of this thesis, raised the question about whether it is possible to predict the timing of the transition to monsoon using the properties of the critical transition? In order to address this question, methods from the bifurcation theory, in particular, the precursor of the critical transition for the analysis of the transition to monsoon has been applied.

In Chapter 4 of this dissertation, a novel method for prediction of the Indian monsoon onset and withdrawal has been proposed based on the identification of the tipping elements of the monsoon - regions of critical behavior prior to the monsoon onset. The time series analysis of observational data from the tipping elements of the monsoon, allowed to reveal the indicator of the monsoon onset and withdrawal and to propose a novel long-range forecasting scheme for the prediction of monsoon onset and withdrawal. The introduced forecasting scheme was able to improve the forecast of the monsoon onset by two weeks and withdrawal by 20 days. The scheme was able to predict the onset date with an accuracy of a week in 74% of years, and withdrawal in 84 %, with an accuracy within 10 days of the considered 50 years. An additional advantage of the proposed forecasting scheme is its possibility to adapt the forecast for abnormal monsoon years, associated with El-Niño-Southern oscillation (ENSO). Particularly successful improvement of the forecast of monsoon onset for the ENSO was observed for the negative phase of ENSO – La-Niña years.

Although the proposed method for forecasting the abrupt transition by identification of the tipping elements of the transition and targeted observation of them for the forecast was introduced for forecasting the onset of the monsoon, this method can be used as a baseline for forecasting the spatio-temporal abrupt critical transitions advancing not only in climate, but also in geophysical, biophysical or other systems.

Associated publication: Stolbova et al. (under review in Geophysical Research Letters, P5).

5.2. Outlook

In this dissertation, the spatial structures of extreme rainfall events and their evolution was investigated by means of complex networks, and influential regions on the extreme events synchronization over the Indian subcontinent were reveal. However, there remain several open questions regarding the propagation of extreme rainfall events during the pre-monsoon, monsoon and post-monsoon seasons. This issue might be addressed by extension of the climate network of extreme precipitation from undirected networks to directed ones and using it to possibly identify the pathways of the extreme event propagation through the Indian subcontinent. Additionally, in the future, higher spatial and temporal resolution data would be available, hopefully, in the North Pakistan region as well, which could extend the accuracy of identification of the influential areas and deepen the understanding of the process of interaction of the monsoon with Westerlies.

In the context of the identification of the tipping elements of the system, which undergoes a spatio-temporal critical transition, it might be interesting to see how the framework introduced in this thesis could be applied to tipping elements in critical transitions of other systems, from sociology and economics to biology and climate. A possible example for application of this methodology, one could apply the methodology to identify tipping elements in the Atlantic Meridional Overturning Circulation (AMOC), in order to reveal optimal observation locations for the prediction of the AMOC collapse. Another example might be identification of the tipping elements as regions in the heart which experience early warning signals of heart arrhythmia or heart attack.

Furthermore, in the framework of the proposed mechanism of abrupt spatio-temporal transition to monsoon, it would be interesting to see whether the cusp catastrophe model would be able to explain the transition to monsoon in other monsoon systems, such as the South American Monsoon System, East-Asian Monsoon, African Monsoon, North American Monsoon and Indo-Australian Monsoon. In addition, it would be very interesting to extend the proposed mechanism to the direction of creating a spatio-temporal forecast of the monsoon onset by identifying characteristic parameters of the region for which the forecast is made every year. This could possibly lead to notable improvements in the forecasting of advance of the monsoon.

Appendix

Appendix A.

On the influence of spatial sampling on climate networks

This appendix is based on the associated publication P2 (Molkenthin et al., 2014), where the influence of spatial sampling on climate networks is discussed. It is widely accepted that the topography as well as other geographical features such as ocean and atmospheric currents have a large impact on the observable time-series similarity. Taking into account that climate networks are reconstructed from time series using correlation measures, it is therefore expected that the spatial sampling will have an impact on the climate networks. Spatial sampling effects in climate networks have been discussed by several authors:Heitzig et al., 2012 proposed weighted measures to deal with differently sized nodes, Rehfeld et al., 2011 discussed this issue from the perspective of temporal and irregularly sampled data, while Rheinwalt et al., 2012 investigated the role of boundary effects on the climate networks measures and proposed a surrogate test which allows to account for this effect.

   In P2 study we investigate the influence of spatial sampling on analytical flow networks, networks generated with toy model of monsoon (START model, Rehfeld et al. (2014)), and networks from temperature data from the Asian monsoon domain. The evaluation of the spatial sampling is revealed through the comparison of networks constructed on a regular grid versus grid with added random jittering. The details regarding the influence of spatial sampling on the analytical flow networks and toy model network can be found in Molkenthin et al. (2014). In this appendix, the influence of spatial sampling on the temperature climate network of the Asian Monsoon domain is discussed.

A.1. Data and Methods

The data analysis was performed on NCEP/NCAR reanalysis daily temperature anomalies composites from January 1, 1970 to December 31, 2010 with a resolution of $2.5°$ on the Asian monsoon domain resulting in 468 nodes. The network was constructed from the anomaly time series using Pearson correlation. The anomalies were calculated as a difference between the original daily temperature time series and long-term daily mean time series for the period 1970–2010. In order to obtain a network from the correlation matrix, the latter was thresholded using a link density of the 5% to yield links corresponding only to strongest correlations. Then, the degree

and betweenness network measures were calculated as shown in Table 1, Chapter 2. The geographical coordinates of each node are marked by a point at the center of each cell (see Figure A.1). To investigate sampling effects, we added a jitter in longitude and latitude at each grid point with a uniformly random number between $\pm a/2$ from the grid center, where a is the size of the grid. The new time series for jittered grid are constructed as Gaussian weighted averages of all of the original time series on the regular grid. The weights of the original time series depend on the euclidean distance between the grid points and the new jittered location.

A.2. Spatial sampling effects in temperature climate network for the Asian monsoon domain

Figure A.1 a) shows the average value of the absolute surface wind speed for the period 1970-2010. This figure indicates the dominant imprint of the monsoon winds on the Asian domain represented by the Arabian Sea, Bay of Bengal and East Asian branches of monsoon highlighted by the highest values of the absolute mean wind speed ($>$10 m/sec). Additionally, high values of the wind speed indicate westerlies over Afganistan and Tibet. Observed high values of wind speed are able to explain the high values of degree in both regular (Figure A.1 c)) and jitter (Figure A.1 d)) climate temperature networks. This result is consistent with model studies by Molkenthin et al., 2014, which have shown that regions along the flow direction tend to have a high degree. Spatial distribution of degree in Figures A.1 c) and d) reveal that highest values of the degree in the climate temperature network of the Asian monsoon domain ($>$48) are associated with Southwest Monsoon ocean current. It allows to conclude that the more persistent ocean currents have a larger influence on the degree than the atmospheric currents (Figure A.1 a)), which are subject to more change. In contrast to the correlation between high velocities and high degrees, which was established earlier in Molkenthin et al., 2014, fast average velocities in the Tibetan plateau (Figure A.1 a)), correspond to some of the lowest degrees in the Asian monsoon domain, as shown in Figure A.1 c), d). It is caused by the fact that the plateau is relatively secluded from the rest of the network due to its high altitude, which means that even if the link density inside the secluded area would be very high, the degree would be low, as connections to other regions are less likely. Comparison of degree of the regular grid network with jittered grid (Figure A.1 c) and d)) shows that the effect of spatial sampling on the degree patterns is reasonably small.

The link length distribution of the climate temperature network for the Asian Monsoon domain is shown on Figure A.1 b). Beige color represents spiky actual link length distribution for the network constructed on the regular grid, while magenta color shows more smooth results for the jittered grid. For the comparison, red and blue colors show the distance distribution between the pair of geographic sites in a complete network (all nodes are connected with all nodes in a square of the Asian monsoon domain) for regular and jittered grid, respectively. It is importanat to note, that the regular arrangement of the grid leads to an overrepresentation of some specific
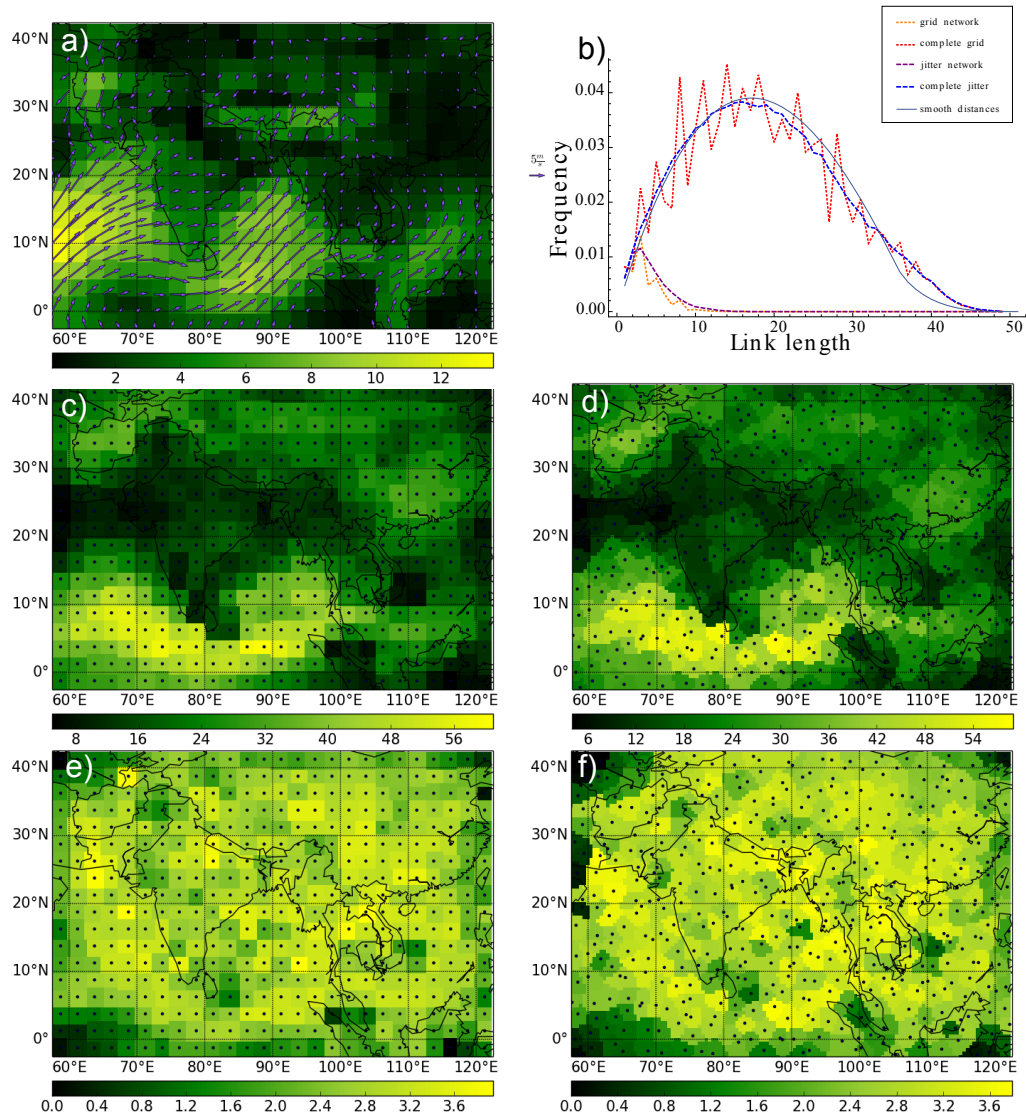
Figure A.1.: The correlation network of temperature data from NCEP/NCAR on a grid and a jittered grid. a) absolute mean wind velocity, b) link length distribution, where link length is expressed in a number of cells between the pair of nodes, c) degree of the grid network, d) degree of the jittered network, e) betweenness of the grid network, f) betweenness of the jittered network.

link lengths (i.e. multiples of the grid constant), while other node-node distances are excluded by the node distribution. Light blue color shows smooth distances distribution obtained by integrating the distances between all pairs of geographic sites i and j, which is equivalent to integrating over the area of the square of the considered domain and all circle segments that lie in the square of radius d. Normalizing the resulting function of d one gets the distance distribution. Obtained function coincides well with the link length distribution of the fully connected nodes of the jittered sampling, while the fully connected regular grid's link length distribution is more spiky, but varies around the same curve.

The bottom row of the Figure A.1 (e) and f)) shows the betweenness for grid and jittered sampling (e,f). The shortest path betweenness varies more spatially than the degree. Most nodes have medium betweenness and those who have higher or lower values do not persist when the sampling is changed. It is shown, for example, at 25°N, 85°E, which in the gridded sampling exhibit one of the lowest values of betweeness, but in the jittered sampling has average value. It is unclear if this effect is due to aliasing or a physical effect, but implies that the betweenness measure is too sensitive to draw conclusions about the system.

A.3. Conclusion

The analysis of the influence of the spatial distribution of nodes on the climate network topology have shown that the degree measure is robust to the spatial re-sampling, while the betweenness reacts more sensitively. Although, the case study example here is related to climate, yet the results can be generalized to all networks coming from discretizations of any continuous system.

An important feature that one constructing spatial networks has to take into account is that in a case of a smooth link length distribution the node to node separation has to cover all possible distances, which is not the situation for the regular grid. A grid does not fulfill that as all distances are of the form: $d(i,j) = a\sqrt{n^2 + m^2}$, where a is the grid constant and n and m are integer numbers. Distances that can not be represented in this way are not present in a grid.

While the effects of the area sizes of nodes are discussed in detail in Heitzig et al., 2012, and this effect can be removed using proposed in this study consistently weighted network measures, this study shows that the problem goes further, when one also considers the underlying physical system. Although, the node size distributions in the regular grid and jittered grid samplings are very similar, their relative position to the underlying flow might be not similar, leading to very different distorting effects on the network structure. In future work it might be interesting to compare different jitter realizations quantitatively, for example using the common component function (CCF) as introduced in P5.

The main finding can be formulated as follows: as long as the node distribution in space is sufficiently homogeneous, the exact chosen spatial sampling has little impact on the topology of the network as in the climate temperature network of the Asian

monsoon domain, discussed here, as well as for the case of analytical flow networks and network generated by the toy model of the monsoon circulation (START, Rehfeld et al., 2014) as it was shown in P2. We have shown that only in cases of significantly inhomogeneous sampling, distortion and misleading structures arose. It is, therefore, important to discuss the sampling and its impact when analyzing spatially sampled data. As a simple test of the spatial sampling we suggest to look at the jittered cell distribution. In a homogeneous sampling this will have a clear peak around $A_{sam} = N_{nod}$, where A_{sam} is the size of the total sampled area and N_{nod} is the number of nodes. If the peak is shifted or very spread out, that suggests poor spatial sampling (see study P2 for the details).

Appendix B.

Inter-annual variability of the Asian Monsoon by means of evolving climate networks

This appendix is based on the associated publications P3 and P6. In P3 study we have developed a novel network measure which allows to characterize the evolution of the climate network with time: *common component function* and applied it to study the inter-annual variability of the Surface Air Temperature (SAT) over the Asian monsoon domain, as it influences the total amount of rainfall and it's spatial distribution during the monsoon season.

B.1. Method

In Tupikina et al. (2014) (P3), we introduce a *common component function (CCF)*. For two unweighted undirected networks defined of the same set of nodes, the *common component function*, $\mathrm{CCF}(N_i, N_j)$, counts the number of common links in a pair of networks N_i and N_j with adjacency matrices A^i and A^j respectively:

$$\mathrm{CCF}(N_i, N_j) = \frac{\sum_{l,k=1(k<l)}^{N} A_{kl}^i A_{kl}^j}{\sum_{l,k=1(k<l)}^{N} A_{kl}^i A_{kl}^i}, \tag{B.1}$$

where

$$\sum_{l,k=1(k<l)}^{N} A_{kl}^i A_{kl}^i = \sum_{l,k=1(k<l)}^{N} A_{kl}^i \tag{B.2}$$

is simply the number of links in the network N_i. Therefore, the normalized common component function $CCF(N_i, N_j)$ takes values between $[0, 1]$.

B.2. Data

We used daily NCEP/NCAR reanalysis temperature anomaly data (NCEP/NCAR, 2015) for the Asian monsoon domain for the years 1970-2010. The spatial resolution was $2.5° \times 2.5°$, covering the area between 2.5°S to 42.5°N and 57.5°E to 122.5°E, resulting in time series for 468 nodes. The temperature climate networks were constructed using Pearson correlation for the window of length 365 days for each full year. The obtained correlation matrix was thresholded in a way that we set a link density of 5% of the strongest links. For the network construction and analysis we used PyUnicorn toolbox, introduced in the publication P6.

B.3. Results

We analyze the inter-annual variability of the surface air temperature over the Asian monsoon domain by means of climate networks. Since climate temperature network was constructed for each year from the period 1970-2010, a set of these networks describes the evolution of climate temperature network and thus, reflects the inter-annual variability of the temperature anomalies in the Asian monsoon domain. First, we identify geographic regions with the highest and lowest variability on inter-annaul time scale using mean degree variability (or variability of connections of the chosen region with other) of the temperature network of the Asian monsoon domain, presented on Figure B.1 A. It shows the lowest degree variability over the Indian subcontinent, Bay of Bengal (BoB) and Arabian Sea - regions of the Indian monsoon activity - a part of the Asian monsoon system, while the highest variability is observed in the Equatorial Indian Ocean - the region influenced by trade winds; Northwest India, Pakistan, Afganistan regions, Tibetan Plateau, South China and South China Sea - regions, influenced mainly by Westerlies and monsoon winds.

In oder to uncover the cause of this variability, we applied the developed network measure - $CCF(N_i, N_j)$ for all pairs of years $i, j \in [1970, 2011]$, where i is kept fixed, yielding a common-links-recurrence-diagram, illustrated in Figure B.1 B. It is important to note the rows and columns with distinct low values (<0.7) for the CCF on this Figure. In these lines the overall sum, $S_i = \sum_j CCF(N_i, N_j)$, takes smaller values in the years $i \in (1971 - 1973, 1975, 1984, 1989, 1993, 1999)$, which indicates less common links in the networks of years corresponding to this lines with the rest of the years. In the previous studies, it has been shown that the Asian monsoon domain on inter-annual timescales experience the influence of El-Nino-Southern Oscillation phenomenon (Turner and Annamalai, 2012). Therefore, we compared the obtained sequence with a list with strong ENSO events according to the NINO 3.4 index (Trenberth et al., 2000), and observed that the break down of links in the climate networks were most likely associated with the strong El-Nino event years in this time period. In particular, our results show that around strong El-Nino years the surface temperature networks have less common links with networks from other years. Since El-Nino events occur during the northern hemisphere winter season, the main effect

of the links breakdown in our networks occur in the year after the event started, specifically, after the strong El-Nino events of 1972, 1983, 1988, 1992 and 1998.
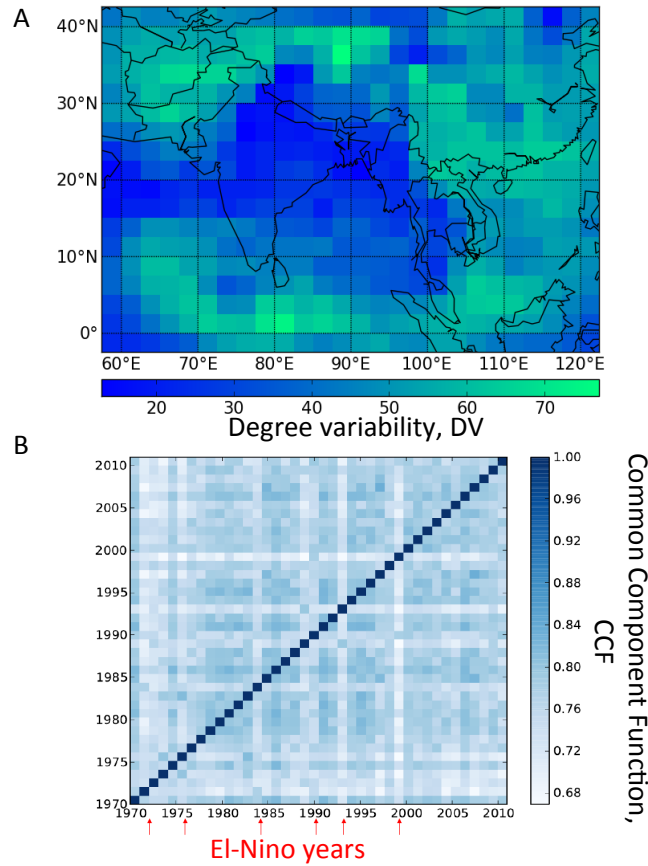
Figure B.1.: A) Degree variability (DV), B) Common-links-recurrence-diagram. Lines with low values (marked at the bottom with arrows) are observed around strong El-Nino years.

B.4. Conclusions

Understanding the inter-annual variability of the Asian monsoon and its interaction with El-Nino-Souther Oscillation remains one of the most vital questions in climatology. Using PyUnicorn toolbox (P6) and novel network measure (common component function) (P3) we were able to analyze these phenomena and their interaction from the climate networks perspective, reveal the temporal evolution of the temperature anomalies over the Asian domain and the influence of El-Nino-Southern Oscillation on the Asian monsoon system.

Analysis of the annual variability of the evolving climate network of the Asian monsoon region using common component function allows us to distinguish between

the permanent component of the climate network, associated with persistent factors influencing temperature of the Asian monsoon domain such as topography and general circulation patterns (trade winds, Westerlies), and annually changing factors, such as connection with variability of other climatic phenomena, in case of Asian domain - El-Nino-Southern Oscillation. It allows us to decompose the temperature variability into permanent and varying component, and conclude that a highly non-random, deterministic general structure is present in the network of the temperature anomalies on which the inter-annual variability is imprinted, (Molkenthin et al., 2014; Tupikina et al., 2014).

In addition, we show that strong El-Nino events dramatically change the organization and structure of the temperature climate network over the Asian Monsoon region influencing the monsoon on annual time scale which is observed in the decreased number of the common links in annual snapshots of the evolving climate network. Our results agree with the previous fundings of Gozolchiani et al. (2011) and Tsonis and Swanson (2008), who show that the "breaking" of links in the global climate network might be a result of the global signature of ENSO on the climate annual variability.

The proposed temporal network measure - common component function can be applied for any type of evolving network where the link but not the node set is changing, and may be particularly useful to characterize nonstationary evolving systems using complex networks.

Appendix C.

Prediction scheme: details

C.1. Time series from the tipping elements of the monsoon for the case study in 2012

As mentioned in the main text, intersection of the time series of air temperature (T) and relative humidity (rh) for each year are in the vicinity of actual onset and withdrawal dates (see Figure C1).

C.2. Parameters for calculation of predicted onset and withdrawal dates. Estimation of onset and withdrawal dates

Here, we describe the parameters used for the estimation of the onset and withdrawal dates. The parameters are gathered into three rows, for each part of the predictability scheme: OD determination using T ($OD_p(T)$), OD determination using rh ($OD_p(rh)$) and WD determination using T ($WD_p(T)$) (see Table 4.1). Columns represent characteristics of the time series related to NP and EG for the mean and given year time series (trends for the given period of time), saturation values (connected with both NP and EG, calculated as values at which intersection of the mean time series from the tipping elements occur), as well as day of the saturation - determined as the day, when T in EG during the given year reached T_{sat}, which is temperature of intersection of the mean T in the EG and NP at the average onset date from the training period (Table 4.1).

C.2.1. *Estimation of* $OD_p(T)$

As the first step, trends are calculated for mean time series from NP ($< NP >$) and EG ($< EG >$) (from the training period) and for time series for the year when the prediction is made, for the periods 30–125 DOY (NP) and 30–100 DOY (EG). Second, T_{sat} is detected as intersection of the mean time series $< NP >$ and $< EG >$. If the difference between the slopes of the current year trend in NP and the mean trend in NP ($< NP >$) is less than 15% of the slope of the mean trend ($< NP >$), we estimate the $OD_p(T)$ as intersection of the trend in NP for the current year of the T_{sat} value. If the estimated value of $OD_p(T)$ lies in the boarders of the onset dates
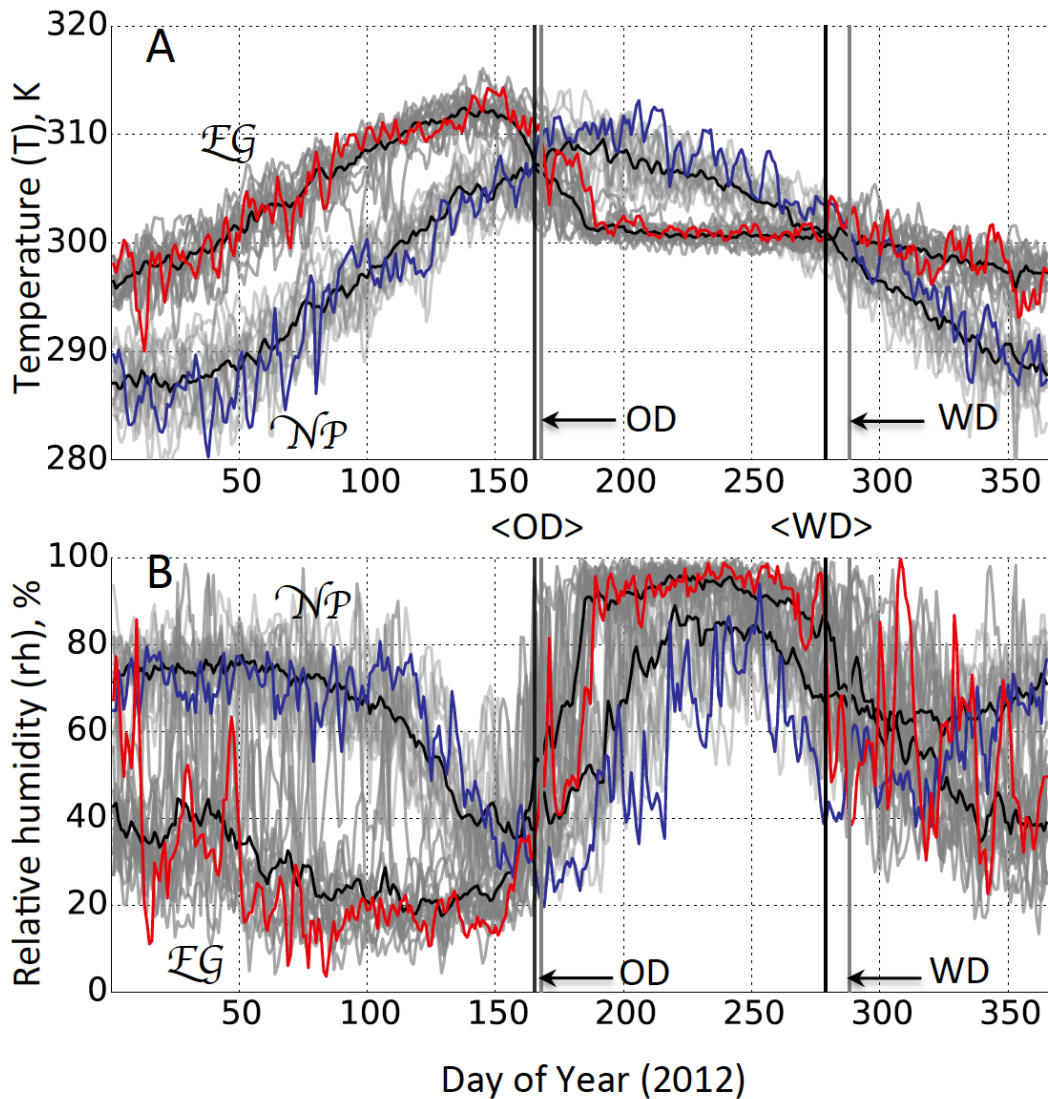
Figure C1.: Time series from tipping elements of monsoon: air temperature at 1000 hPa (A) and relative humidity at 1000 hPa (B); 14-year mean (black) and 2012 values for NP (blue) and the EG (red). Grey lines on the background show time series from the NP and EG for the training period of 14 years. Black solid lines indicate mean values of the OD ($< OD >$) and WD ($< WD >$) for the training period, while solid grey lines - actual onset (OD) and withdrawal dates (WD) for 2012.

from the corresponding training period, we use this value as predicted OD. Otherwise, if the deviation of the trend in NP for the current year is more than 15% or the estimated values is outside of the range determined by the corresponding training period, the $OD_p(T)$ is determined using the mean trend from the training period.

C.2.2. *Estimation of $OD_p(rh)$*

We detect rh_{sat} as a near surface relative humidity at which rh values intersect from the tipping elements of the monsoon. Second, we calculate the trend of rh in NP for the period 81–172 DOY. Third, from the time series of near surface air temperature we identify d_{sat} as the date when mean T in EG for the first time reaches T_{sat}, and we calculate the trend of rh in NP from this date untill 125 DOY. Then, $OD_p(rh)$ is estimated as an intersection of this trend with rh_{sat}. When the estimated value lies outside the boundaries determined by the onset dates from the training period, we estimate $OD_p(rh)$ using the mean trend from NP from the training period and rh_{sat}.

C.2.3. *Estimation of $WD_p(T)$*

Estimation of the WD is based on the fact that on average, the slope of the linear trend of $<NP>$ for the period 30–125 DOY is equal with an opposite sign to the slope of the decrease of the average T in NP from the training period at the end of the monsoon season. We call this trend a *reversed trend*. We force the reversed trend to the mean time series from NP to intersect the average T in the EG at the $<WD>$ of the training period. We note, that this reversed trend intersects the normal mean trend close to the day when T of the mean T in NP reaches it's maximum during the year. Based on this observation, we estimate the WD for the given year as follows: First, we identify the maximum value of T in NP for the period 195–205 DOY and mark the date when it happens. Second, we reconstruct the reversed trend in NP from the current year trend in NP including the condition that the obtained trend should intersect with the normal trend at the detected date of the maximum of T in NP. Third, we identify T_{mon} in the EG (monsoon temperature) from the training period by finding T in the EG at the $<WD>$. Finally, we estimate $WD_p(T)$ as the intersection of the reversed trend of NP and baseline for T_{mon}. When the predicted WD lies outside of the boundaries from the values from the training period for a given year, we estimate the WD using trends of the mean time series from the training period from the tipping elements of monsoon for this year.

C.3. Identification of the optimal training period

Skills of the proposed prediction scheme depend on the training period for the estimation of the onset and withdrawal dates. Here we define a correct prediction as a year when the difference in days between the predicted and real onset dates is equal or less than 7 days for the OD and 10 days for the WD. Therefore, the number of correctly predicted onset dates is what we call the true positive rate (TPR).
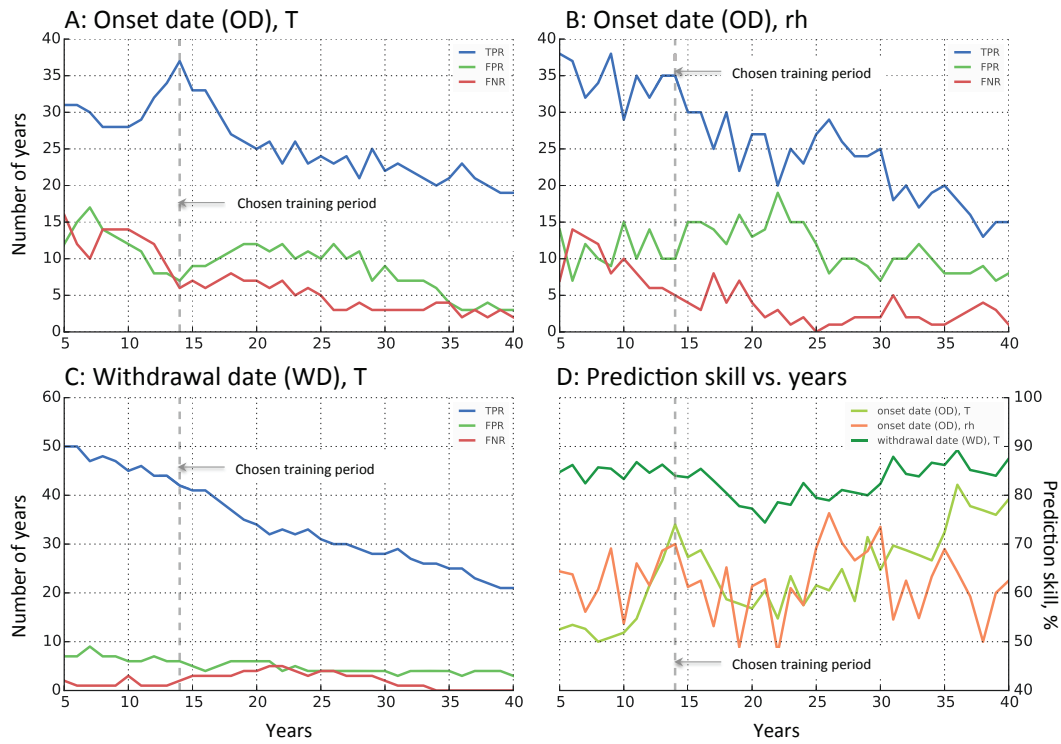
Figure C.2.: Sensitivity of the accuracy of prediction scheme to the length of the training period. A, B, C - Dependence of the TPR, FPR and FNR in years versus length of the training period. Number of the considered years for each value of training period=TPR+FPR+FNR. D - Dependence of prediction skill on the number of considered years.

Similarly, we define a false positive predicted date when the predicted onset date is more than a week earlier than real onset date (FPR) and false negative when predicted onset date was more than a week later than the real onset date (FNR). We test our predictability scheme for the different training periods. The result is shown in the Figure C.2.

Bibliography

Achuthavarier, Deepthi, V. Krishnamurthy, Ben P. Kirtman, and Bohua Huang (2012). "Role of the Indian Ocean in the ENSOâIndian Summer Monsoon Teleconnection in the NCEP Climate Forecast System". In: *Journal of Climate* 25.7, pp. 2490–2508. ISSN: 0894-8755. DOI: 10.1175/JCLI-D-11-00111.1.

Alessandri, Andrea, Andrea Borrelli, Annalisa Cherchi, Stefano Materia, Antonio Navarra, June-Yi Lee, and Bin Wang (2014). "Prediction of Indian summer monsoon onset using dynamical sub-seasonal forecasts: effects of realistic initialization of the atmosphere". In: *Monthly Weather Review*, p. 141113122228007. DOI: 10.1175/MWR-D-14-00187.1.

Ananthakrishnan, R. and M. K. Soman (1990). "The onset of the southwest monsoon in 1990". In: *Current Science* 61.7, pp. 447–453.

Barreiro, Marcelo, Arturo C Marti, and Cristina Masoller (2011). "Inferring long memory processes in the climate network via ordinal pattern analysis." In: *Chaos (Woodbury, N.Y.)* 21.1, p. 013101. ISSN: 1089-7682. DOI: 10.1063/1.3545273.

Boers, Niklas, Bodo Bookhagen, Norbert Marwan, Jürgen Kurths, and José Marengo (2013). "Complex networks identify spatial patterns of extreme rainfall events of the South American Monsoon System". In: *Geophysical Research Letters* 40.16, pp. 4386–4392. DOI: 10.1002/grl.50681.

Bookhagen, Bodo and Douglas W. Burbank (2010). "Toward a complete Himalayan hydrological budget: Spatiotemporal distribution of snowmelt and rainfall and their impact on river discharge". In: *Journal of Geophysical Research* 115.F3, F03019. ISSN: 0148-0227. DOI: 10.1029/2009JF001426.

Boos, William R and Zhiming Kuang (2010). "Dominant control of the South Asian monsoon by orographic insulation versus plateau heating". In: *Nature* 463.7278, pp. 218–222. ISSN: 0028-0836.

Byshev, V. I., V. G. Neiman, Yu. a. Romanov, and I. V. Serykh (2012). "On El Niñoâs impact upon the climate characteristics of the Indian monsoon". In: *Oceanology* 52.2, pp. 147–156. DOI: 10.1134/S0001437012010043.

Cannon, Forest, Leila M. V. Carvalho, Charles Jones, and Bodo Bookhagen (2014). "Multi-annual variations in winter westerly disturbance activity affecting the Himalaya". In: *Climate Dynamics* 44.1-2, pp. 441–455. DOI: 10.1007/s00382-014-2248-8.

Chakraborty, a. (2002). "Role of Asian and African orography in Indian summer monsoon". In: *Geophysical Research Letters* 29.20, p. 1989. ISSN: 0094-8276. DOI: 10.1029/2002GL015522.

Chappel (1983). "Thresholds and lags in geomorphologic changes". In: *Australian Geographer* 15, pp. 357–366.

Bibliography

Choudhury, Ayantika Dey and R. Krishnan (2011). "Dynamical Response of the South Asian Monsoon Trough to Latent Heating from Stratiform and Convective Precipitation". In: *Journal of the Atmospheric Sciences* 68.6, pp. 1347–1363. ISSN: 0022-4928. DOI: `10.1175/2011JAS3705.1`.

Das, Anindya (2011). "Farmersâ Suicide in India: Implications for Public Mental Health". In: *Psychiatry.*

Das, P.K. (1987). "Short- and long-term prediction in India". In: *In Monsoons, edited by J.S.Fein and P.L. Stephens, John Wiley and Sons, New York*, pp. 549–578.

Das, Someshwar, a. K. Mitra, G. R. Iyengar, and J. Singh (2002). "Skill of Medium-Range Forecasts over the Indian Monsoon Region Using Different Parameterizations of Deep Convection". In: *Weather and Forecasting* 17.1992, pp. 1194–1210. ISSN: 0882-8156. DOI: `10.1175/1520-0434(2002)017<1194:SOMRFO>2.0.CO;2`.

Deza, J I, C Masoller, and M Barreiro (2013a). "Distinguishing the effects of internal and forced atmospheric variability in climate networks arXiv : 1311 . 3089v1 [nlin . CD] 13 Nov 2013". In: November. arXiv: `arXiv:1311.3089v1`.

Deza, J.I., M. Barreiro, and C. Masoller (2013b). "Inferring interdependencies in climate networks constructed at inter-annual, intra-season and longer time scales". In: *The European Physical Journal Special Topics* 222.2, pp. 511–523. ISSN: 1951-6355. DOI: `10.1140/epjst/e2013-01856-5`.

Donges, J. F., Y. Zou, N. Marwan, and J. Kurths (2009a). "Complex networks in climate dynamics". In: *The European Physical Journal Special Topics* 174.1, pp. 157–179. ISSN: 1951-6355. DOI: `10.1140/epjst/e2009-01098-2`.

– (2009b). "The backbone of the climate network". In: *EPL (Europhysics Letters)* 87.4, p. 48007. ISSN: 0295-5075. DOI: `10.1209/0295-5075/87/48007`.

Durai, V. R. and S. K. Roy Bhowmik (2014). "Prediction of Indian summer monsoon in short to medium range time scale with high resolution global forecast system (GFS) T574 and T382". In: *Climate Dynamics* 42, pp. 1527–1551. DOI: `10.1007/s00382-013-1895-5`.

Ebeling, Werner and I.M Sokolov (2005). *Fluctuations and Linear Irreversible Processes. Statistical Thermodynamics and Stochastic Theory of Nonequilibrium Systems*, pp. 97–110.

ERA40 (2015). URL: `http://apps.ecmwf.int/datasets/data/era40-daily/` (visited on 09/20/2015).

Fasullo, John and P. J. Webster (2003). "A hydrological definition of Indian Monsoon onset and withdrawal". In: *Journal of Climate* 16, pp. 3200–3211. ISSN: 08948755. DOI: `10.1175/1520-0442(2003)016<3200a:AHDOIM>2.0.CO;2`.

Feldhoff, J. H., R. V. Donner, J. F. Donges, N. Marwan, and J. Kurths (2013). "Geometric signature of complex synchronisation scenarios". In: *EPL (Europhysics Letters)* 102.3, p. 30007. ISSN: 0295-5075. DOI: `10.1209/0295-5075/102/30007`.

Feng, Qing Yi, Jan P Viebahn, and Henk A Dijkstra (2014). "Deep ocean early warning signals of an Atlantic MOC collapse". In: pp. 6008–6014. DOI: `10.1002/2014GL061019.Received`.

Feng, Song (2005). "Regulation of Tibetan Plateau heating on variation of Indian summer monsoon in the last two millennia". In: *Geophysical Research Letters* 32.2, p. L02702. ISSN: 0094-8276. DOI: 10.1029/2004GL021246.

Flatau, M. K., P. J. Flatau, and D. Rudnick (2001). "The dynamics of double monsoon onsets". In: *Journal of Climate* 14.May 1979, pp. 4130–4146. DOI: 10.1175/1520-0442(2001)014<4130:TDODMO>2.0.CO;2.

Gadgil, Sulochana (2003). "The Indian Monsoon and Its Variability". In: *Annual Review of Earth and Planetary Sciences* 31.1998, pp. 429–467. DOI: 10.1146/annurev.earth.31.100901.141251.

– (2004). "Extremes of the Indian summer monsoon rainfall, ENSO and equatorial Indian Ocean oscillation". In: *Geophysical Research Letters* 31.12, p. L12213. ISSN: 0094-8276. DOI: 10.1029/2004GL019733.

GEBCO.

Goswami, B. N., Guoxiong Wu, and T. Yasunari (2006). "The annual cycle, intraseasonal oscillations, and roadblock to seasonal predictability of the Asian summer monsoon". In: *Journal of Climate* 19, pp. 5078–5099. DOI: 10.1175/JCLI3901.1.

Goswami, B. N., J. R. Kulkarni, V. R. Mujumdar, and R. Chattopadhyay (2010). "On factors responsible for recent secular trend in the onset phase of monsoon intraseasonal oscillations". In: *International Journal of Climatology* 30.14, pp. 2240–2246. DOI: 10.1002/joc.2041.

Goswami, P. and K. C. Gouda (2010). "Evaluation of a Dynamical Basis for Advance Forecasting of the Date of Onset of Monsoon Rainfall over India". In: *Monthly Weather Review* 138. DOI: 10.1175/2010MWR2978.1.

Gozolchiani, a., K. Yamasaki, O. Gazit, and S. Havlin (2008). "Pattern of climate network blinking links follows El Niño events". In: *EPL (Europhysics Letters)* 83.2, p. 28005. ISSN: 0295-5075. DOI: 10.1209/0295-5075/83/28005.

Gozolchiani, a., S. Havlin, and K. Yamasaki (2011). "Emergence of El Niño as an Autonomous Component in the Climate Network". In: *Physical Review Letters* 107.14, p. 148501. ISSN: 0031-9007. DOI: 10.1103/PhysRevLett.107.148501.

Graf, W.L. (1979). "Catastrophe theory as a model for changes in fluvial systems". In: *D.D. Rhodes, G.P. Williams (Eds.), Adjustments of the Fluvial System, Kendall Hunt, Dubuque*, pp. 13–32.

Heitzig, Jobst, Jonathan F Donges, Yong Zou, and Norbert Marwan (2012). "Node-weighted measures for complex networks with spatially embedded , sampled , or differently sized nodes". In: pp. 1–21. arXiv: arXiv:1101.4757v2.

Henley, S (1976). "Catastrophe theory models in geology". In: *Mathematical Geology* 8, pp. 649–655.

– (1983). "Evolutionary geomorphology". In: *Geography* 68, pp. 225–235.

Hlinka, J., D. Hartman, N. Jajcay, M. Vejmelka, R. Donner, N. Marwan, J. Kurths, and M. Paluš (2014). "Regional and inter-regional effects in evolving climate networks". In: *Nonlinear Processes in Geophysics* 21.2, pp. 451–462. ISSN: 16077946. DOI: 10.5194/npg-21-451-2014.

Holloway, Christopher and J. D. Neelin (2009). "Moisture vertical structure, column water vapor, and tropical deep convection". In: *Journal of the Atmospheric Sciences*, pp. 1665–1683. DOI: `10.1175/2008JAS2806.1`.

Huffman, George J., David T. Bolvin, Eric J. Nelkin, David B. Wolff, Robert F. Adler, Guojun Gu, Yang Hong, Kenneth P. Bowman, and Erich F. Stocker (2007). "The TRMM Multisatellite Precipitation Analysis (TMPA): Quasi-Global, Multiyear, Combined-Sensor Precipitation Estimates at Fine Scales". In: *Journal of Hydrometeorology* 8.1, pp. 38–55.

IMD (2015). *Indian Meteorological Department.*

Joseph, Porathur V., Jon K. Eischeid, and Robert J. Pyle (1994). "Interannual Variability of the Onset of the Indian Summer Monsoon and Its Association with Atmospheric Features, El Niño, and Sea Surface Temperature Anomalies". In: *Journal of Climate* 7, pp. 81–105. DOI: `10.1175/1520-0442(1994)007<0081:IVOTOO>2.0.CO;2`.

Joseph P.V. Sooraj, K. P. and Rajan. C. K (2006). "The Summer Monsoon onset over Process over South Asia and an Objective method for the Date of Monsoon Onset over Kerala". In: *International Journal of Climatology* 26, pp. 1871–1893.

Kalnay, E, M Kanamitsu, R Kistler, W Collins, D Deaven, L Gandin, M Iredell, S Saha, G White, J Woollen, Y Zhu, M Chelliah, W Ebisuzaki, W Higgins, J Janowiak, K C Mo, C Ropelewski, J Wang, A Leetmaa, R Reynolds, R Jenne, and D Joseph (1996). "The NCEP/NCAR 40-year reanalysis project". In: *Bull. Amer. Meteor. Soc.* 77, pp. 437–440.

Kim, J., J. Sanjay, C. Mattmann, M. Boustani, M. V. S. Ramarao, R. Krishnan, and D. Waliser (2015). "Uncertainties in estimating spatial and interannual variations in precipitation climatology in the India-Tibet region from multiple gridded precipitation datasets". In: *International Journal of Climatology*, n/a–n/a. ISSN: 08998418. DOI: `10.1002/joc.4306`.

Krishna Kumar, K. (2005). "Advancing dynamical prediction of Indian monsoon rainfall". In: *Geophysical Research Letters* 32.8, p. L08704. ISSN: 0094-8276. DOI: `10.1029/2004GL021979`.

Krishnamurthy, V. and J. Shukla (2007). "Intraseasonal and seasonally persisting patterns of indian monsoon rainfall". In: *Journal of Climate* 20, pp. 3–20. ISSN: 08948755. DOI: `10.1175/JCLI3981.1`.

Krishnamurti, T N (1971). "Tropical East-Wesr Circulations During the Northern Summer". In: *Journal of the Atmospheric Sciences* 28, pp. 1342–1347.

Krishnamurti, T. N. and Y. Ramanathan (1982). *Sensitivity of the Monsoon Onset to Differential Heating.* DOI: `10.1175/1520-0469(1982)039<1290:SOTMOT>2.0.CO;2`.

Krishnan, R., C. Zhang, and M. Sugi (2000). "Dynamics of Breaks in the Indian Summer Monsoon". In: *Journal of the Atmospheric Sciences* 57.1969, pp. 1354–1372. ISSN: 0022-4928. DOI: `10.1175/1520-0469(2000)057<1354:DOBITI>2.0.CO;2`.

Lenton, Timothy M. (2011). "Early warning of climate tipping points". In: *Nature Climate Change* 1.4, pp. 201–209.

Lenton, Timothy M, Hermann Held, Elmar Kriegler, Jim W Hall, Wolfgang Lucht, Stefan Rahmstorf, and Hans Joachim Schellnhuber (2008). "Tipping elements in the Earth's climate system". In: *Proceedings of the National Academy of Sciences of the United States of America* 105.6, pp. 1786–93.

Levermann, Anders, Jacob Schewe, Vladimir Petoukhov, and Hermann Held (2009). "Basic mechanism for abrupt monsoon transitions". In: *Proceedings of the National Academy of Sciences of the United States of America* 106.49, pp. 20572–7. ISSN: 1091-6490.

Ludescher, Josef, Avi Gozolchiani, Mikhail I Bogachev, Armin Bunde, Shlomo Havlin, and Hans Joachim Schellnhuber (2014). "Very early warning of next El Niño." In: *Proceedings of the National Academy of Sciences of the United States of America* 111.6, pp. 2064–6. ISSN: 1091-6490. DOI: 10.1073/pnas.1323058111.

Madhura, R. K., R. Krishnan, J. V. Revadekar, M. Mujumdar, and B. N. Goswami (2015). "Changes in western disturbances over the Western Himalayas in a warming environment". In: *Climate Dynamics* 44.3-4, pp. 1157–1168. ISSN: 09307575. DOI: 10.1007/s00382-014-2166-9.

Majumdar, Apala, John Ockendon, Peter Howell, and Elena Surovyatkina (2013). "Transitions through critical temperatures in nematic liquid crystals". In: *Physical Review E* 88.2, p. 022501. ISSN: 1539-3755. DOI: 10.1103/PhysRevE.88.022501.

Malik, N., N. Marwan, and J. Kurths (2010). "Spatial structures and directionalities in Monsoonal precipitation over South Asia". In: *Nonlinear Processes in Geophysics* 17.5, pp. 371–381. ISSN: 1607-7946. DOI: 10.5194/npg-17-371-2010.

Malik, Nishant, Bodo Bookhagen, Norbert Marwan, and Jürgen Kurths (2011). "Analysis of spatial and temporal extreme monsoonal rainfall over South Asia using complex networks". In: *Climate Dynamics* 39.3-4, pp. 971–987. ISSN: 0930-7575. DOI: 10.1007/s00382-011-1156-4.

Martin, E. a., M. Paczuski, and J. Davidsen (2013). "Interpretation of link fluctuations in climate networks during El Niño periods". In: *EPL (Europhysics Letters)* 102.4, p. 48003. ISSN: 0295-5075. DOI: 10.1209/0295-5075/102/48003.

Marwan, Norbert and Stefan Schinkel (2013). "Recurrence plots 25 years later â Gaining confidence in dynamical transitions AN INVITATION TO". In: 101.

Marwan, Norbert, Jonathan F. Donges, Yong Zou, Reik V. Donner, and Jürgen Kurths (2009). "Complex network approach for recurrence analysis of time series". In: *Physics Letters A* 373.46, pp. 4246–4254. ISSN: 03759601. DOI: 10.1016/j.physleta.2009.09.042.

Mishra, Vimal, Devashish Kumar, Auroop R Ganguly, J Sanjay, Milind Mujumdar, R Krishnan, and Reepal D Shah (2014). "Reliability of regional and global climate models to simulate precipitation extremes over India". In: *Journal of Geophysical Research : Atmospheres*, pp. 9301–9323. DOI: 10.1002/2014JD021636.Received.

Molkenthin, Nora, Kira Rehfeld, Norbert Marwan, and Jürgen Kurths (2014). "Networks from flows - from dynamics to topology." In: *Scientific reports* 4, p. 4119. ISSN: 2045-2322. DOI: 10.1038/srep04119.

Bibliography

Munot, a. a. and K. Krishna Kumar (2007). "Long range prediction of Indian summer monsoon rainfall". In: *Journal of Earth System Science* 116.1, pp. 73–79. DOI: `10.1007/s12040-007-0008-4`.

NCEP/NCAR (2015). URL: `http://www.erls.noaa.gov/psd` (visited on 09/20/2015).

NCMRF. *National Center for Medium Range Forecasts*.

Neelin, J. David, Ole Peters, and Katrina Hales (2009). "The Transition to Strong Convection". In: *Journal of the Atmospheric Sciences* 66.8, pp. 2367–2384. ISSN: 0022-4928. DOI: `10.1175/2009JAS2962.1`.

Neiman, Alexander, Alexander Silchenko, Vadim Anishchenko, and Lutz Schimansky-Geier (1998). "Stochastic resonance: Noise-enhanced phase coherence". In: *Phys. Rev. E* 58 (6), pp. 7118–7125. DOI: `10.1103/PhysRevE.58.7118`.

Neiman, Alexander, Lutz Schimansky-Geier, Ann Cornell-Bell, and Frank Moss (1999). "Noise-Enhanced Phase Synchronization in Excitable Media". In: *Phys. Rev. Lett.* 83 (23), pp. 4896–4899. DOI: `10.1103/PhysRevLett.83.4896`.

Pai, D.S. and RajeevanM. Nair (2009). "Summer monsoon onset over Kerala: New definition and prediction". In: *Journal of Earth System Science* 118.2. DOI: `10.1007/s12040-009-0020-y`.

Paluš, M., D. Hartman, J. Hlinka, and M. Vejmelka (2011). "Discerning connectivity from dynamics in climate networks". In: *Nonlinear Processes in Geophysics* 18.5, pp. 751–763. ISSN: 1607-7946. DOI: `10.5194/npg-18-751-2011`.

Pattanaik, D. R. and M. Rajeevan (2009). "Variability of extreme rainfall events over India during southwest monsoon season". In: *Meteorological Applications* November 2015, n/a–n/a. ISSN: 13504827. DOI: `10.1002/met.164`.

Peters, Ole, J. David Neelin, and Stephen W. Nesbitt (2009). "Mesoscale Convective Systems and Critical Clusters". In: *Journal of the Atmospheric Sciences* 66.9, pp. 2913–2924. ISSN: 0022-4928. DOI: `10.1175/2008JAS2761.1`.

Poston, Tim and Ian Stewart (1989). "Catastrophe: Theory and Its Applications." In: *New York: Dover, 1998. ISBN 0-486-69271-X*. ISSN: 0-486-69271-X.

Prasad, V. S. (2005). "Onset and withdrawal of Indian summer monsoon". In: *Geophysical Research Letters* 32.20, p. L20715. DOI: `10.1029/2005GL023269`.

Puranik, S S, K C Sinha Ray, P N Sen, and P Pradeep Kumar (2013). "An index for predicting the onset of monsoon over Kerala". In: *Current Science* 105.7.

Qin, S.Q., J.J. Jiao, S.J. Wang, and H. Long (2001). "A nonlinear catastrophe model of instability of planar-slip slope and chaotic dynamical mechanisms of its evolutionary process". In: *International Journal of Solids and Structures* 38, pp. 8093–8109.

Rajagopalan, Balaji and Peter Molnar (2013). "Signatures of Tibetan Plateau heating on Indian summer monsoon rainfall variability". In: *Journal of Geophysical Research: Atmospheres* 118.3, pp. 1170–1178. ISSN: 2169897X. DOI: `10.1002/jgrd.50124`.

– (2014). "Combining Regional Moist Static Energy and ENSO for Forecasting of Early and Late Season Indian Monsoon Rainfall and its Extremes". In: *Geophysical Research Letters*.

Rajkumari, G and R Narasimha (1996). "Statistical analysis of the position of the monsoon trough". In: *Proc. Indian Acad. Sci. (Earth Platen Sci.)* 105, pp. 343–355.

Rao, Nageswara G (1999). "Variations of the SO Relationship with Summer and Winter Monsoon Rainfall over India: 1872â1993". In: *Journal of Climate* 12, pp. 3486–3495.

Rao, P (1976). "Southwest monsoon". In: *Meteorological monograph, Synoptic Meteorology, Indian Meteorological Department, New Delhi* 1.

Rao, P. L. S., U. C. Mohanty, and K. J. Ramesh (2005). "The evolution and retreat features of the summer monsoon over India". In: *Meteorological Applications* 12, p. 241. DOI: 10.1017/S1350482705001775.

Rehfeld, K., N. Marwan, J. Heitzig, and J. Kurths (2011). "Comparison of correlation analysis techniques for irregularly sampled time series". In: *Nonlinear Processes in Geophysics* 18.3, pp. 389–404. ISSN: 1607-7946. DOI: 10.5194/npg-18-389-2011.

Rehfeld, K., N. Molkenthin, and J. Kurths (2014). "Testing the detectability of spatio-temporal climate transitions from paleoclimate networks with the START model". In: *Nonlinear Processes in Geophysics* 21.3, pp. 691–703. DOI: 10.5194/npg-21-691-2014.

Rehfeld, Kira, Norbert Marwan, Sebastian F. M. Breitenbach, Jürgen Kurths, and Climate Dynamics (2012). "Late Holocene Asian Summer Monsoon dynamics from small but complex networks of palaeoclimate data (in press)". In: *Climate Dynamics*. ISSN: 0930-7575.

Revadekar, J. V. and B. Preethi (2012). "Statistical analysis of the relationship between summer monsoon precipitation extremes and foodgrain yield over India". In: *International Journal of Climatology* 32.3, pp. 419–429. ISSN: 08998418. DOI: 10.1002/joc.2282.

Rheinwalt, Aljoscha, Norbert Marwan, Jürgen Kurths, Peter Werner, and Friedrich-Wilhelm Gerstengarbe (2012). "Boundary effects in network measures of spatially embedded networks". In: *EPL (Europhysics Letters)* 100.2, p. 28002. ISSN: 0295-5075. DOI: 10.1209/0295-5075/100/28002.

Sabeerali, C. T., Suryachandra a. Rao, R. S. Ajayamohan, and Raghu Murtugudde (2011). "On the relationship between Indian summer monsoon withdrawal and Indo-Pacific SST anomalies before and after 1976/1977 climate shift". In: *Climate Dynamics* 39.3-4, pp. 841–859. ISSN: 0930-7575. DOI: 10.1007/s00382-011-1269-9.

Saha, Suranjana and Kshudiram Saha (1980). "A hypothesis on onset, advance and withdrawal of the Indian summer monsoon". In: *Pure and Applied Geophysics PAGEOPH* 118.2, pp. 1066–1075. ISSN: 0033-4553. DOI: 10.1007/BF01593050.

Sankar, Syam, M R Ramesh Kumar, Chris Reason, and Dona Paula (2011). "On the Relative Roles of El Nino and Indian Ocean Dipole Events on the Monsoon Onset over Kerala". In: *Theor. Appl. Clim.* 103.

Scarsoglio, Stefania, Francesco Laio, and Luca Ridolfi (2013). "Climate dynamics: a network-based approach for the analysis of global precipitation." In: *PloS one* 8.8, e71129. ISSN: 1932-6203. DOI: 10.1371/journal.pone.0071129.

Shukla, J. and D. A. Mooley (1987). "Empirical prediction of the summer monsoon rainfall over India". In: *Monthly Weather Review* 115.

Sikka, D R and S Gadgil (1980). "On the maximum cloud zone and the ITCZ over Indian longutudes during the south-west monsoon". In: *Monthly Weather Review* 108, pp. 1840–1853.

Singh, Nityanand and Ashwini A Ranade (2010). *Determination of Onset and Withdrawal Dates of Summer Monsoon across India using NCEP/NCAR Re-analysis data set.* Indian Institute of Tropical Meteorology.

Singh, Ramesh P., Sudipta Sarkar, and Ashbindu Singh (2000). "Effect of El Niæo observed over Indian continent from satellite-derived ozone data". In: *Eos, Transactions American Geophysical Union* 81.36, p. 409. ISSN: 0096-3941. DOI: `10.1029/00EO000304`.

Sinha, P., U. C. Mohanty, S. C. Kar, and S. Kumari (2013). "Role of the Himalayan Orography in Simulation of the Indian Summer Monsoon using RegCM3". In: *Pure and Applied Geophysics.* ISSN: 0033-4553. DOI: `10.1007/s00024-013-0675-9`.

Soman, M K and K Krishna Kumar (1993). "Space-time evolution of the meteorological features associated with the onset of th Indian summer monsoon". In: *Monthly Weather Review* 121, pp. 1177–1194.

Stolbova, Veronika, Paige Martin, Bodo Bookhagen, Norbert Marwan, and Juergen Kurths (2014). "Topology and seasonal evolution of the network of extreme precipitation over the Indian subcontinent and Sri Lanka". In: *Nonlinear Processes in Geophysics* 21, pp. 901–917.

Subash, N. and B. Gangwar (2014). "Statistical analysis of Indian rainfall and rice productivity anomalies over the last decades". In: *International Journal of Climatology* 34.7, pp. 2378–2392. DOI: `10.1002/joc.3845`.

Surovyatkina, E., Yu. Kravtsov, and J. Kurths (2005). "Fluctuation growth and saturation in nonlinear oscillators on the threshold of bifurcation of spontaneous symmetry breaking". In: *Physical Review E* 72.4, p. 046125. DOI: `10.1103/PhysRevE.72.046125`.

Syed, F. S., J. H. Yoo, H. Körnich, and F. Kucharski (2012). "Extratropical influences on the inter-annual variability of South-Asian monsoon". In: *Climate Dynamics* 38.7-8, pp. 1661–1674. DOI: `10.1007/s00382-011-1059-4`.

Taniguchi, Kenji and Toshio Koike (2006). "Comparison of definitions of Indian summer monsoon onset: Better representation of rapid transitions of atmospheric conditions". In: *Geophysical Research Letters* 33.2, p. L02709. DOI: `10.1029/2005GL024526`.

Thom, Rene (1989). "Structural Stability and Morphogenesis: An Outline of a General Theory of Models." In: *Reading, MA: Addison-Wesley.* ISSN: 0-201-09419-3.

Tirabassi, G and C Masoller (2013). "On the effects of lag-times in networks constructed from similarities of monthly fluctuations of climate fields AN INVITATION TO". In: 102.

Trenberth, K. E., D. P. Stepaniak, and J. M. Caron (2000). "The global monsoon as seen through the divergent atmospheric circulation". In: *Journal of Climate* 13, pp. 3969–3993.

TRMM.

Tsonis, A.A and P.J. Roebber (2004). "The architecture of the climate network". In: *Physica A: Statistical Mechanics and its Applications* 333, pp. 497–504. ISSN: 03784371. DOI: `10.1016/j.physa.2003.10.045`.

Tsonis, Anastasios and Kyle Swanson (2008). "Topology and Predictability of El Niño and La Niña Networks". In: *Physical Review Letters* 100.22, p. 228502. ISSN: 0031-9007. DOI: `10.1103/PhysRevLett.100.228502`.

Tsonis, Anastasios a., Kyle L. Swanson, and Paul J. Roebber (2006). "What Do Networks Have to Do with Climate?" In: *Bulletin of the American Meteorological Society* 87.5, pp. 585–595. ISSN: 0003-0007. DOI: `10.1175/BAMS-87-5-585`.

Tsonis, Anastasios a., Kyle L. Swanson, and Geli Wang (2008). "On the Role of Atmospheric Teleconnections in Climate". In: *Journal of Climate* 21.12, pp. 2990–3001. ISSN: 0894-8755. DOI: `10.1175/2007JCLI1907.1`.

Tsonis, Anastasios A., Geli Wang, Kyle L. Swanson, Francisco A. Rodrigues, and Luciano Da Fontura Costa (2010). "Community structure and dynamics in climate networks". In: *Climate Dynamics* 37.5-6, pp. 933–940. ISSN: 0930-7575. DOI: `10.1007/s00382-010-0874-3`.

Tupikina, L., K. Rehfeld, N. Molkenthin, V. Stolbova, N. Marwan, and J. Kurths (2014). "Characterizing the evolution of climate networks". In: *Nonlinear Processes in Geophysics* 21.3, pp. 705–711. ISSN: 1607-7946. DOI: `10.5194/npg-21-705-2014`.

Turner, Andrew G. and H. Annamalai (2012). "Climate change and the South Asian summer monsoon". In: *Nature Climate Change* 2.8, pp. 587–595. ISSN: 1758-678X. DOI: `10.1038/nclimate1495`.

Uppala, S. M., P. W. Kallberg, A. J. Simmons, U. Andrae, V. Da Costa Bechtold, M. Fiorino, J. K. Gibson, J. Haseler, A. Hernandez, G. A. Kelly, X. Li, K. Onogi, S. Saarinen, N. Sokka, R. P. Allan, E. Andersson, K. Arpe, M. A. Balmaseda, A. C. M. Beljaars, L. Van De Berg, J. Bidlot, N. Bormann, S. Caires, F. Chevallier, A. Dethof, M. Dragosavac, M. Fisher, M. Fuentes, S. Hagemann, E. Holm, B. J. Hoskins, L. Isaksen, P. A. E. M. Janssen, R. Jenne, A. P. Mcnally, J.-F. Mahfouf, J.-J. Morcrette, N. A. Rayner, R. W. Saunders, P. Simon, A. Sterl, K. E. Trenberth, A. Untch, D. Vasiljevic, P. Viterbo, and J. Woollen (2005). "The ERA-40 re-analysis". In: *Quarterly Journal of the Royal Meteorological Society* 131.612, pp. 2961–3012. DOI: `10.1256/qj.04.176`.

Waliser, Duane E., W Stern, S Schubert, and K M Lau (2003). "Dynamic predictability of intraseasonal variability associated with the Asian summer monsoon a) India b) S E Asia". In: *Q. J. R. Meteorol. Soc.* 129, pp. 2897–2925. DOI: `10.1256/qj.02.51`.

Wang, Bin (2006). *The Asian Monsoon*. Springer Praxis Books.

Wang, Bin, Qinghua Ding, and P. V. Joseph (2009). "Objective Definition of the Indian Summer Monsoon Onset". In: *Journal of Climate* 22.12, pp. 3303–3316.

Wang, Yang, Avi Gozolchiani, Yosef Ashkenazy, Yehiel Berezin, Oded Guez, and Shlomo Havlin (2013). "The dominant imprint of Rossby waves in the climate network". In: d, pp. 1–5.

Webster, P J, V O Magafia, T N Palmer, J Shukla, R A Tomas, M Yanai, and T Yasunari (1998). "Monsoons : Processes , predictability , and the prospects for prediction". In: 103.

Bibliography

Webster, Peter J (2013). "Improve weather forecasts for the developing world". In: *Nature* 493, pp. 17–19. DOI: `10.1038/493017a`.

Wiesenfeld, K (1985). *Virtual Hopf phenomenon: A new precursor of period-doubling bifurcations*. DOI: `10.1103/PhysRevA.32.1744`.

Wu, Renguang and Ben P. Kirtman (2003). "On the impacts of the Indian summer monsoon on ENSO in a coupled GCM". In: *Quarterly Journal of the Royal Meteorological Society* 129.595, pp. 3439–3468. ISSN: 00359009. DOI: `10.1256/qj.02.214`.

Wu, Renguang, Jilong Chen, and Wen Chen (2012). "Different Types of ENSO Influences on the Indian Summer Monsoon Variability". In: *Journal of Climate* 2.3, pp. 903–920. ISSN: 0894-8755. DOI: `10.1175/JCLI-D-11-00039.1`.

Yamasaki, K., a. Gozolchiani, and S. Havlin (2008). "Climate Networks around the Globe are Significantly Affected by El Niño". In: *Physical Review Letters* 100.22, p. 228501. ISSN: 0031-9007. DOI: `10.1103/PhysRevLett.100.228501`.

Yamasaki, Kazuko, Avi Gozolchiani, Shlomo Havlin, and Ramat Gan (2009). "Climate Networks Based on Phase Synchronization Analysis Track El-Ni Ë". In: 179, pp. 178–188.

Yang, Song, Zuqiang Zhang, Vernon E. Kousky, R. Wayne Higgins, Soo Hyun Yoo, Jianyin Liang, and Yun Fan (2008). "Simulations and seasonal prediction of the Asian summer monsoon in the NCEP climate forecast system". In: *Journal of Climate* 21, pp. 3755–3775. DOI: `10.1175/2008JCLI1961.1`.

Yatagai, Akiyo, Osamu Arakawa, Kenji Kamiguchi, and Haruko Kawamoto (2009). "A 44-Year Daily Gridded Precipitation Dataset for Asia". In: 5, pp. 3–6.

Selbständigkeitserklärung

Ich erkläre, dass ich die vorliegende Arbeit selbständig und nur unter Verwendung der angegebenen Literatur und Hilfsmittel angefertigt habe.

Potsdam, den 3. November 2015 Veronika Stolbova